GAC-MAC
WINNIPEG
2013

AT THE
CENTRE OF
THE CONTINENT

AU
CENTRE DU
CONTINENT

FIELD TRIP GUIDEBOOK

Field Trip Guidebook FT-A2 / Open File OF2013-3
Volcanological and Structural Setting of Paleoproterozoic VMS and Gold deposits at Snow Lake, Manitoba

Alan Bailes, Kate Rubingh, Simon Gagné, Craig Taylor, Alan Galley, Sarah Bernauer and Darren Simms

GAC® | AGC®

Held in conjunction with
GAC®-MAC • AGC®-AMC
Joint Annual Meeting • Congrès annuel conjoint
May 22–24, 2013

MAC | AMC

This field trip was sponsored by the Mineral Deposits Division of the Geological Association of Canada

In-kind support provided by HudBay Minerals Inc.

HUDBAY

Open File OF2013-3

Field Trip Guidebook FT-A2

Volcanological and Structural Setting of Paleoproterozoic VMS and Gold deposits at Snow Lake, Manitoba

by Alan Bailes, Kate Rubingh, Simon Gagné, Craig Taylor, Alan Galley, Sarah Bernauer and Darren Simms

Geological Association of Canada–Mineralogical Association of Canada Joint Annual Meeting, Winnipeg

May, 2013

Innovation, Energy and Mines

Hon. Dave Chomiak
Minister

Grant Doak
Deputy Minister

Mineral Resources Division

John Fox
Assistant Deputy Minister

Manitoba Geological Survey

C.H. Böhm
A/Director

Bailes, A., Rubingh, K., Gagné, S., Taylor, C., Galley, A., Bernaeur, S. and Simms, D. 2013: Volcanological and Structural Setting of Paleoproterozoic VMS and Gold deposits at Snow Lake, Manitoba; Geological Association of Canada–Mineralogical Association of Canada Joint Annual Meeting, Field Trip Guidebook FT-A2; Manitoba Innovation, Energy and Mines, Manitoba Geological Survey, Open File OF2013-3, 63 p.

NTS grid: 63K16

Keywords: Manitoba; Trans Hudson Orogen; Flin Flon Belt; Snow Lake; Paleoproterozoic; volcanology; VMS; altered rocks; metamorphism; Cu; Zn; Au

Author addresses:

Alan Bailes, Simon Gagné
Manitoba Geological Survey, 360-1395 Ellice Avenue, Winnipeg, Manitoba R3G 2P2

Alan Bailes
Bailes Geoscience, 6 Park Grove Drive, Winnipeg, MB, R2J 3L6

Kate Rubingh
Mineral Exploration Research Centre, Laurentian University, Sudbury, ON P3E 2C6

Craig Taylor
HudBay Minerals Inc., P.O. Box 1500, Flin Flon, MB, R8A 0A2

Alan Galley
CMIC, 2-250-155 Queens Street, Ottawa, ON

Sarah Bernauer, Darren Simms
HudBay Minerals Inc., P.O. Box 130, Snow Lake, MB, R0B 1M0

Published by:

Manitoba Innovation, Energy and Mines
Manitoba Geological Survey
360–1395 Ellice Avenue
Winnipeg, Manitoba
R3G 3P2 Canada
Telephone: (800) 223-5215 (General Enquiry)
(204) 945-4154 (Publication Sales)
Fax: (204) 945-8427
E-mail: minesinfo@gov.mb.ca
Website: manitoba.ca/minerals

This publication is available to download free of charge at manitoba.ca/minerals

Cover illustration: Quartz-feldspar-rich altered rims on pillows in Welch basalt 200 m east of north end of Stroud Lake. This zone of alteration, which characterizes the upper 300–500 m of Welch basalt, has been traced for an over 20 km strike length.

SAFETY INFORMATION

General Information

The Geological Association of Canada (GAC) recognizes that its field trips may involve hazards to the leaders and participants. It is the policy of the GAC to provide for the safety of participants during field trips, and to take every precaution, reasonable in the circumstances, to ensure that field trips are run with due regard for the safety of leaders and participants. Field trip safety is a shared responsibility. The GAC has a responsibility to take all reasonable care to provide for the safety of the participants on its field trips. Participants have a responsibility to give careful attention to safety-related matters and to conduct themselves with due regard to the safety of themselves and others while on the field trips.

Field trip participants should be aware that any geological fieldwork, including field trips, can present significant safety hazards. Foreseeable hazards of a general nature include inclement weather, slips and falls on uneven terrain, falling or rolling rock, insect bites or stings, animal encounters and flying rock from hammering. **The provision and use of appropriate personal protective equipment (e.g., rain gear, sunscreen, insect repellent, safety glasses, work gloves and sturdy boots) is the responsibility of each participant.** Each field trip vehicle will be equipped with a moderate sized first-aid kit, and the lead vehicle will carry a larger, more comprehensive kit of the type used by the Manitoba Geological Survey for remote field parties.

Participants should be prepared for the possibility of inclement weather. In Manitoba, the weather in May is highly unpredictable. The average daily temperature in Winnipeg is 12°C, with record extremes of 37°C and -11°C. North-central Manitoba (Thompson) has an average daily temperature of 7°C, with record extremes of 33°C and -18°C (*Source:* Environment Canada). Consequently, participants should be prepared for a wide range of temperature and weather conditions, and should plan to dress in layers. A full rain suit and warm sweater are essential. Gloves and a warm hat could prove invaluable if it is cold and wet, and a sunhat and sunscreen might be just as essential in the heat and sun.

Above all, field trip participants are responsible for acting in a manner that is safe for themselves and their co-participants. This responsibility includes using personal protective equipment (PPE) when necessary or when recommended by the field trip leader, or upon personal identification of a hazard requiring PPE use. It also includes informing the field trip leaders of any matters of which they have knowledge that may affect their health and safety or that of co-participants. Field Trip participants should pay close attention to instructions from the trip leaders and GAC representatives at all field trip stops. Specific dangers and precautions will be reiterated at individual localities.

Specific Hazards

Some of the stops on this field trip may require short hikes, in some cases over rough, rocky, uneven or wet terrain. Participants should be in good physical condition and accustomed to exercise. Sturdy footwear that provides ankle support is strongly recommended. Some participants may find a hiking stick a useful aid in walking safely. Steep outcrop surfaces require special care, especially after rain. Access to bush outcrops may require traverses across muddy or boggy areas; in some cases it may be necessary to cross small streams or ditches. Field trip leaders are responsible for identifying such stops and making participants aware well in advance if waterproof footwear is required. Field trip leaders will also ensure that participants do not go into areas for which their footwear is inadequate for safety. In all cases, field trip participants must stay with the group.

Other field trip stops are located adjacent to roads, some of which may be prone to fast-moving traffic. At these stops, participants should pay careful attention to oncoming traffic, which may be distracted by the field trip group. Participants should exit vehicles on the shoulder-side of the road, stay off roads when examining or photographing outcrops, and exercise extreme caution in crossing roads.

Road cuts or rock quarries also present specific hazards, and participants MUST behave appropriately for the safety of all. Participants must be aware of the danger from falling debris and should stay well back from overhanging cliffs or steep faces. Participants must stay clear of abrupt drop-offs at all times, stay with the field trip group, and follow instructions from leaders.

Participants are asked to refrain from hammering rock. It represents a significant hazard to the individual and other participants, and is in most cases unnecessary. Many stops on this field trip include outcrop with unusual features that should be preserved for future visitors. If a genuine reason exists for collecting a sample, please inform the field trip leader, and then make sure it is done safely and with concern for others, ideally after the main group has departed the outcrop.

Subsequent sections of this guidebook contain the stop descriptions and outcrop information for the field trip. In addition to the general precautions and hazards noted above, the introductions for specific localities make note of any specific safety concerns. Field trip participants must read these cautions carefully and take appropriate precautions for their own safety and the safety of others.

TABLE OF CONTENTS

Page

Safety information iii
Introduction 1
Regional geology and background 4
Regional Setting 4
Structural Evolution 4
Part 1: Volcanological and structural setting of VMS deposits in the Snow Lake arc assemblage (by Alan Bailes and Alan Galley) 5
Introduction 5
Stratigraphy 5
Anderson sequence (Primitive Arc) 5
Chisel sequence (Mature Arc) 5
Snow Creek Sequence (Rifted Arc) 9
VMS mineralization in the Snow Lake arc assemblage 9
Large synvolcanic alteration zones associated with the Snow Lake VMS deposits 9
Stop Descriptions 1 to 12: Geology and alteration features in the Chisel Lake section 11
Introduction 11
STOP 1 (UTM: 6072978N; 429289E): Welch Lake boninite, Anderson sequence 11
Introduction 11
Location A (UTM: 6072929N; 0429293E): “High-Ca boninite” 12
Location B (UTM: 6072972N; 0429281E): Contact between flows 1 and 3 12
Location C (UTM: 6072989N; 0429272E): Contact between flows 3 and 4 13
STOP 2: Silicified/feldspathized Welch Lake low-Ti basaltic andesite and andesite 13
Introduction 13
Alteration 14
Location A (UTM: 6073148N; 0429335E): Intensely silicified/feldspathized pillows, plagioclase phyric mafic flow 15
Location B (UTM: 6073143N; 0423322E): Fragments of silicified/feldspathized pillows in a heterolithologic breccia bed 15
Location C (UTM: 6073140N; 0429294E): Silicified/feldspathized pillows in aphyric mafic flow 16
Location D (UTM: 6073158; 0429250): Patches of silicification/feldspathization and epidotization in a massive aphyric flow 16
STOP 3 (UTM: 6073475N; 0428851E): Silicified/feldspathized Welch Lake basaltic andesite and Foot-Mud sulphide horizon 16
Introduction 16
Outcrop Description 17
Geochemistry of alteration 17
Relative mass change 17
Nature of hydrothermal fluids 17
STOP 4 (UTM: 06073516N; 0428973E): Stroud Lake felsic breccia 17
Introduction 17
Stop Description 19
Location A 19
Location B 20
Location C 20
Location D 20
STOP 5: Richard Lake Intrusive Complex (virtual stop) 20
Hydrothermal alteration 21

Emplacement history 21
STOP 6: Silicification/feldspathization associated with dacite dikes in the Edwards Lake formation (UTM 6074287N; 0428607E) 22
STOP 7: Alteration of the Edwards Lake mafic tuff and heterolithologic breccia: Roots of a VMS hydrothermal system 23
Location A (UTM: 426441E, 6076208N): Synvolcanic dikes intruding heterolithic mafic breccia 24
Location B (UTM: 426456E, 6076111N): Multiple episodes of dike emplacement and alteration 24
Location C (UTM: 426436E, 6076107N): Orbicular quartz-plagioclase rich domains overprinting both matrix and fragments 26
Location D (UTM: 426511E, 6076091N): Zoned alteration in breccia fragments 26
STOP 8: Highly altered Moore Lake mafic breccias (UTM: 6075801N/0427304E) 26
Location A (UTM: 6075801N; 0427304E): Silicified/feldspathized and chlorite-rich altered mafic monolithologic breccia 27
Location B (UTM: 6075801N; 0427304E): Staurolite-garnet-chlorite-biotite-rich altered rocks 27
STOP 9: Distal part of the discordant Chisel Mine footwall alteration zone (in Powderhouse dacite) 27
Location A: Relatively unaltered Powderhouse dacite UTM: 427628E/ 6076332N) 28
Location B: Altered Powderhouse dacite (UTM: 6076263N; 427748E) 28
STOP 10 (UTM: 6076471N; 0429000E): Surface expression of the Ghost Lake “mine horizon” 28
STOP 11: Threehouse mafic volcaniclastic rocks 29
Introduction 29
Location A (UTM: 6076584N; 0428868E): Large scour channel and bomb sag in mafic tuff 29
Location B (UTM: 6076580N; 0428831E): Cross bedded mafic tuff and lapilli tuff 29
Stop 12: Drill cross section, Lalor VMS deposit (virtual stop) 29
Stop Descriptions 13 to 16: Geology and hydrothermal alteration features in the Anderson Lake-Stall Lake mine area 31
Introduction 31
STOP 13: Sneath Lake Synvolcanic Intrusive Complex (UTM: 6077921N; 439143E) 32
STOP 14 (UTM: 60798509N; 438915E): Altered Anderson rhyolite adjacent to Stall alteration pipe 34
STOP 15 (UTM: 6079683N; 437009E): Anderson alteration pipe 36
STOP 16 (UTM: 6079347N; 439327E): Hangingwall alteration above Stall Lake VMS mine 36
Location A (UTM: 6079365N; 439290E): Relatively unaltered Welch Lake pillowed basaltic andesite 36
Location B (UTM: 6079445N; 439240E): Strongly silicified/albitized Welch Lake pillowed basaltic andesite 37
Location C (UTM: 6079383N; 439429E): Contact between Anderson and Upper Chisel sequences 37
Part 2: Stratigraphy, structure and orogenic lode gold mineralization within the McLeod Road-Birch Lake thrust panel (by Kate Rubingh and Simon Gagné) 38
Introduction 38
Stratigraphy 38
Description of stratigraphic units 38
Unit 1: Mafic volcaniclastic rocks 38
Unit 2: Felsic volcaniclastic rocks 38
Unit 3: Heterolithic felsic volcaniclastic rocks 38
Unit 4: Felsic volcanic and volcaniclastic rocks 38
Unit 5: Mafic volcanic and volcaniclastic rocks 39
Unit 6: Felsic volcanic rocks 39
Unit 7: Mafic volcanic and volcaniclastic rocks 39
Structural geology 40
Mineralization 41
Stop descriptions 17 to 22: Structural Features in Post-Accretion Sedimentary Rocks 41
STOP 17 (UTM NAD 83 – 0 434 760 mE, 6 080 710 mN: Burntwood Group, Snow Lake 43
STOP 18 (UTM NAD 83 – 0 434 781 mE, 6 080 953 mN): Burntwood Group, Snow Lake 43

STOP 19 (UTM NAD 83 – 0 434 929 mE, 6 081 099 mN): Burntwood Group, Snow Lake 44
STOP 20 (UTM NAD 83– 0 434 924 mE, 6 081 255 mN): Burntwood Group, Crystal View Park 45
STOP 21 (UTM NAD 83 – 0 434 355 mE, 6 081 614 mN): Corley Lake member of the Burntwood Group 45
STOP 22 (UTM: 6081670 N; 0434365 E): McLeod Road Thrust (MRT); examination of the contact between the Burntwood Group and the volcanics of the MB panel 45
Introduction 45
Stop Description 47
Stop Descriptions 23 to 26: Structural relationships observed in the volcanic rocks of the MB panel and the implications for the setting of gold mineralization 47
Introduction 47
STOP 23 (UTM: 6082438N; 0433614E) Howe Sound Fault 47
Introduction 47
Stop Description 47
STOP 24 (UTM: 6083561N; 0433511E): Boundary zone 50
Introduction 50
Outcrop Description 50
STOP 25 (UTM: 6084071N; 0433238E): The No. 3 zone 52
Introduction 52
Location A 53
Location B 53
STOP 26 (UTM: 6084810N; 0432097E): McLeod Road Thrust 53
Introduction 53
Outcrop Description 53
Part 3: Geological Setting of the Au-rich Lalor Lake Zn-Cu VMS mine (by Alan Bailes, Craig Taylor, Sarah Bernauer and Darren Simms) 57
Introduction 57
Deposit history 57
References 59

FIGURES

Figure 1: Location of the Flin Flon Belt(FF) in northern Manitoba and Saskatchewan 1
Figure 2: Simplified geology of the central and eastern portions of the Flin Flon Belt showing major tectonostratigraphic assemblages and plutons, and locations of mined VMS deposits 3
Figure 3: Bivariate plot of gold grade versus tonnage for VMS deposits from Mercier-Langevin et al. (2011). Data are shown for 513 deposits worldwide (dataset modified from Franklin et al. 2005). 4
Figure 4: Plan view of the 1.89 Ga Anderson sequence, Chisel sequence and Snow Creek sequence components of the Snow Lake arc assemblage. 6
Figure 5: Simplified geological map of the Snow Lake area. 7
Figure 6: Schematic stratigraphic cross sections (not to scale) depicting the interpreted chronology of geological and hydrothermal events that controlled formation of the large regional-scale alteration zones at Snow Lake. 8
Figure 7: Simplified geology map showing the distribution of altered rocks within the Snow Lake arc assemblage 10
Figure 8: Location of field trip stops on a schematic stratigraphic section showing setting of VMS deposits in the ca. 1.89 Ga Snow Lake arc assemblage. 12
Figure 9: Location of field trip stops on a schematic cross section illustrating discordant, subconcordant and semi-conformable zones of alteration developed within strata of the Snow Lake arc assemblage. 13
Figure 10: Geological map of the Snow Lake area showing the locations of all whole-rock samples analyzed for oxygen isotopes and the regional oxygen isotope zoning based after Taylor and Timbal (1998). 14
Figure 11: Series of boninite and boninite-like flows in the Welch formation of the Anderson sequence. 15

Figure 12: Series of pillowed and massive Welch low-Ti basalt flows showing varying degrees of silicification/albitization 16
Figure 13: Map of outcrop at Stop 3 detailing various types of alteration (from Surka, 2001). 18
Figure 14: Schematic cross section through the Chisel sequence.... 19
Figure 15: Stratigraphic section of Stroud felsic breccia exposed at Stop 4. 21
Figure 16: Geology of the Richard Lake Intrusive Complex (RLIC) and b) "cartoon" showing possible stages (1-3) in evolution of the RLIC. 22
Figure 17: Sketch of two dacite dikes at Stop 6 that display flow banded margins and have silica-feldspar rich alteration domains developed in the adjacent mafic tuff.... 23
Figure 18: Outcrop maps of Edwards formation volcaniclastic rocks that were altered within the high temperature hydrothermal reservoir 1.5 to 2 km below the Chisel-North Chisel-Lalor VMS deposits 25
Figure 19: Plan view of the distribution of rock units hosting the Chisel, Lost and Ghost lakes VMS deposits. 28
Figure 20: Sketch of outcrop at Stop 11 showing well-bedded Threehouse mafic volcaniclastic rocks with numerous primary features. 30
Figure 21: Vertical cross section (looking west) showing the Chisel and Chisel North VMS deposits (modified from Galley et al., 1993).... 30
Figure 22: Vertical section of the geology on S5200N based on re-logging of drill holes by Bailes (2008, 2009).. 31
Figure 23: a) Generalized geology of the Anderson sequence, which hosts the Anderson, Stall, Rod and Linda VMS deposits 33
Figure 24: Reconstruction of the Anderson rhyolite in cross section to illustrate the different flow units and the position of the VMS deposits and major base metal sulphide occurrences.... 34
Figure 25: Cartoon illustrating the evolution of the Sneath Lake intrusive complex in relation to the development of the Anderson-Stall hydrothermal system within the Anderson sequence.... 35
Figure 26: Sketch of outcrop at Stop 16, Location C 37
Figure 27: Simplified geological map of the McLeod Road-Birch Lake thrust panel.... 39
Figure 28: Simplified "stratigraphic" column for the McLeod Road-Birch Lake thrust panel. 40
Figure 29: Two layer model illustrating the modification of S2 during F2 and F3 from Kraus and Wiliams (1994b). 42
Figure 30: Sketch map showing the inferred MRT contact between the Burntwood Group metasedimentary rocks and the metavolcanic rocks of the McLeod Road-Birch Lake (MB) panel at Stop 22. 44
Figure 31: a) S2 fabric in the Burntwood Group overprinting the S0/S1 fabric; b) S2 fabric in the Burntwood Group is folded and the S3 fabric is axial planar to the Z asymmetric folds.... 46
Figure 32: Outcrop map of the Toots zone at Stop 23 modified from (Galley et al., 1991) 48
Figure 33: Simplified map to show the regional fabric relationships of the Howe Sound Fault and the MRT 49
Figure 34: Sketch to show the S-C fabric which represents a potential splay of the MRT 50
Figure 35: Outcrop map of the Boundary zone at Stop 24 51
Figure 36: Sketch to show the sinistral shear fracture at the Boundary Zone. 51
Figure 37: Sketch to show the fabric relationships at the No.3 Zone portal.... 52
Figure 38: a) F1 folds with an axial planar fabric and S3 axial planar cleavage to small tight folds, b) S2 cleavage overprints iron carbonate vein. 54
Figure 39: Sketch of features on outcrop at Stop 26, Location C.... 55
Figure 40: Deep EM anomalies from gound geophysics over the Chisel Lake-Photo Lake-Lalor Lake property.... 56
Figure 41: Proposed Lalor Mine development plan (December 2010) in cross section.... 58
Figure 42: Major geological units encountered in drill core projected onto S5200N (Bailes, 2012) at the Lalor Lake mine along with the distribution of rocks with Hashimoto Indices >90.... 58
Figure 43: The distribution of rocks with a chlorite-carbonate-pyrite index (CCPI) >90 on S5200N.... 59

TABLES

Table 1: Producing and past producing VMS mines of the Flin Flon Domain.... 2
Table 2: Comparison of deformational events identified by various authors in the McLeod Road-Birch Lake thrust panel 41

Introduction

The Flin Flon Belt (FFB; Lucas et al., 1996) consists of Paleoproterozoic volcanic, plutonic and minor sedimentary rocks within the juvenile internal zone of the Trans-Hudson Orogen (**Figure 1**). Flin Flon volcanic rocks are exposed in an easterly trending 250 km long by 75 km wide belt that is tectonically bounded to the north by the gneissic metasedimentary, metavolcanic and plutonic rocks (Kisseynew domain,KD) and concealed to the south by Phanerozoic platformal cover rocks. The apparent easterly trend of the FFB is an artifact of its tectonic contact to the north with the KD and the easterly trace of overlapping Phanerozoic cover rocks to the south. The internal subdomains in the FFB and, in fact, the FFB itself trend to the south-southwest, with the FFB continuing for hundreds of kilometres to the south beneath Phanerozoic cover.

The FFB is composed of structurally juxtaposed volcanic and sedimentary assemblages that were emplaced in a variety of tectonic environments (Lucas et al., 1996; Syme et al., 1999). The major 1.92–1.88 Ga components include areally significant juvenile arc and juvenile ocean-floor rocks, and minor ocean plateau/ocean island basalt (Stern et al., 1995a,b; Syme et al., 1999). The juvenile arc assemblage comprises tholeiitic, calc-alkaline and lesser shoshonitic and boninitic rocks similar in major and trace element geochemistry to modern intraoceanic arcs (Stern et al., 1995a). Ocean-floor basalt sequences are exclusively tholeiitic, and are geochemically similar to modern N- and E-type MORBs erupted in back-arc basins (Stern et al., 1995b). Evolved arc assemblages and Archean crustal slices are present within the FFB as minor components.

Collectively, these tectonostratigraphic assemblages were juxtaposed in an accretionary complex at ca. 1.88–1.87 Ga, presumably as a result of arc-arc collisions. The collage was basement to 1.87–1.83 Ga post-accretion arc magmatism, expressed as voluminous calc-alkaline plutons and rarely preserved calc-alkaline to alkaline volcanic rocks. Unroofing of the accretionary collage and deposition of continental alluvial-fluvial sedimentary rocks (Missi Group) and marine turbidites (Burntwood Group) occurred ca. 1.85–1.84 Ga, coeval with the waning stages of post-accretion arc magmatism. The sedimentary suites were imbricated with volcanic assemblages in the eastern FFB during 1.85–1.82 Ga juxtaposition of the supracrustal rocks along pre-peak metamorphic structures. Post ca. 1.83 Ga structures formed the present southwest-verging fold style at the northeastern end of the FFB.

The FFB is one of the premier volcanogenic massive sulphide (VMS) districts in the world with 29 developed deposits containing over 176 Mt. of sulphide ore (**Table 1**). Most of the

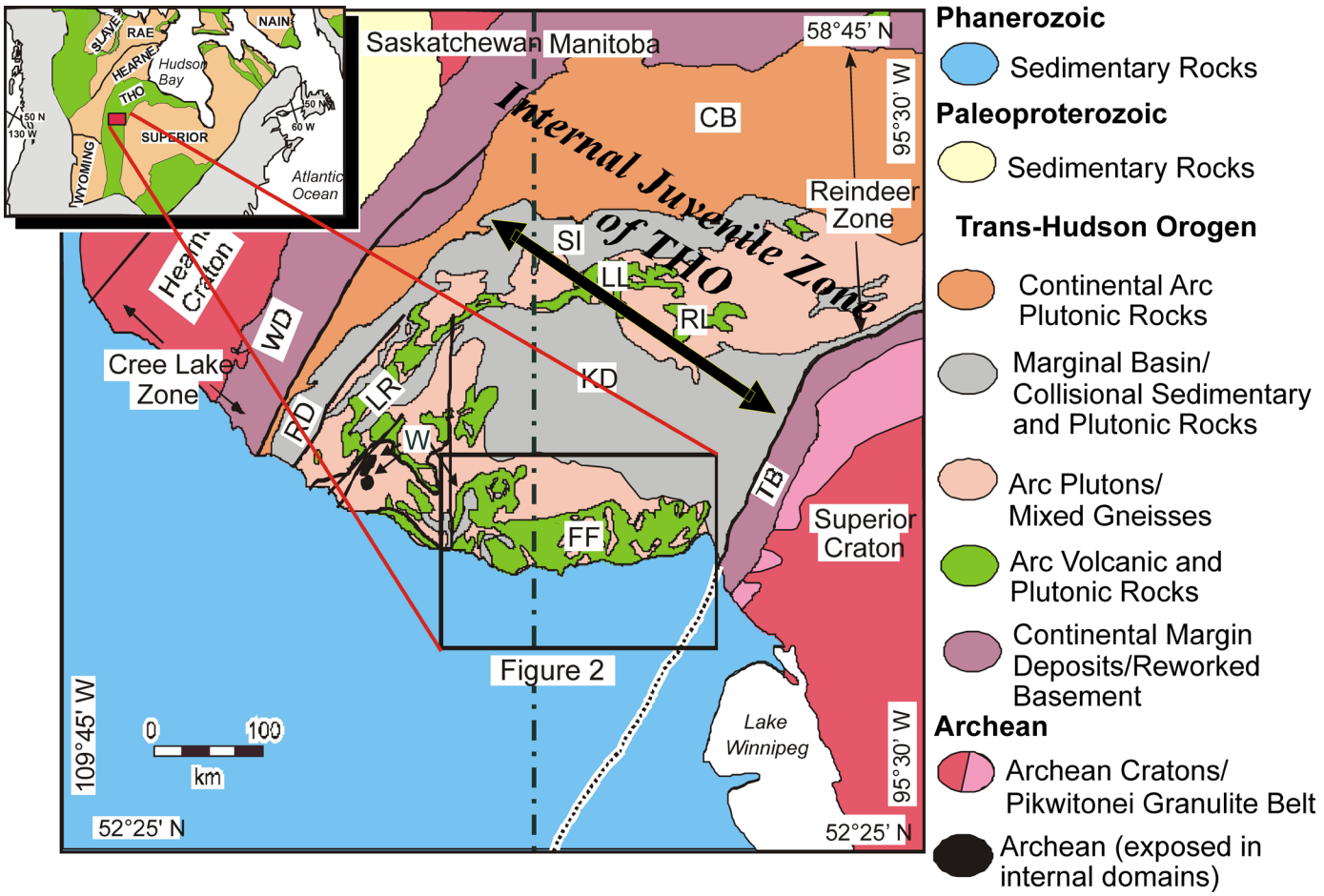

Figure 1: *Location of the Flin Flon Belt (FF) in northern Manitoba and Saskatchewan. Other greenstone belts in the juvenile core (Reindeer Zone) of the Trans-Hudson orogen (THO) are Lynn Lake (LL), Rusty Lake (RL) and La Ronge (LR). Also shown are the Chipewyan batholith belt (CB), Southern Indian domain (SI), Kisseynew domain (KD), Wollaston domain (WD), the Thompson nickel belt (TB) and structural windows of Sask craton (W). The inset diagram shows the location of Figure 2 (red rectangle) relative to major Archean cratons and Paleoproterozoic Orogens in North America after Hoffman (1988). Figure after Lucas et al. (1996).*

Table 1: Producing and past-producing VMS mines of the Flin Flon Belt. Producing mines include remaining resource; Lalor Lake includes the inferred resource. Resource estimates are not 43-101 compliant. In the Snow Lake area the Photo Lake and Lalor Lake deposits are gold-rich by the criteria of Mercier-Langevin et al. (2011).

Mine	Tonnes	Au g/t	Ag g/t	Cu %	Zn %	Discovered	Method
Mandy	125000	3.02	60.15	8.22	11.38	1915	Prospecting
Flin Flon	62485362	2.72	41.28	2.21	4.11	1915	Prospecting
Sherridon	7739471	0.63	18.96	2.37	2.28	1922	Prospecting
Dickstone	1077462	1.56	9.49	3.91	2.15	1935	Prospecting
Cuprus	462094	1.3	28.8	3.25	6.4	1941	Prospecting
Birch Lake	272898	0.1	4.11	6.21	0	1950	Prospecting
Schist Lake	1846656	1.3	37.03	4.3	7.27	1947	Geological
Don Jon	79329	0.96	15.09	3.09	0.01	1950	Geophysics
North Star	241691	0.34	0.57	6.11	0	1950	Geophysics
Flexar	305937	1.3	6.51	3.76	0.5	1952	Geophysics
Coronation	1281719	2.06	5.14	4.25	0.24	1953	Geophysics
Osborne	2807471	0. 27	4. 11	3. 14	1.5	1953	Prospecting
Chisel	7153532	1.76	44.76	0.54	10.6	1956	Geophysics
Stall	6381129	1.41	12.34	4.41	0.5	1956	Geophysics
Ghost & Lost	581438	1.2	39.09	1.34	8.6	1956	Geophysics
Anderson	2510000	0.62	7.54	3.4	0.1	1963	Geophysics
White Lake	849784	0.72	27.1	1.98	4.64	1963	Geophysics
Centennial	2366000	1.51	26.4	1.56	2.2	1969	Geophysics
Rod	735219	1.71	16.11	6.63	2.9	1970	Geological
Westarm	1394149	1.56	17.49	3.21	1.48	1973	Geophysics
Spruce Point	1865095	1.68	19.54	2.06	2.4	1973	Geophysics
Trout Lake	21612296	1.56	16.02	1.74	4.97	1976	Geophysics
Hanson Lake	147332	1.09	137.14	0.51	9.99	1984	Geophysics
Callinan	7773725	2.06	24.63	1.36	4	1984	Geological
Chisel North	2606 212	0. 58	21. 43	0. 21	9. 49	1985	Geological
777	21903539	2.12	26.94	2.59	4.39	1993	Geological
Konuto	1645691	1.99	8.91	4.2	1.63	1994	Geophysics
Photo Lake	689885	4.9	29.38	4.58	6.35	1995	Geophysics
Lalor Lake Zn-Cu	18100000	0.64	25.24	0.64	8.97	2007	Geophysics
Lalor Lake Cu-Au	5400000	4.7	30.6	0.47	0.46	2007	Geophysics
Reed Lake	2720000	0.62	7.63	4.5	0.89	2007	Geophysics

mined VMS deposits in the Flin Flon Belt are hosted by 1.89 Ga juvenile oceanic arc volcanic rocks at Flin Flon and Snow Lake, located near the west-central and eastern end of FFB respectively (**Figure 1** and **Figure 2**). Most gold mineralization in the FFB is associated with late brittle-ductile shear zones formed after peak tectonic and metamorphic activity within the Trans-Hudson Orogen. At Snow Lake, however, preliminary investigations suggest a long history of gold mineralization, with at least some gold introduced prior to metamorphism. The largest orogenic lode gold deposit (1.4 million oz Au production between 1949–1958 and 1996–2006) in the Trans Hudson Orogen is the Snow Lake mine, located just north of the town of Snow Lake.

Flin Flon Belt VMS deposits have high metal contents, with many of them displaying exceptionally high Au content (**Figure 3**; **Table 1**). The Flin Flon deposit, which contained an average 2.64 g/t Au for a total of 165 tonnes (Hannington et al., 1999), is second only to the Horne deposit in Canada for amount of gold contained in a VMS deposit. In the Snow Lake area, both the Photo Lake and Lalor Lake deposits are gold-rich (>3.46g/t; **Table 1**).

The principal objectives of the field trip are to:

1. Place the Snow Lake VMS and gold deposits in the context of the tectonic and magmatic evolution of the eastern portion of the Flin Flon Domain.
2. Introduce the stratigraphy, lithofacies and structural elements of the VMS and lode-gold hosting portions of the Snow Lake region.
3. Examine three regional-scale alteration zones of which two are a product of VMS-producing hydrothermal activity.
4. Illustrate the effects of metamorphic recrystallization of VMS-associated alteration zones to almandine-amphibolite facies mineral assemblages.
5. Demonstrate the role of fold- and thrust-events in the Snow Lake area in localizing lode gold mineralization.

The field trip is divided into 3 parts with each presented separately. Part 1 deals with the Snow Lake Arc Assemblage, and concentrates on the stratigraphic setting and synvolcanic hydrothermal alteration in this VMS-rich volcanic sequence. Part 2 deals with the stratigraphic and structural setting of orogenic lode gold mineralization in the McLeod Road-Birch lake allochthon. Part 3 deals with the underground mine tour of the Lalor Lake Zn-Cu gold-rich VMS deposit.

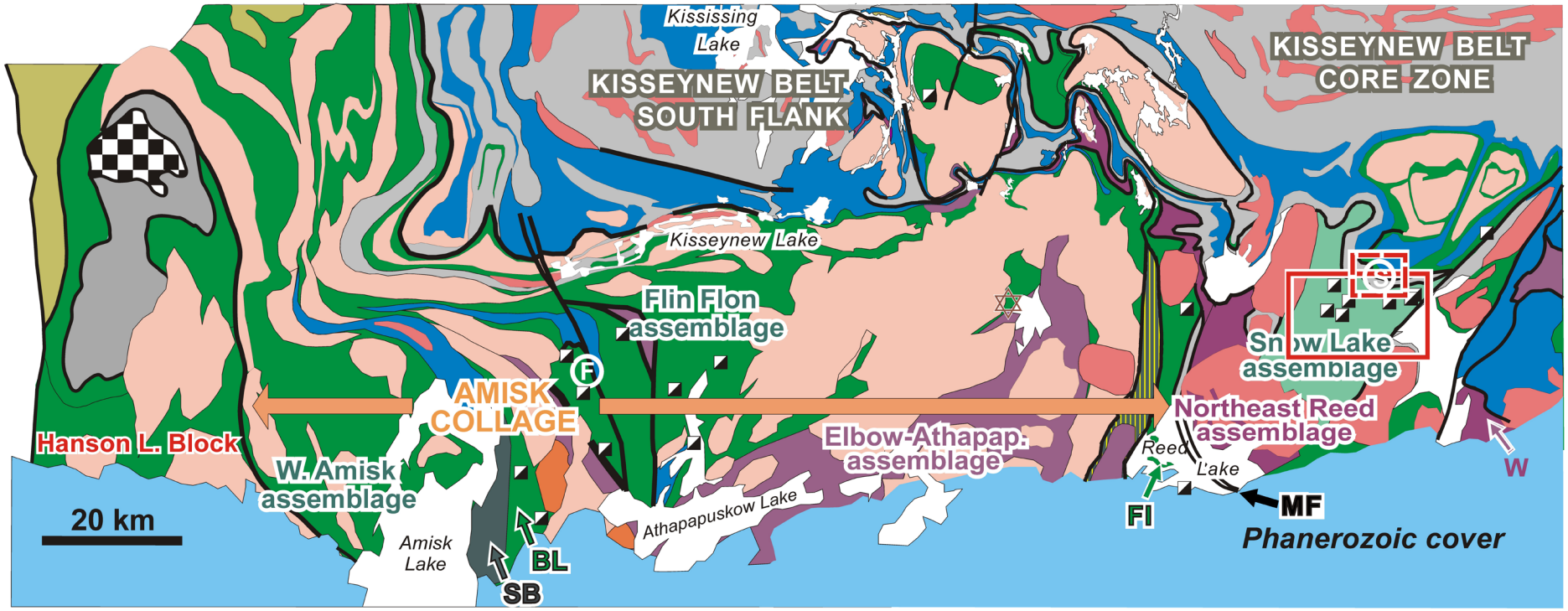

Figure 2: *Simplified geology of the central and eastern portions of the Flin Flon Belt showing major tectonostratigraphic assemblages and plutons, and locations of mined VMS deposits. F: Flin Flon, S: Snow Lake. The Snow Lake area is characterized by a structural style and by lithologies that are more comparable to the Kisseynew domain than those in the Amisk Collage of the central Flin Flon Belt. The Snow Lake area consists of a series of allochthons of 1.89 Ga volcanic and 1.85–1.83 Ga sedimentary rocks soled by the Morton Lake fault zone (MF; Syme et al. 1995). The red rectangle shows the area depicted in* ***Figure 4****. The smaller dashed rectangle shows the area depicted in* ***Figure 27****.*

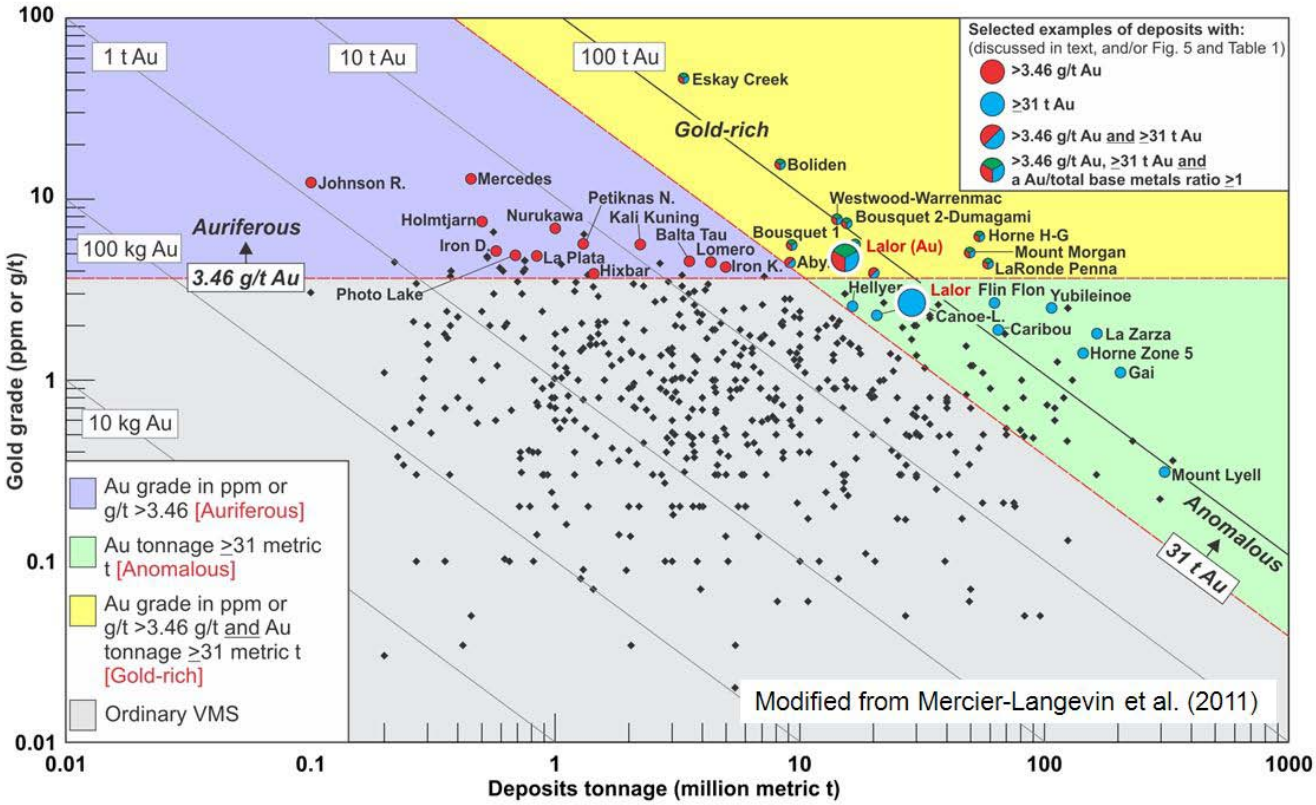

Figure 3: *Bivariate plot of gold grade versus tonnage for VMS deposits from Mercier-Langevin et al. (2011). Data are shown for 513 deposits worldwide (dataset modified from Franklin et al. 2005).*

Regional geology and background

Regional Setting

The Flin Flon Belt comprises, from east to west, the Snow Lake-Kisseynew fold-thrust subdomain (informal term), the Amisk Collage and the Hanson Lake Block (**Figure 2**), all amalgamated during ca. 1.87–1.85 Ga intraoceanic accretion and subsequent 1.84–1.81 terminal collision in the THO (Lewry and Collerson 1990; Lucas et al. 1996). The Flin Flon Belt is preserved in fold-repeated and thrust-stacked tectonostratigraphic assemblages, which structurally overlie the Archean to earliest-Paleoproterozoic Sask Craton (Ashton et al. 2005).

The Snow Lake-Kisseynew subdomain, situated between the east end of the Amisk Collage and the Superior Craton (**Figure 1** and **Figure 2**), is dominated by 1.84–1.81 Ga fold-thrust–style tectonics and by southwest-verging allochthons of volcanic rocks (e.g., Snow Lake arc assemblage, Northeast Reed assemblage). It likely followed an independent evolution from the remainder of the Flin Flon Belt prior to 1.84–1.81Ga terminal collision (Stern et al., 1992; Percival et al., 2006; Corrigan et al., 2007). This area includes a diverse sequence of deformed and metamorphosed volcanic, sedimentary and intrusive rocks, and contains 9 of the FFB's 29 base metal mines. These include 8 past-producers and the Lalor Lake mine discovered in 2007. Production at the Lalor Lake mine began in 2012.

Structural evolution

Numerous detailed structural studies carried out in the Flin Flon Belt (e.g., Syme et al., 1995; Connors, 1996; Lucas et al., 1996; Ansdell et al., 1999; Connors et al., 1999; Lafrance, in press) have identified deformation events spanning early accretion (1.88–1.87 Ga) to late tectonic continental collisions (1.83–1.77 Ga). Deformation events that accompanied the pre–1.85 Ga tectonic accretion and amalgamation have yet to be recognized in the Snow Lake-Kisseynew fold and thrust belt, probably due to overprinting by subsequent deformation and metamorphism. The oldest recognized structures (D_1) in the area, which are best developed in successor arc supracrustal units such as the Burntwood Group sedimentary rocks , are <1.84 Ga in age. Four deformation events have been recognized (D_1–D_4; Kraus and Williams, 1999). The first two (D_1 and D_2) are interpreted to result from the southwest tectonic transport of Burntwood Group greywacke turbidite from the Kisseynew Domain over the Flin Flon Belt (Kraus and Williams, 1999). Both the D_1 and D_2 events are characterized by tight isoclinal folding and associated low-angle 'thrust' faults (e.g., McLeod Road Thrust). The D_3 event is interpreted to result from northwest-southeast transpressional shortening that accompanied syn– to post–peak regional metamorphism (Connors et al., 1999). It is largely manifest by upright, open to closed F_3 folds (e.g., Threehouse Lake synform) and associated, steeply dipping faults (e.g., Berry Creek Fault). The D_4 structures are east-trending open upright folds that overprint F_3 folds (Connors, 1996; Kraus and Williams, 1999).

Both D_1 and D_2 faults typically define contacts between lithotectonic assemblages and are curvilinear due to subsequent folding, partly during D_3 deformation. The Snow Lake arc assemblage (Stern et al., 1995b; Lucas et al., 1996) cores a large, map-scale allochthon that is expressed in the Snow Lake

arc assemblage as a doubly plunging F_2 antiform (Anderson Bay antiform). The F_1 folds and D_1 thrust faults are bracketed in age by crosscutting 1.84–1.83 Ga (David et al., 1996) granitic plutons and the youngest 1.84 Ga detrital zircon (Machado et al., 1999) in the Burntwood Group greywacke. Fold structures belonging to D_2 were originally identified by Kraus and Williams (1999) at Snow Lake, but can also be demonstrated to occur locally in Burntwood Group sedimentary rocks on Wekusko Lake. Both Connors et al. (1999) and Kraus and Williams (1999) indicated that D_2 deformation, similar to the earlier D_1 deformation, involves low-angle 'thrust' faults.

Deformation structures belonging to D_3 are ubiquitous in the eastern Flin Flon Domain. In the Snow Lake area, they are mainly manifest as east-northeast–trending, open F_3 folds (e.g., Threehouse synform), which are syn- to post-peak regional metamorphism (ca. 1.81 Ga; David et al., 1996). Other manifestations of D_3 deformation are S_3 foliations, which are axial planar to the folds. The crescentic configuration of the McLeod Road Thrust and F_{1-2} folds at Snow Lake is a product of broad folding during D_3 deformation.

Part 1: Volcanological and structural setting of VMS deposits in the Snow Lake arc assemblage (by Alan Bailes and Alan Galley)

Introduction

The volcanogenic massive sulphide (VMS) deposits at Snow Lake occur in an approximately 6 km thick succession (**Figure 4** and **Figure 5**) of volcanic rocks (Snow Lake arc assemblage) that records, in its stratigraphy and geochemistry, a temporal evolution in geodynamic setting from a 'primitive arc' (Anderson sequence), to a 'mature arc' (Chisel sequence) and then to an 'arc-rift' (Snow Creek sequence). The VMS-hosting Anderson and Chisel sequences contain evidence of intra-arc rifting. In the Anderson sequence, this includes the combination of boninite, low-Ti basalt and isotopically juvenile rhyolite flows, an association of rock types that has been attributed (Bailes and Galley, 1999) in both modern and Phanerozoic arcs to high-temperature hydrous melting of refractory mantle sources in an extensional and/or proto-arc environment. Rifting in the Chisel sequence is indicated by indirect criteria that includes voluminous volcaniclastic detritus; prominent synvolcanic dike sets; and the local presence of highly fractionated, differentiated magma series. The VMS deposits in both sequences are spatially associated with juvenile rhyolite complexes, synvolcanic intrusive rocks (dominated by two large trondhjemitic bodies) and extensive areas of rocks that underwent hydrothermal alteration. Schematic stratigraphic cross sections (not to scale) which depict the interpreted chronology of geological and hydrothermal events that controlled formation of alteration zones and VMS at Snow Lake are depicted in **Figure 6**.

Stratigraphy

Anderson sequence (primitive arc)

The Anderson sequence is a compositionally bimodal geochemically primitive arc sequence dominated by the Welch basalt/basaltic andesite, which contains at least three rhyolite flow complexes, and is intruded by the subvolcanic Sneath Lake tonalite-trondhjemite intrusive complex (**Figure 4** and **Figure 5**). The >3 km of Welch formation consists of subaqueous low-Ti tholeiitic basalt to andesite flows, and a subunit of high-Ca boninite (Stern et al., 1995a). High-Ca boninite is relatively rare in modern settings, having only been identified within the northern end of the Tongan forearc (Falloon et al., 1992) and in the upper Pillow Lavas of the Cretaceous Troodos ophiolite (Duncan and Green, 1987). On the basis of the high-Ca boninite and low-Ti basalt association, Stern et al. (1995a) suggest that the Anderson sequence formed in a nascent arc tectonic setting.

The mafic volcanic succession contains three discrete rhyolite flow complexes, known from west to east as the Daly, Sneath and Anderson (**Figure 4** and **Figure 5**). Each consists of a series of massive and lobe and hyaloclastite flows. Like the host mafic volcanics, the rhyolite complexes contain little evidence for interflow volcaniclastic or epiclastic units. The Anderson rhyolite complex is the largest, extending approximately 8 km in strike length and 2 km in thickness. Both it and the Daly rhyolite complex consist of a number of texturally distinct flows.

Both mafic and felsic flows of the Anderson sequence are intruded by the 22 km long by 2 km thick Sneath Lake tonalite-trondhjemite subvolcanic intrusive complex (**Figure 4** and **Figure 5**). The Anderson and Daly rhyolites lie directly above the composite intrusion near its two ends (**Figure 6a** and **Figure 6b**). The various trondhjemite phases are compositionally similar to the rhyolites. Its subvolcanic nature is further reinforced by the presence of large cobbles of trondhjemite intercalated with Anderson rhyolite flows and within the overlying Stroud rhyolite of the Chisel sequence.

The last rock type within the Anderson sequence is a 1–5 m thick, finely layered, sulfidic, mixed argillite, epiclastic-chert unit known as the "Foot-Mud Horizon" (**Figure 4**, **Figure 5** and **Figure 6b**). This sedimentary unit appears similar in origin to exhalites described in other Precambrian VMS camps, including the "C" Contact tuff in Noranda (Kalogeropoulos and Scott, 1989) and the Key Tuffite at Mattagami Lake (Liaghat and MacLean, 1992). The Foot-Mud Horizon extends along the top of the primitive bimodal sequence for the entire strike length of the underlying Sneath Lake Intrusive Complex (SLIC).

Chisel sequence (mature arc)

The transition from the Anderson to the Chisel sequences is characterized by an abrupt change from a chemically bimodal succession dominated by subaqueous mafic flows to a chemically diverse succession dominated by units of heterolithic volcaniclastic detritus. It is also marked by distinctive changes in geochemical character of associated mafic flows. The Chisel

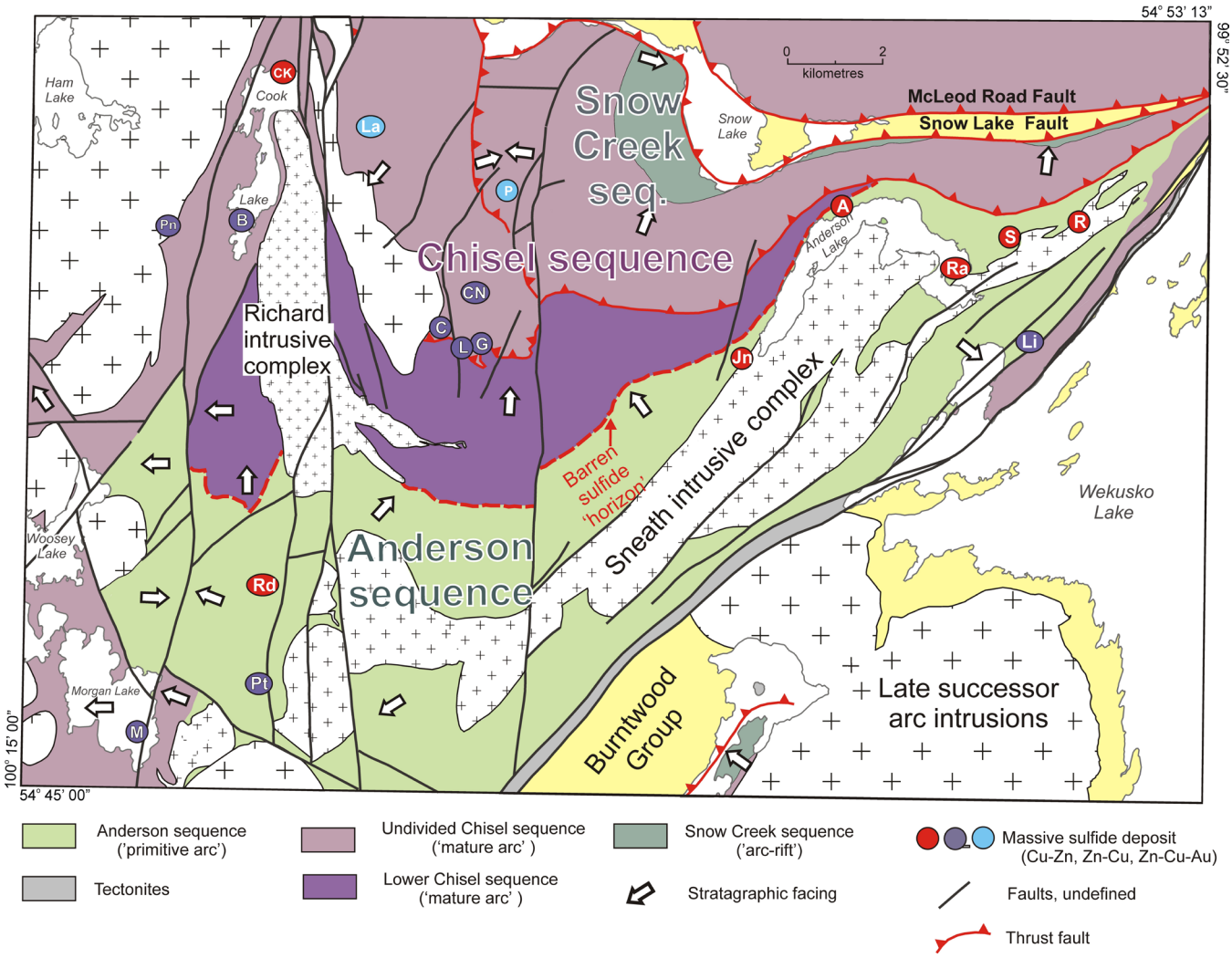

Figure 4: *Plan view of the 1.89 Ga Anderson sequence, Chisel sequence and Snow Creek sequence components of the Snow Lake arc assemblage. Arrows show facing direction of supracrustal rocks. Also shown are ca. 1.84–1.83 Ga successor arc sedimentary and intrusive rocks, ca. 1.84 Ga thrust faults (red, teeth on hangingwall) and ca. 1.78 Ga normal faults (solid black lines). Coloured circles and ellipses show distribution of VMS deposits: A, Anderson Lake; B, Bomber; C, Chisel Lake; CK, Cook Lake; CN, Chisel North; G, Ghost Lake; Jn, Joannie zone; L, Lost Lake; La, Lalor Lake; Li, Linda; M, Morgan Lake; P, Photo Lake; Pn, Pen zone; Pt, Pot Lake; R, Rod; Ra, Ram zone; Rd, Raindrop; S, Stall Lake. The barren sulphide 'horizon' (locally known as the Foot-Mud horizon) is a sulphide-bearing, fine-grained, volcaniclastic unit located at the contact between the Anderson (primitive arc) and Chisel (mature arc) sequences.*

mafic flows typically have higher Th/Nb, Th/Yb and La/Yb ratios and lower ε_{Nd} values (0 to +2.7) than do those in the underlying Anderson sequence (+3; Stern et al., 1992; Bailes and Galley, 1999). Stern et al. (1992) suggested that the Chisel magmas were affected by within-plate enrichment, derivation from a more fertile mantle source, lower average extents of melting at greater depths, and/or contamination from older crustal fragments. Intracrustal contamination during Chisel magma genesis is supported by the presence of an inherited zircon population with ages of 2650–2824 Ma in the 1892 Ma Stroud breccia (David et al., 1996).

Chisel sequence units (**Figure 5** and **Figure 6**) are typically thin (compared to the Anderson sequence) and discontinuous, display rapid lateral facies variations and include a large volume of volcaniclastic material. The high proportion of volcaniclastic rocks (40–50%) in the Chisel section suggest that considerable topographic relief was developed, possibly as a result of intra-arc extension, rifting and caldera development.

The Chisel sequence, >3 km thick, is subdivided into lower and upper parts (**Figure 4**). The contact between these subdivisions coincides with a break, initially interpreted to be a hiatus in volcanism (Bailes and Galley, 2007) but now interpreted to be a thrust fault (Bailes et al., 2009). Chisel sequence rocks of uncertain stratigraphic position (likely part of a hanging wall to the thrust fault) occur northwest of Chisel Lake and west of the Richard Lake Intrusive Complex (RLIC).

The Chisel sequence is cut by a wide variety of intrusive rocks, ranging from dikes less than a metre across to large plutons several kilometres in diameter. Most of these intrusions are demonstrably synvolcanic, and many can be clearly related to specific extrusive equivalents. Two groups of synvolcanic intrusions are recognized: one of these feeds Lower Chisel

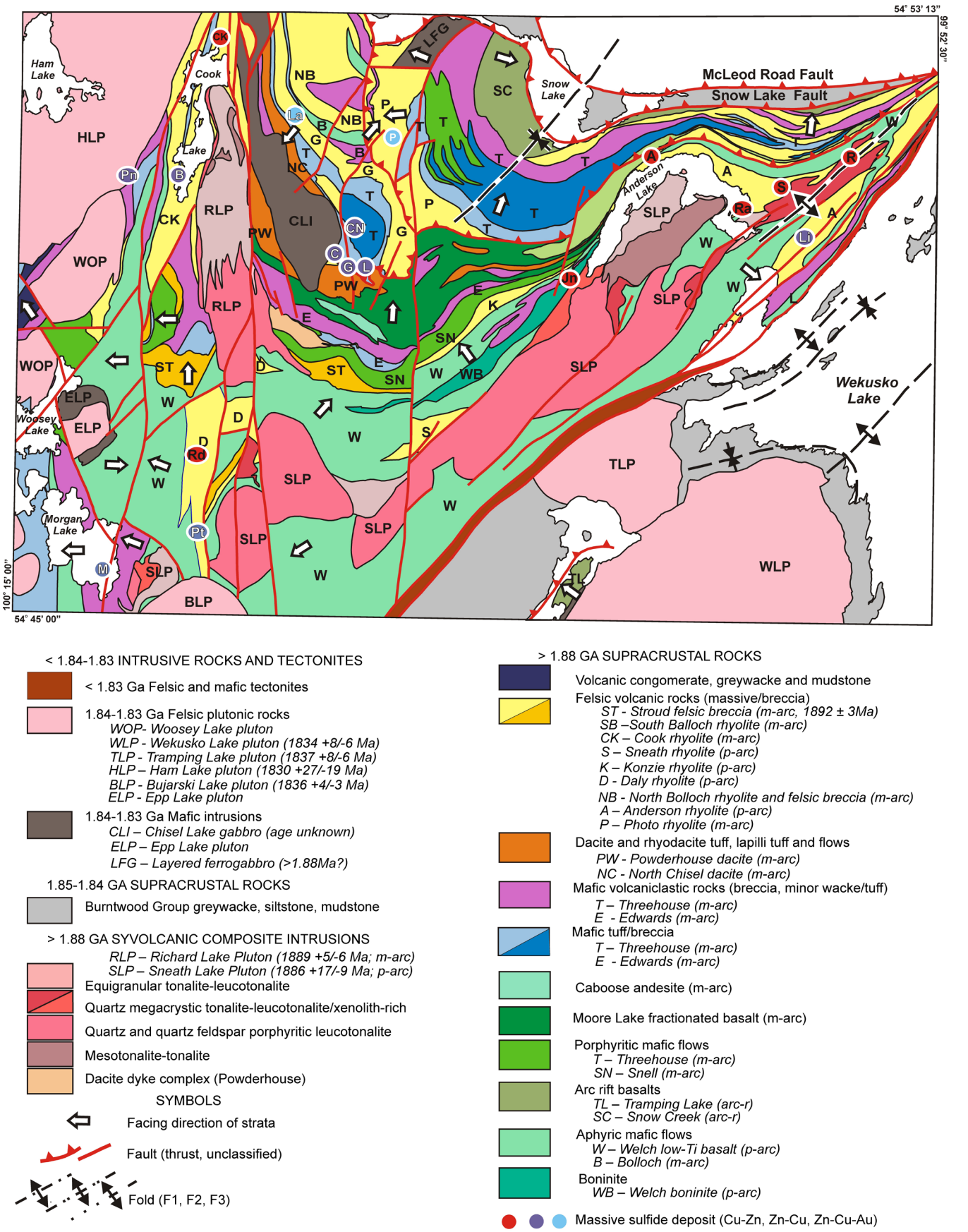

Figure 5: *Simplified geological map of the Snow Lake area. Letters indicate informal names of units (identified in legend). The designations after the unit name (e.g., p-arc) in the legend indicate which sequence it belongs to: p-arc for Anderson sequence, m-arc for Chisel sequence and arc-r for Snow Creek sequence. VMS deposit names and designations are the same as those given in the caption for* ***Figure 4****.*

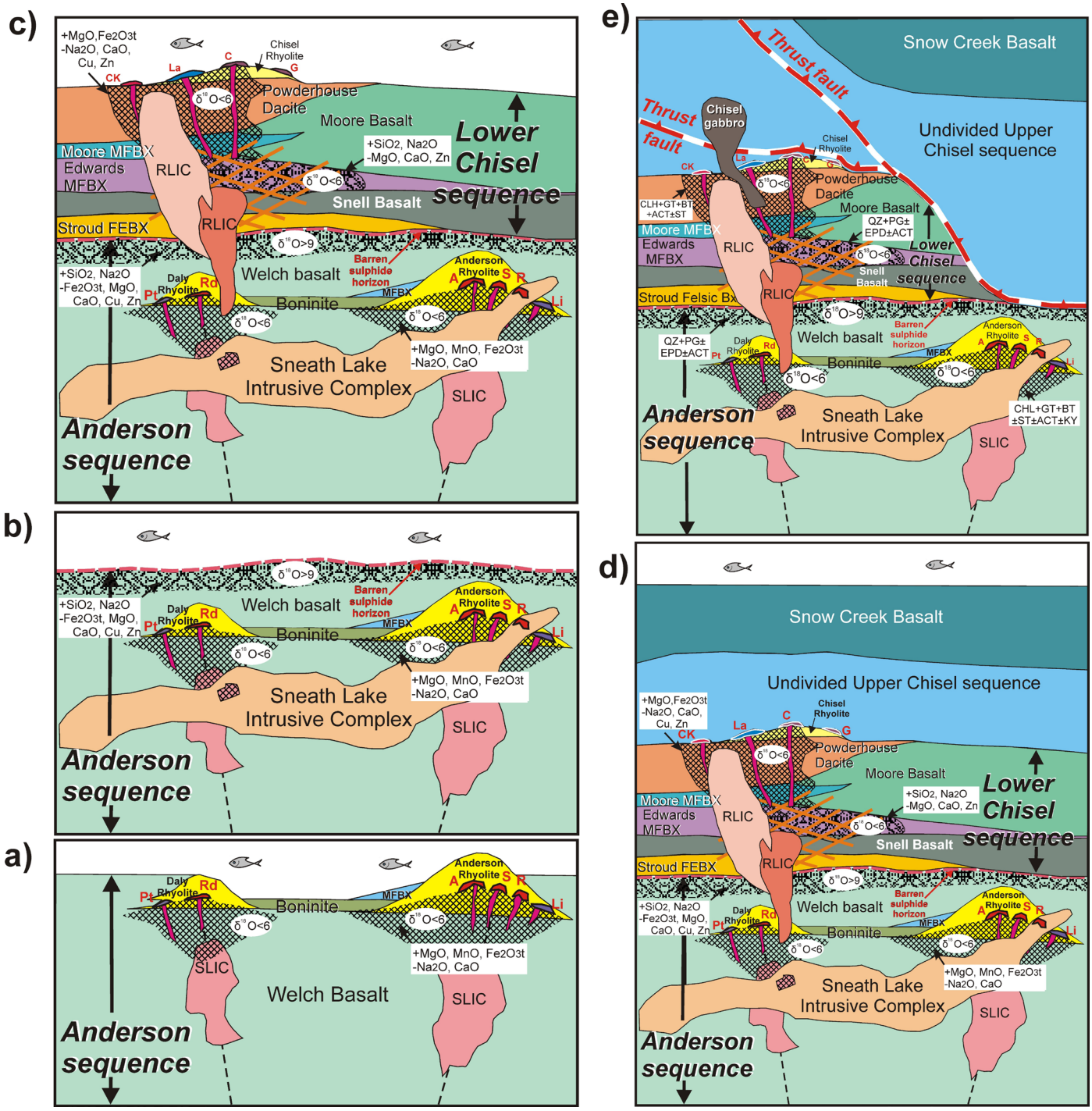

Figure 6: *Schematic stratigraphic cross sections (not to scale) depicting the interpreted chronology of geological and hydrothermal events that controlled formation of the large regional-scale alteration zones at Snow Lake (from Bailes et al., in press).* **(a)** *1.89 Ga extrusion of low Ti basalts and associated bonninites (Welch), emplacement of early phases of the SLIC, extrusion of co-genetic rhyolite complexes (Anderson, Daly), >350º hydrothermal activity and formation of Cu-rich VMS deposits.* **(b)** *Continued mafic volcanism (Welch), emplacement of late phases of the SLIC, diffuse and waning <250ºC hydrothermal activity at sea floor, and formation of a regional barren sulphide unit.* **(c)** *Debris flow deposition of volcaniclastic units (Stroud, Edwards), extrusion of basalt flows (Snell), emplacement of synvolcanic dikes and plutons (includes early phases of RLIC), extrusion of co-genetic basalt (Moore) and felsic flows (Powderhouse, Chisel), >350ºC hydrothermal activity (shallow water?, boiling?) and formation of Zn-rich auriferous VMS deposits.* **(d)** *1.89 Ga emplacement of late phases of RLIC, extrusion of undivided Upper Chisel sequence volcanic rocks, and extrusion of back arc-arc rift Snow Creek basalts.* **(e)** *1.84-1.835 Ga thrust and fold deformation, 1.835-1.815 Ga emplacement of Chisel Lake gabbro, and 1.815 Ga regional metamorphism that recrystallized altered rocks to middle almandine-amphibolite facies mineral assemblages. Note that the 1.89 Ga RLIC intrudes across the contact between the Anderson and Chisel sequences supporting the interpretation of this being a structurally intact, depositional contact.*

volcanism and the other is related to Upper Chisel volcanism. The abundant (locally up to 50% by volume) synvolcanic dikes support the hypothesis that rifting and caldera development accompanied accumulation of the Chisel sequence.

Snow Creek sequence (rifted arc)

The debris flows of the upper part of the Chisel sequence are abruptly overlain by a thick succession of massive to pillowed basalt flows and associated basalt sills. This monotonous flow succession contains very little interflow hyaloclastite or flow breccia, suggesting very rapid deposition. The MORB-like lithogeochemistry of these flows suggests they represent the rifting of the Snow Lake arc assemblage and development of back-arc ocean-floor (**Figure 6**). Another interpretation is that the Snow Creek sequence is unrelated to the Chisel sequence with a thrust fault marking their contact.

VMS mineralization in the Snow Lake arc assemblage

The VMS deposits in the Snow Lake arc assemblage can be subdivided into two distinct groups: Cu-Zn-rich (Cu-Zn) and Zn-Cu-rich (Zn-Cu and Zn-Cu-Au) types. The Cu-Zn-rich deposits occur principally in the Anderson sequence and the Zn-Cu and Zn-Cu-Au rich deposits occur in the Chisel sequence.

Cu-Zn-rich deposits and occurrences in the Anderson sequence (**Figure 5**) are confined almost entirely to within the Anderson and Daly rhyolite complexes. All of the developed deposits are within the larger Anderson rhyolite. The Anderson, Stall and Rod orebodies contained an aggregate 10.1 million tonnes of ore with an average grade of 4.15% Cu, 0.53% Zn, and averaged 1.5 g/t Au (Bailes and Galley, 1996). This rhyolite complex also hosts the uneconomic 13 Mt Linda deposit grading 0.3% Cu and 0.79% Zn (Inmet Inc., pers. comm., 1992), and the small uneconomic, Cu-rich stockwork-type Joannie and Ram zones. The Daly rhyolite hosts the Raindrop zone grading 3.52% Cu and 0.82 % Zn over 8.36 m (Hodges and Manojlovic, 1993), as well as the Pot deposit grading 1.43% Cu and 4.5% Zn over 2.1 m (HBED, pers. comm., 1972) (**Figure 5**). The integral role played by the SLIC in VMS generation is most clearly evident in the Anderson Lake area where there is a steady increase in both intensity of alteration of supracrustal rocks and of the Cu/Zn ratio (Cu/Cu+Zn) of contained VMS deposits, from 27 (Linda) to 97 (Anderson Lake), as distance to the pluton decreases. The latter is interpreted to result from higher temperature for pluton-proximal portions of the regional synvolcanic hydrothermal system (Bailes and Galley, 1996). The Photo Lake VMS deposit is a Cu-Zn-Au massive sulphide mineralization within the upper Chisel sequence. It occurs within a thick section of rhyolite (Bailes and Simms, 1994). The current interpretation is that the Photo Lake VMS deposit occurs in the hangingwall structural panel to the Chisel-Lalor VMS system and is part of a separate VMS forming event (Bailes et al., 2009).

Five Zn-rich VMS deposits are located in the Chisel sequence, approximately 2 km stratigraphically above its base. They occur near the contact between the Lower and Upper parts of the Chisel sequence. Chisel Lake, Chisel North, Lost Lake and Ghost Lake deposits contained an aggregate 10.6 Mt (production plus reserves) grading 0.42% Cu and 10.06% Zn, and 30–60 g/t Ag and 0.4–1.7 g/t Au. The Lalor Lake deposit, the only currently operating mine in the Snow Lake area, contains 18.1 Mt of Zn-Cu ore grading 0.7% Cu, 8.97% Zn, 34 g/t Ag and 2.87 g/t Au, with an additional inferred Cu-Au resource of 5.4 million tonnes grading 0.46% Zn, 0.47% Cu, 4.7g/tonne Au and 30.6g/tonne Ag (HBED, March, 2010). All five deposits overlie the Powderhouse dacite and local discrete rhyolite flow complexes, where they appear to have originally formed blanket-like accumulations whose high aspect ratios are now obscured by polyphase folding. These deposits are characterized by remnants of dolomite. The association of carbonate with these Zn-Pb-Cu-Ag VMS deposits is a characteristic of several Paleoproterozoic massive sulphide camps, including parts of the Bergslagen and Skellefte districts of Sweden, the VMS deposits of northern Wisconsin, and the Errington and Vermilion deposits within the Sudbury Basin (Galley, 1996; Galley and Ames, 1998). A combination of overprinting high temperature hydrothermal activity and later regional metamorphism recrystallization of the dolomitic material has converted them to coarse-grained calc-silicate assemblages similar to those commonly displayed by magmatic skarn deposits (Galley and Ames, 1998).

Large synvolcanic alteration zones associated with the Snow Lake VMS deposits

The volcanic sequences of the Snow Lake arc assemblage contain prominent zones of alteration that affect approximately 15% (16 km^2) of the volcanic strata and associated synvolcanic intrusions (**Figure 7**). These alteration zones, which were formed by synvolcanic hydrothermal activity, were subsequently recrystallized during a 1.81 Ga regional metamorphic episode and can be readily recognized by their unique metamorphic mineral assemblages. Centimetre-scale, euhedral crystals of chlorite, phlogopitic biotite, amphibole, muscovite, garnet and staurolite are common metamorphic minerals within the recrystallized semi-conformable alteration zones. Large-scale alteration zones at Snow Lake, which are typically subparallel to host stratigraphy, are up to 20 km in strike length and 0.8 km wide. For comparison, recrystallized discordant alteration zones, which are substantially smaller (0.4 km^2 or <0.3%) in area, may cut across up to 1.5 km of stratigraphy and are frequently characterized by coarse-grained aluminosilicate minerals such as kyanite.

Large-scale semi-conformable alteration zones at Snow Lake vary considerably in their metamorphic mineral assemblages, but can be divided into two types: “regional semi-conformable” and “subconcordant”. The “regional semi-conformable” zones form up to 6% of the supracrustal volcanic rocks, have significant lateral extent and continuity, and display a bleached appearance due to the replacement of mafic groundmass minerals by feldspar, epidote and/or quartz (**Figure 7**). They are mineralogically and morphologically similar to “regional semi-conformable” alteration zones discussed in the literature by Gibson et al. (1983), Hannington et al. (2003) and Franklin et al. (2005). The “subconcordant” zones form up to 9% of the supracrustal volcanic rocks and are characterized

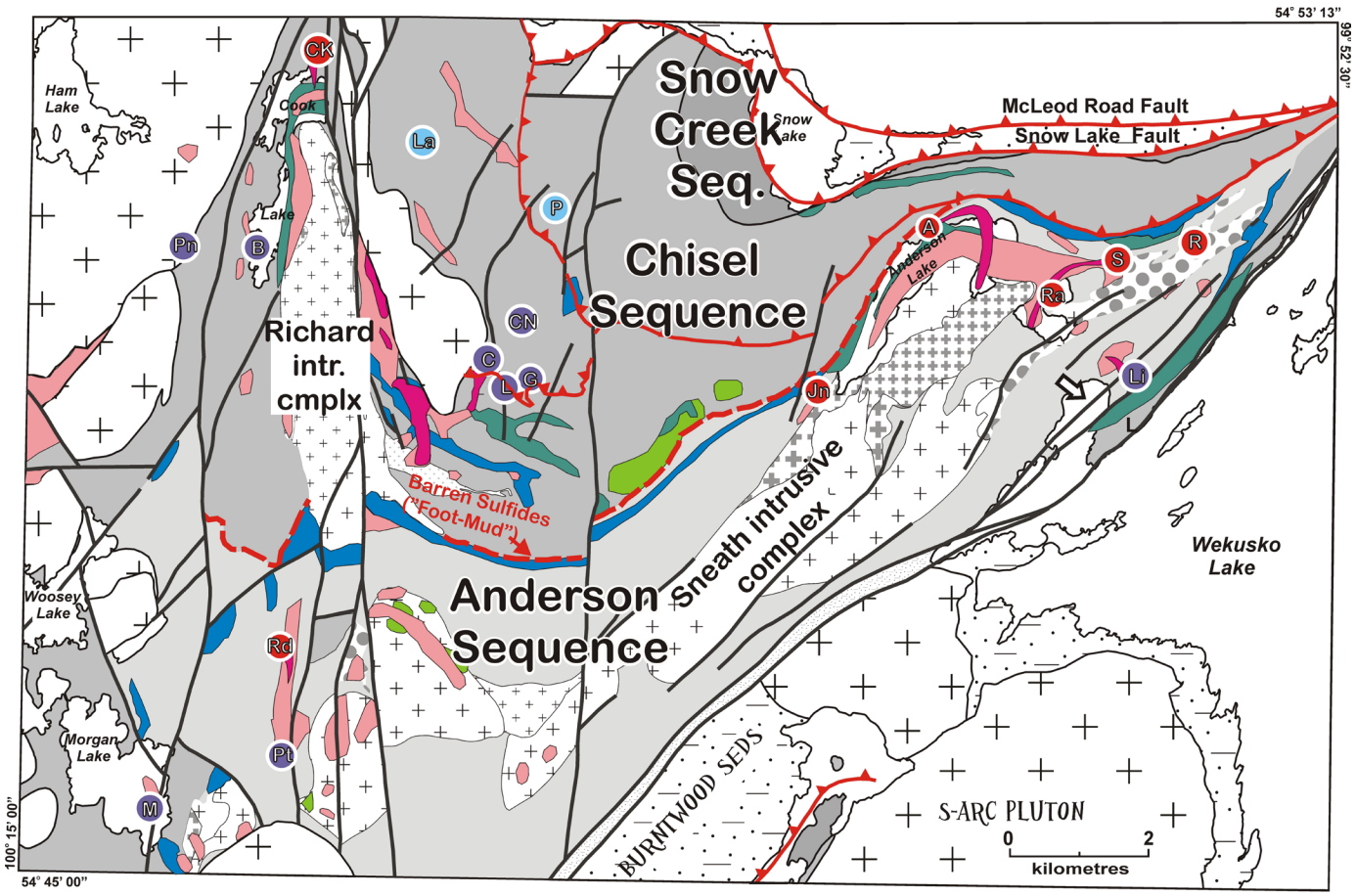

ALTERED ROCKS (METAMORPHOSED AT 1.82-1.81 GA)

Discordant zones

Completely altered rocks (mineral assemblages depend on protolith)

Subconcordant zones

Chlorite+garnet+biotite-rich rocks ± staurolite ± actinolite

Regional semi-conformable zones

Amphibole-rich rocks ± garnet

Epidote-rich rocks

Quartz+plagioclase-rich rocks ± epidote ± actinolite (derived from a mafic protolith)

> 1.88 GA SYNVOLCANIC INTRUSIVE ROCKS

Quartz megacrystic tonalite/xenolith-rich

Quartz feldspar porphyry

Equigranular leucotonalite

Hornblende tonalite – mesotonalite

Dacite dyke complex (Powderhouse)

> 1.88 GA SUPRACRUSTAL ROCKS

Snow Creek Seq. (arc rift) supracrustals

Chisel Seq. (mature arc) supracrustals

Anderson Seq. (primitive arc) supracrustals

ROCKS POSTDATING ALTERATION

< 1.84-1.83 Intrusive rocks

1.85-1.84 Ga Burntwood Group greywacke

SYMBOLS

Fault (thrust, unclassified)

VMS deposit (Cu-Zn, Zn-Cu, Zn-Cu-Au)

Figure 7: *Simplified geology map showing the distribution of altered rocks. The altered rocks, which formed during 1.89 Ga synvolcanic hydrothermal activity, contain unique metamophic mineral assemblages that reflect 1.81 Ga regional metamorphism to middle amphibolite facies mineral assemblages. The altered rocks comprise 15–20% of the volcanic rocks and synvolcanic intrusions exposed in the Snow Lake area.*

by 20–50% groundmass chlorite, biotite, and/or sericite with up to 2 cm porphyroblasts of garnet, staurolite, kyanite and/or amphibole (**Figure 7**). Although the subconcordant zones display considerable lateral continuity (over 7 kilometers strike length and 10:1 length to width ratios), they commonly merge with and share the chemical attributes and mineral assemblages of discordant alteration zones. At Snow Lake the large-scale "subconcordant" zones have been variably referred to as an alteration "apron" (Hodges and Manojlovic, 1993) and "lower conformable" zone (Walford and Franklin, 1982).

Three periods of robust hydrothermal activity are identified within the Snow Lake arc assemblage (Bailes and Galley, 1996). The first, and oldest, hydrothermal event (**Figure 6a**) is focused within the Anderson and Daly felsic extrusive complexes, and is interpreted to be genetically related to formation of the Anderson, Stall and Rod Cu-Zn VMS deposits in the former complex, and the Raindrop and Pot Lake base metal occurrences in the latter. This hydrothermal activity also affected the underlying SLIC, where it is manifest, most typically, as 'fracture-controlled' zones of alteration. These are interpreted to result from 'collapse' of the hydrothermal system into the subvolcanic intrusion as it cooled. The alteration caused by this hydrothermal activity includes both sub-conformable, 3–5 km long and as much as 1000 m in total thickness, and discordant alteration zones that commonly terminate upsection at known VMS deposits and occurrences. These alteration zones are truncated by a late phase of the SLIC, which is considered evidence of the coeval nature of the volcanism, alteration and plutonism.

The second hydrothermal event took place at the end of Anderson sequence volcanism. This hydrothermal activity resulted in a semi-conformable zone of silica and epidote addition in the Welch basalt at the top of the Anderson sequence (**Figure 4**, **Figure 6** and **Figure 7**). A 300–500 m thick zone of alteration was produced directly underlying the 'Foot-Mud tuff-exhalite' at the top of the Anderson sequence. Both the alteration and the Foot-Mud exhalite have the same strike length as the underlying SLIC.

The third hydrothermal event is located within Lower Chisel volcanic rocks (**Figure 4**, **Figure 6** and **Figure 7**) and is spatially associated with Lower Chisel intrusive rocks, in particular dikes of the Powderhouse dacite and early phases of the Richard Lake intrusive complex. Resultant alteration by the hydrothermal fluids, which is largely confined to the Edwards mafic volcaniclastic rocks, is interpreted to be synvolcanic and related to generation of VMS deposits, as it only affects strata underlying the Chisel–Chisel North–Ghost–Lost-Lalor VMS horizon.

Stop descriptions 1 to 12: geology and alteration features in the Chisel Lake section

Introduction

Stops 1 to 12 begins in the upper part of the Anderson sequence and ends at the mine-hosting portion of the Chisel sequence (**Figure 8** and **Figure 9**). Although the stops will emphasize features produced by the footwall hydrothermal alteration system below the Chisel area VMS deposits, a number of the stops will be of unaltered rocks with the objective of presenting the stratigraphic and tectonic setting of the VMS deposits. Two stops will be virtual stops to describe and discuss features that are too remote to examine on this trip. The extent of hydrothermal alteration within this section of the mature arc has been defined both mineralogically (**Figure 7**) and isotopically (**Figure 10**).

At Stops 1 to 3 we will examine low-Ti tholeiite basalts and boninite flows, which characterize the Anderson primitive arc sequence, as well as a prominent zone of seafloor, semi-conformable feldspathization/silicification that affects the upper 500 m of this succession (**Figure 9**). Stops 4 to 9, which are typically within the volcaniclastic units which dominate the Chisel mature arc sequence, present the relationship between subvolcanic intrusions, sub-seafloor hydrothermal activity and alteration in these permeable rock formations. At Stops 10 and 11 we will examine the host stratigraphy of the Lost Lake and Ghost Lake VMS deposits and present evidence for a thrust along the contact between the Lower and Upper Chisel sequences.

To get to Stop 5, from the town of Snow Lake, head south on highway 392 and turn right on provincial road 395 (approximately 2.1 km south of town). Follow provincial highway 395 to the past-producing Chisel Lake mine. From the minesite follow the abandoned rail bed 1.2 km to the south and then follow a short trail/road to the east to join up with the Edwards Lake trail/road. Follow the Edwards Lake road 2.6 km to the south and park vehicle at UTM 429295E/ 6072985N.

STOP 1 (UTM: 6072978N; 429289E; UTM zone 14, NAD 83[1]): Welch Lake boninite, Anderson sequence

Introduction

At Stop 1 (**Figure 8** and **Figure 9**) three well preserved north-facing mafic flows (**Figure 11**), which outcrop directly west of the road, will be examined. The lowermost flow displays the chemical characteristics of a high-Ca boninite (Stern et al., 1995a; Bailes and Galley, 1999), and the overlying two flows display boninite-like lithogeochemistry (*e.g.* higher MgO, Ni and Cr values than most tholeiitic rocks at Snow Lake).

The high-Ca boninites at Snow Lake are intimately associated with low-Ti tholeiitic basalts and isotopically juvenile felsic rhyolite. This rock association has been interpreted in both the modern (Beccaluva and Serri, 1988; Crawford et al. 1989) and Phanerozoic (Swinden 1996) to be a product of high temperature, hydrous partial melting of refractory mantle sources in proto-arc environments during arc extension. According to Crawford et al. (1989), boninitic and refractory magmas are a reflection of zones of extremely high heat flow because, to form, they require high heat of fusion. This rock association has been linked with VMS deposits (Swinden 1996) possibly reflecting a common genetic affiliation with zones of high heat flow, rifting and attendant increase in fluid circulation and geothermal activity (Bailes and Galley, 1999, and references therein).

[1] All UTM references in this guidebook are UTM Zone 14, NAD 83.

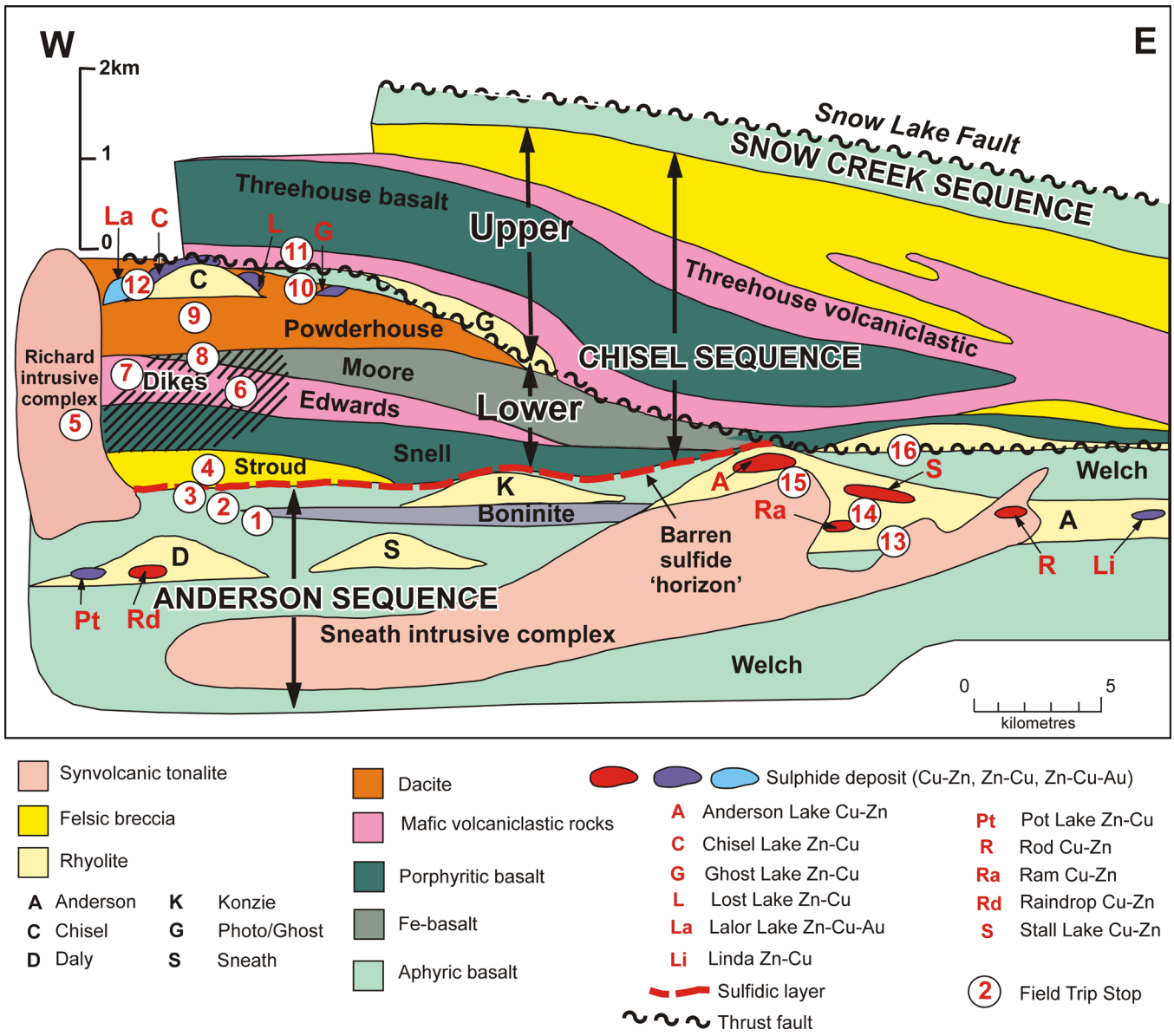

Figure 8: *Location of field trip stops on a schematic stratigraphic section showing setting of VMS deposits in the eastern two thirds of the ca. 1.89 Ga Snow Lake arc assemblage. Note the spatial association of deposits with rhyolite complexes (names of rhyolite complexes indicated by letters). The Sneath Lake and Richard Lake plutons are intrusive complexes that include several phases, with younger phases (shown in Figure 6 but not shown separately in this diagram) intruding VMS-hosting rhyolites and alteration zones. For example, a late phase of the Sneath Lake intrusive complex has intruded and enveloped the Rod VMS deposit (R). The U-Pb zircon age for the Sneath Lake pluton is poorly constrained (1886 +17/-9 Ma; David et al. 1996) and only indicates the subvolcanic nature of the pluton and not an actual age relative to the younger Stroud Lake felsic breccia (1892 ± 3 Ma; David et al. 1996) and subvolcanic Richard Lake pluton (1889 +8/-6 Ma; Bailes et al. , 1988, 1991). Note vertical exaggeration due to differing horizontal and vertical scales.*

Location A (UTM: 6072929N; 429293E): "High-Ca boninite"

The "high-Ca boninite" (flow 1) is over 35 m thick, aphyric, pillowed, and has a distinctive pale pistachio green weathering colour. Pillows are blocky, display narrow (<5 cm) selvages, are 30-80 cm in diameter, contain 10-15% quartz and carbonate amygdales (0.5-3 mm), and are surrounded by light tan coloured, recrystallized interpillow hyaloclastite. A 1 m wide synvolcanic porphyritic mafic dike, which intrudes between but never across pillows, is texturally identical to the overlying flow 3.

Location B (UTM: 6072972N; 429281E): Contact between flows 1 and 3

The contact between flow 1 and 3 is covered by a narrow (<0.5 m wide) gully. The upper 4 m of flow 1 displays higher vesicularity and thicker domains of interpillow hyaloclastite than at location A. Flow 3 is easily distinguished from flow 1 by its pyroxene (pseudomorphed by amphibole)-plagioclase phyric character, medium to dark grey green weathering colour, and smoothly curving pillow morphologies. Pillows in flow 3 are locally imbricated consistent with flow transport from southwest to northeast (present geographic coordinates). Pil-

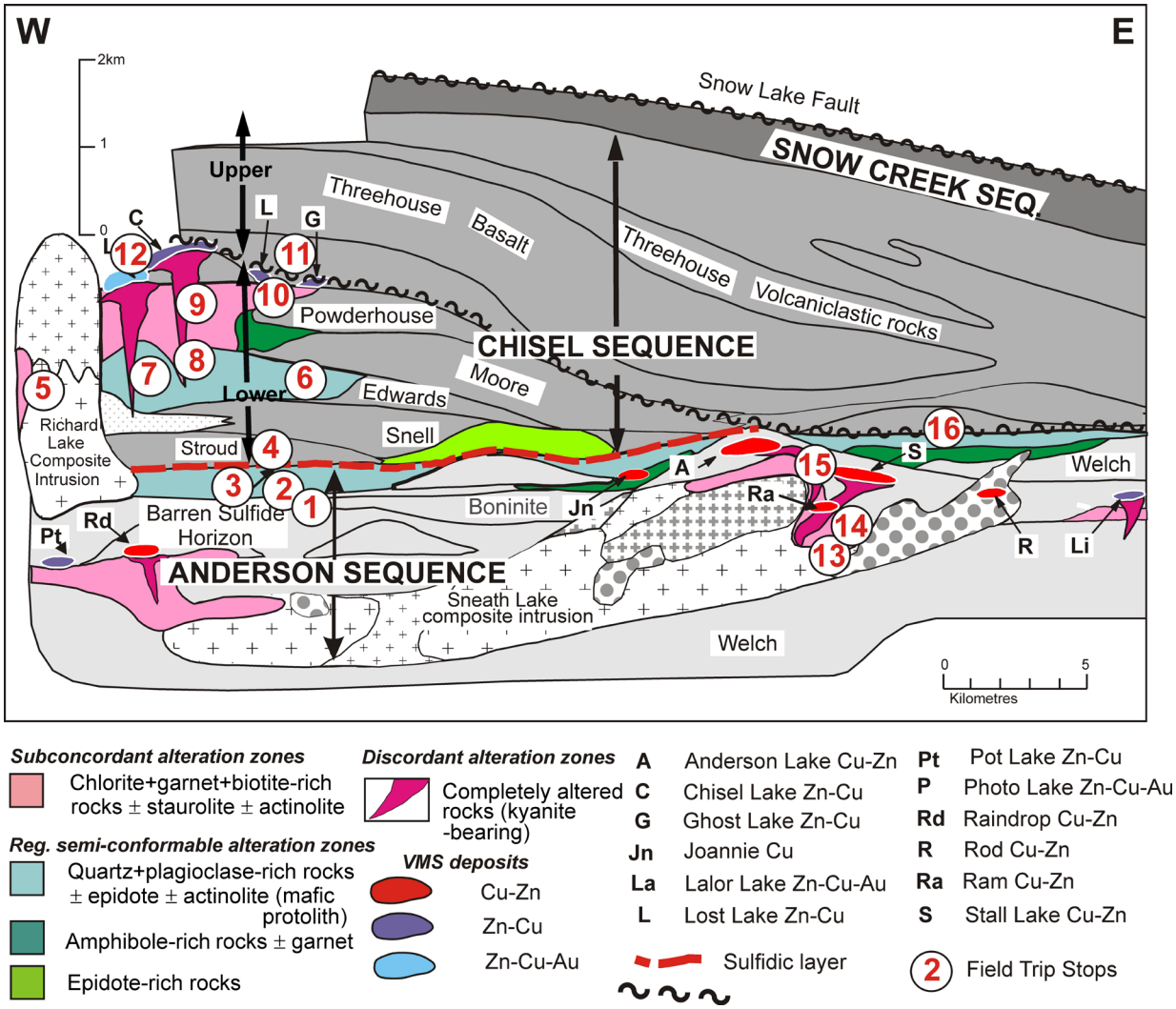

Figure 9: *Location of field trip stops on a schematic cross section illustrating discordant, subconcordant and semi-conformable zones of alteration developed within strata of the eastern two thirds of the Snow Lake arc assemblage. Note thrust fault between Lower and Upper parts of the Chisel Sequence as documented by Bailes et al. (2009). Note the prominent discordant zones of alteration stratigraphically beneath the Anderson Lake (A), Stall Lake (S), Linda (L), Raindrop (Rd), Chisel Lake (C) and Lalor Lake (La) VMS deposits.*

lows in flow 3 display narrow selvages and up to 1 cm of rusty weathering interpillow hyaloclastite. Pillow size is relatively constant from bottom to top of this 5 m thick flow. Southwest of location B, flows 1 and 3 are separated by up to 6 m of laminated mafic scoria tuff and lapilli tuff which includes a narrow porphyritic pillowed flow that is locally only one pillow thick.

Location C (UTM: 6072989N; 429272E): Contact between flows 3 and 4

Flows 3 and 4 are separated by a 0.3–3 m unit of mafic scoria tuff and lapilli tuff that displays both reverse and normal size grading, and, in one locality, current lamination; the latter indicates the same southwest to northeast component of transport as the pillow imbrication in flow 3. The tuff/lapilli tuff contains local accessory clasts that are identical to the underlying flow. Flow 4 is similar in textural and composition to flow 3, but has a slightly lower phenocryst population than flow 3 and contains 1-3% quartz-filled radial pipe vesicles (up to 5 cm in length) that are not observed in flow 3.

Turn vehicle around and set odometer to zero. Proceed north on road to 0.25 km. Follow trail to east of road to access filed trip outcrops.

STOP 2: Silicified/feldspathized Welch Lake low-Ti basaltic andesite and andesite

Introduction

Low-Ti arc tholeiites of the Welch Lake suite form a >3 km thick sequence that dominates the Anderson sequence (Figure 8). They display high contents of large ion lithophile elements (LIL; e.g. Rb, Ba, Th, Sr), low contents of high field strength elements (HFSE; e.g. Hf, Ti, Zr, Y), and very low Ni and Cr relative to N-MORB; these features characterize subduction-related magmas (Gill, 1981; Tarney et al., 1981) formed within modern oceanic arc tectonic settings. The Welch Lake arc tholeiites display flat to slightly LREE depleted patterns, similar to those displayed by the boninitic flows but with higher overall REE values (3–10X chondrite).

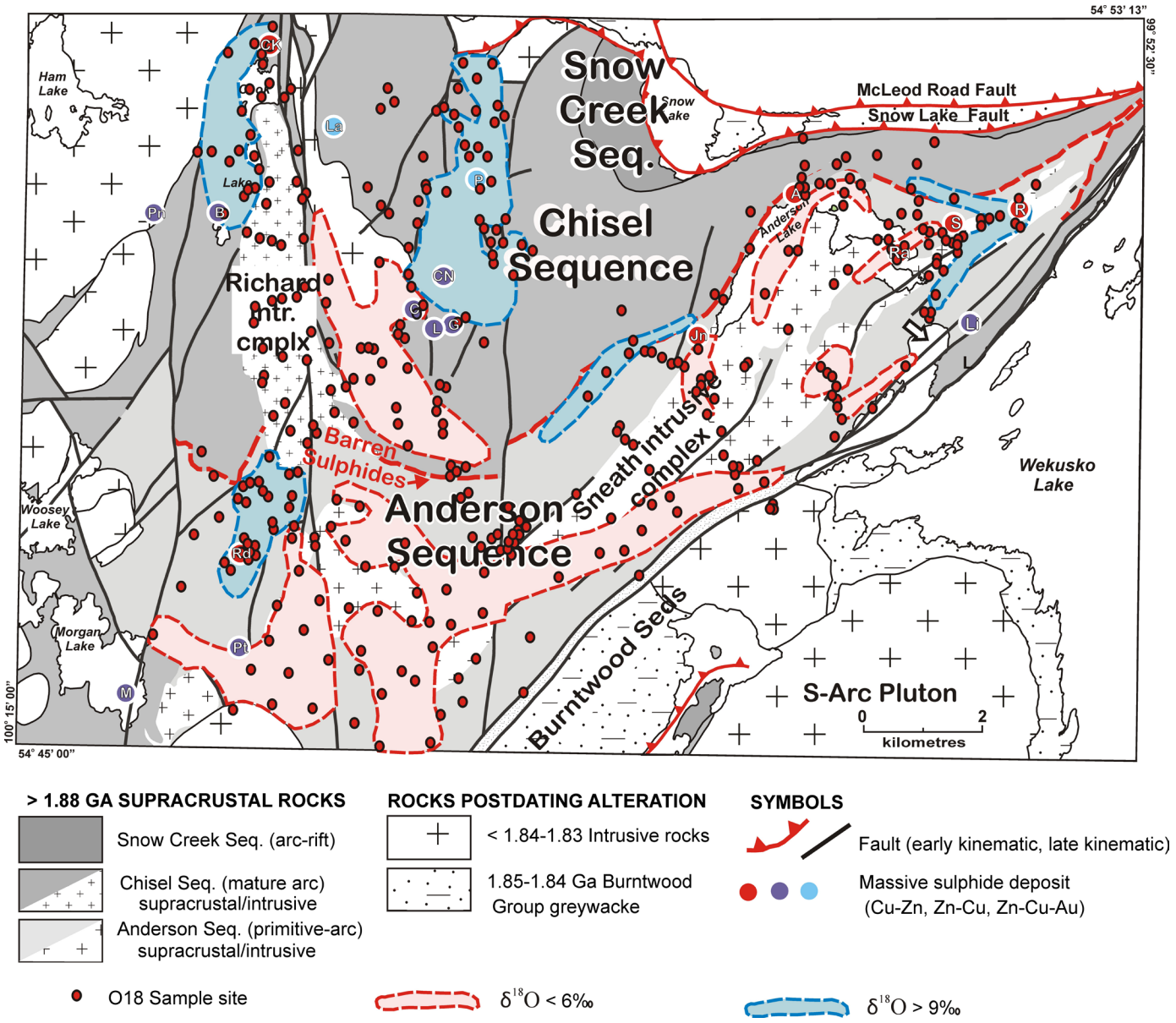

Figure 10: *Geologic map of the Snow Lake area showing the locations of all whole-rock samples analyzed for oxygen isotopes and the regional oxygen isotope zoning based after Taylor and Timbal (1998). Note that high-temperature alteration from beneath the Chisel Lake Gabbro is projected to the surface.*

The silicified/feldspathized mafic flows at this stop (Figure 12) are part of a 0.5 by >20 km semi-conformable alteration zone at the top of the Anderson sequence in the Welch Lake formation (**Figure 9**). The alteration zone underlies a thin zone of <5m sulphidic sediments known locally as the Foot-Mud horizon. The close proximity of the alteration zone and the directly overlying Foot-Mud unit suggests that the geothermal activity responsible for the alteration zone may also have produced the sulphidic sediments. The couplet of silicified/feldspathized basaltic andesite and overlying sulphidic exhalite occurs in the Noranda and Mattagami Lake VMS camps (Gibson et al., 1983; Piché et al., 1990) and also with base metal mineralization in the Chibougamau mining district (Couture, 1986). The Foot-Mud unit postdates the prominent Cu-rich VMS deposits of the Anderson primitive arc sequence, which are associated with rhyolite flow complexes lower in the stratigraphic sequence (Figure 8).

At this stop, located less than 300 m below the top of the Anderson primitive arc sequence (**Figure 8**, **Figure 9** and **Figure 12**) we will examine a series of moderately silicified and feldspathized low-Ti arc tholeiite flows (locations A, B, C and D). The stop descriptions are based on work by Skirrow (1987), who studied alteration of these flows as part of his M.Sc. thesis at Carleton University. The results of this study are fully discussed in a paper by Skirrow and Franklin (1994).

Alteration

Silicified/feldspathized pillows at this stop are strongly zoned, generally with an outer 1-2 cm wide selvage of hornblende-oligoclase-quartz, a 10-20 cm thick silicified margin, and an interior zone with 10-30 cm diameter domains of yellow-green clinozoisite and quartz. Elemental gains and losses during alteration of pillows discussed below were calculated

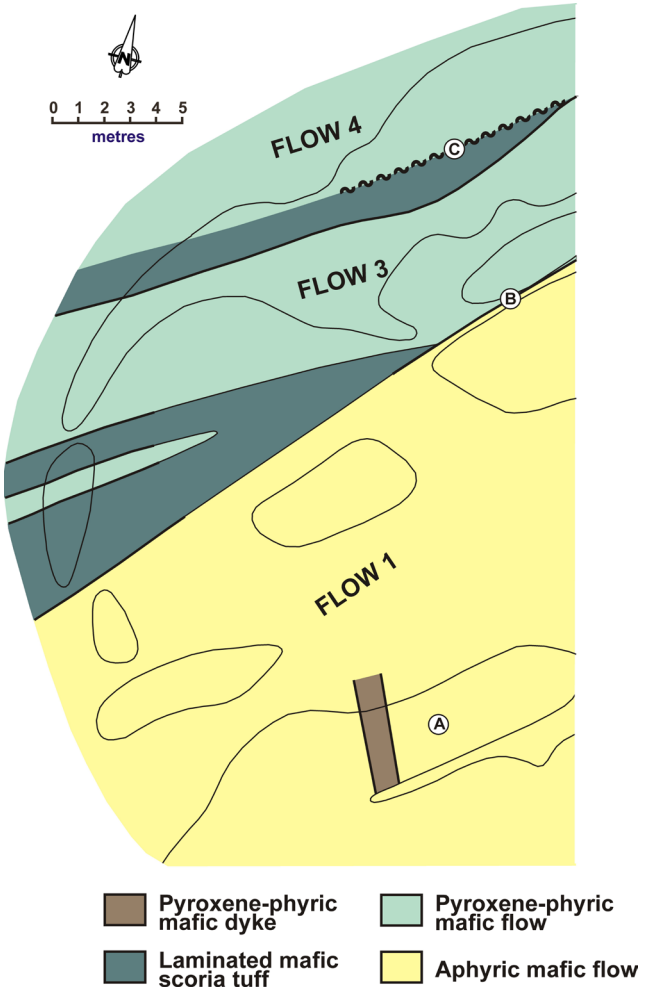

Figure 11: *Series of boninite and boninite-like flows in the Welch formation of the Anderson sequence. Three locations marked by circled letters will be examined.*

using the method of Grant (1986) and reported by Skirrow (1987).

Pillow margins show gains in SiO_2 that cannot be accounted for by redistribution of SiO_2 within a particular pillow; therefore, a source of SiO_2 external to the pillow is indicated; the latter is supported by a more recent study by Surka (2001) of similarly altered pillowed basalt at Stop 3. An overall small loss of Fe_2O_3(T) and MgO from altered pillows is likely. Epidotization of pillow cores involves large gains of CaO, oxidation of ferrous to ferric iron and large losses of Na_2O. Chemical changes in zones of patchy epidotization are similar to that displayed in epidotized pillow cores.

Skirrow (1987) interpreted alteration of mafic flows at this stop to be a product of interaction of diffuse, near-seafloor silica-rich hydrothermal fluids with still hot Welch Lake mafic lava flows. The heat source producing the silica-rich hydrothermal discharge is suggested by Skirrow (1987) to have been the subvolcanic Sneath Lake tonalite intrusive complex. The silica could have been derived locally from alteration of glassy pillow selvages and interpillow hyaloclastite, or from lower parts of the volcanic pile (Skirrow and Franklin, 1994).

The observed zonation of alteration in pillows at this stop was interpreted by Skirrow (1987) to have been produced by rapid cooling of the outermost parts of the hot lava pillows against cold seawater, producing a glassy selvage, and establishing a large temperature gradient between the selvage and the hot pillow margin and core. Skirrow (1987) interpreted the silica precipitation in the pillow margins to have been a result of raising the temperature of the invading silica-rich hydrothermal fluid to >350° C (Kennedy, 1950). *Note: this is not supported by the $\delta^{18}O$ isotopic studies of Bruce (1998) and Holk (1998) which suggest that the alteration of the pillows at this stop took place at low temperatures (< 250°C).*

Silicification/feldspathization of pillows and flows is variable. A broad correlation between intensity of alteration with portions of pillows and flows that display abundant thermal contraction cracks suggests that altering fluids may have gained access to the interior of pillows and flows via these cracks.

Location A (UTM: 6073148N; 429335E): Intensely silicified/feldspathized pillows, plagioclase phyric mafic flow

At this location the upper 15 m of a strongly silicified/feldspathized plagioclase-phyric mafic flow, overlain to the north by heterolithologic breccia (location B), is exposed. Pillows in this flow are relatively large, contain 5-10% plagioclase phenocrysts, and exhibit quartz-filled concentric thermal contraction cracks. Vesicles increase slightly in abundance towards the top of the flow (northwards) and are filled with quartz or quartz-epidote. Some of the features accompanying silicification/ feldspathization of a pillowed mafic flow are well displayed at this outcrop.

Altered pillows at this outcrop show a characteristic zonation from margin to core: a) a 1–2 cm wide medium grey selvage composed of hornblende + oligoclase + quartz and, in places, garnet + chlorite + biotite; b) a 10–20 cm silicified light grey margin containing quartz + oligoclase + hornblende + magnetite + garnet; c) and a core with 10–30 cm diameter yellowish-green, epidotized domains composed mainly of clinozoisite and quartz. The silicified margin typically includes white weathering intensely silicified domains (5–20 cm) composed of quartz + oligoclase (+ magnetite + hornblende), generally localized near the top and bottom of pillows. In strongly altered pillows these white weathering zones of intense silicification continue completely around the pillow forming "doughnut" structures (this feature is well developed at Stop 3).

Patches of yellow-green epidosite on this outcrop are surrounded by light grey to white domains of silicification similar to those at the margin of altered pillows. Thermal contraction cracks pass through both the silicified and epidotized domains without deviation indicating alteration was an approximately constant volume exchange of elements.

Location B (UTM: 6073143N; 423322E): Fragments of silicified/feldspathized pillows in a heterolithologic breccia bed

A normally graded, heterolithologic breccia bed overlies and fills depressions in the plagioclase-phyric pillowed mafic flow of location A. The breccia bed has a massive base and indistinctly stratified top, contains angular to subangular clasts

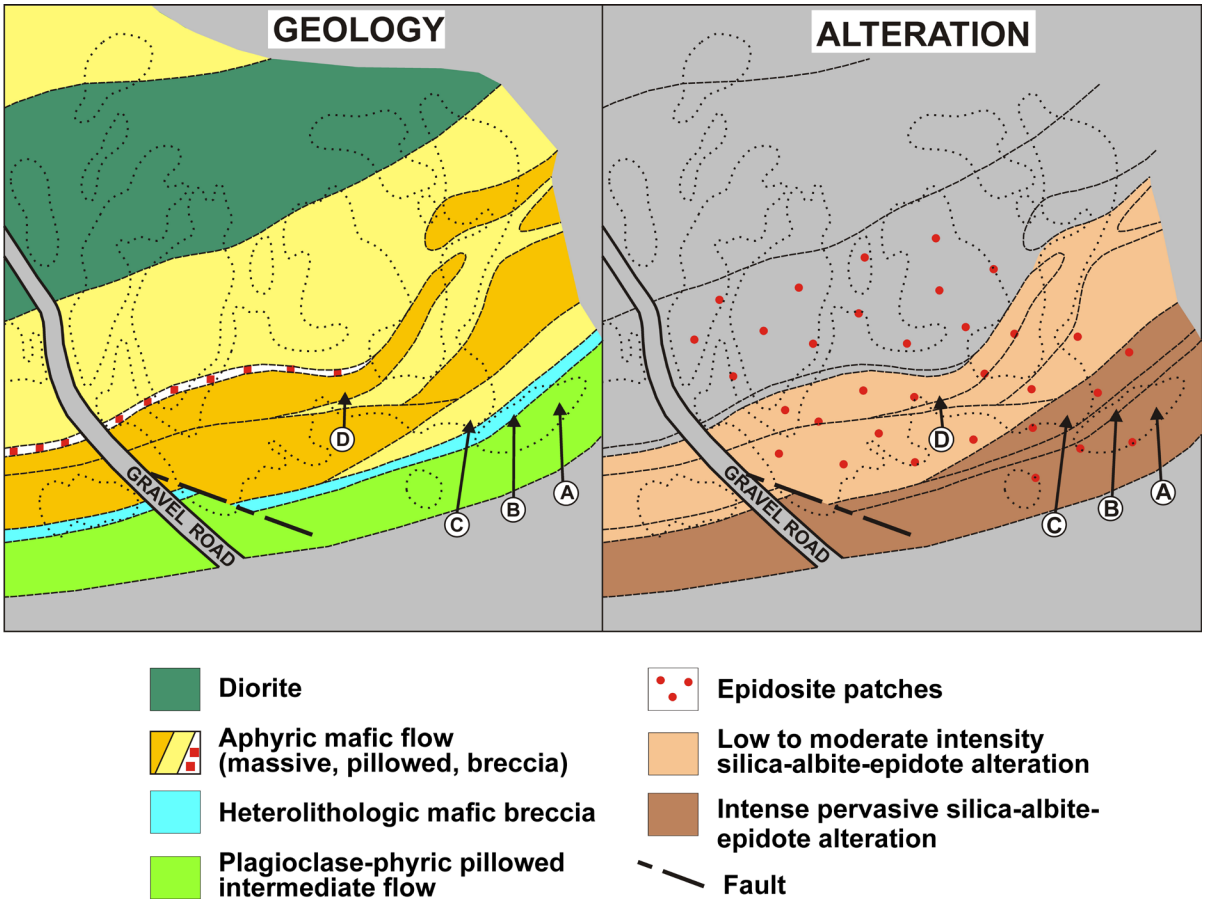

Figure 12: *Series of pillowed and massive Welch low-Ti basalt flows showing varying degrees of silicification/albitization. The distribution of flows and alteration facies was mapped by Skirrow (1987). Four locations marked by circled letters will be examined.*

up to 40 cm in diameter, grades upwards into granule-sized detritus, and is framework-supported. The important feature at this location is the presence of previously silicified/feldspathized fragments of plagioclase-phyric pillows (identical to the flow at location A) in this directly overlying breccia bed. This indicates that silicification/feldspathization of the underlying flow (location A) preceded deposition of the heterolithologic breccia bed. For this reason Skirrow (1987) interpreted the alteration to have occurred very close to, or at, the seafloor.

Location C (UTM: 6073140N; 429294E): Silicified/ feldspathized pillows in aphyric mafic flow

A less intensely silicified/feldspathized pillowed mafic flow than that at location A is exposed here. The zonation of alteration within the pillows is almost identical to that at location A. However, here pillows are smaller, selvages are more hornblendic, and intensely silicified patches (and associated thermal contraction cracks) occur closer to the selvages.

Location D (UTM: 6073158N; 429250E): Patches of silicification/feldspathization and epidotization in a massive aphyric flow

A massive 20 m thick mafic flow with distinctive patches of silicification/feldspathization and epidotization overlies, and is separated from, the silicified flow at location C by several massive and pillowed flows, including a pillow fragment breccia. Alteration patches at location 4 are sinuous, typically 0.3 to 1.5 m long, and elongate parallel to thermal contraction cracks (i.e. they are subparallel to lower contact of the flow). Most are concentrically zoned from an outer dark green hornblende-rich periphery, to a middle light grey quartz, plagioclase, hornblende and magnetite-bearing silicic zone, to an interior light yellowish green core composed of clinozoisite, quartz and minor titanite and carbonate. Some alteration patches are connected and appear to form an anastomizing network. Thermal contraction cracks in this flow are typically filled by hornblende, but where they pass through the silicic peripheries of alteration patches they are filled with quartz and plagioclase.

Return to vehicles and proceed north on road to 0.7 km (UTM: 6073461N; 428914E).Field trip outcrop is accessed by following trail east of road.

STOP 3 (UTM: 6073475N; 428851E): Silicified/ feldspathized Welch Lake basaltic andesite and Foot-Mud sulphide horizon

Introduction

This outcrop at Stop 3 (**Figure 8**, **Figure 9** and **Figure 13**) provides a particularly photogenic and well preserved example of a silicified/feldspathized aphyric pillowed basaltic andesite. The alteration is part of the same zone of silicification /feldspathization observed at Stop 2, but here it is located at the very

top of the Anderson sequence and is directly overlain by Foot-Mud sulphidic sedimentary rocks. Overlying Chisel sequence Stroud Lake felsic breccias are unaffected by the prominent silicification/feldspathization at this outcrop. Because the alteration does not affect overlying strata and is cross cut by the Chisel sequence Richard Lake subvolcanic intrusion, this supports the interpretation by Skirrow (1987) and Skirrow and Franklin (1994) that it formed very close to, or at, the paleo-seafloor.

Outcrop Description

Proceeding west (along strike) by trail from the road, weakly to moderately silicified/feldspathized pillows are crossed on route to the intensely altered pillowed flow at Stop 3. Primary features in the altered flow at the stop are well preserved and include excellent pillow shapes, thermal contraction cracks, amygdales, and interpillow hyaloclastite. Prominent white weathering zones of intense silicification form a complete ring around the inner margin of pillows, and enclose less altered or epidotized pillow cores. Strongly gossaned sulphidic sedimentary rocks of the Foot-Mud horizon are located just northeast of the main outcrop area. Primary features and zones of alteration were mapped on this outcrop at 1:10 scale by Surka (2001) as part of a B.Sc. study at the University of Manitoba; this study is drawn upon extensively for the description of this stop. Eight alteration facies and two varieties of interpillow hyaloclastite (**Figure 13**) were identified by Surka (2001).

Geochemistry of alteration

Surka (2001) collected representative samples of each alteration facies at Stop 3 and a series of unaltered basalt from Stop 2 (Location E), including samples from the pillow margin, pillow core and interpillow hyaloclastite for comparison. A sample of the least altered basaltic andesite from Stop 3 was taken from Facies E. SiO_2 and other major elements show dramatic variations (e.g., SiO_2 varies from 47 to 74%). In addition mobile metal ions vary dramatically, with this likely a result of the alteration process.

Relative mass change

Surka (2001) examined the relative mass change of elements at this stop by comparing the altered rocks to least altered equivalents. The objective was two-fold. The first objective was to establish whether the alteration at this stop represented a simple redistribution of elements in a closed system or whether the alteration took place in an open system with introduction and loss of elements. A second objective was to determine the mobility of metal ions during alteration and to establish the potential of this alteration to generate VMS mineralization. Because all of the rocks at Stop 3 have almost certainly been altered to some extent, samples taken from the much less altered flow at Stop 2 were considered to potentially be a good candidate for comparison for relative mass change calculations. However, the trace element geochemistry of the flows at Stop 2 and 3 are quite different with the consequence that immobile trace elements could not be used for the mass change calculations and the possibility that the two flows may have had distinctly different original chemistry could not be ruled out.

Surka concluded that significant addition and loss of both major and trace elements occurred during alteration. It is clear that SiO_2 and K_2O were added, and Fe_2O_3T, Cu and Zn were lost during alteration of the basalt at this location. A rough calculation of the amount of metals lost from this zone of silicification/feldspathization during alteration was determined to be 17.5 Mt Cu and 1.0 Mt Zn or 583 Mt of 3% Cu and 17.5 Mt of 6% Zn. Although this is a large amount of Cu and Zn, there is no way of knowing whether the metals were concentrated by the resultant mineralized hydrothermal fluids or were lost in the seawater column and deposited as widespread but sub-economic sulphides in the Foot-Mud horizon.

Nature of hydrothermal fluids

The presence of semi-conformable zones of silicification in several Precambrian VMS camps makes it necessary to gain an understanding as to their origin. In many cases there appears to be at least two origins for these zones. The Welch Lake silicification zones, and comparable zones in the Noranda and Matagami Lake camps, immediately underlie units of comparable strike length that consist of mixed epiclastic-tuffaceous and sulphidic exhalative material. This would suggest a genetic relationship between the two. If this is the case, then silicification had to occur in the immediate sub-seafloor. This would contradict earlier models for silicification, such as that invoked by Galley (1993) that suggests that silicification is a high temperature phenomenon that takes place in the deeper parts of a convective hydrothermal system. In these deeper parts, the elevation of fluid temperatures over 380°C results in the retrograde solubility of silica and rapid precipitation (Kennedy, 1950). Examples of this type of silicification will be observed at Stop 6. A shallow sub-seafloor silicification event would intuitively take place at lower temperatures.

Return to road via trail and walk up road 200 m (UTM 6073504N; 428911E) and take cut line to east of road. Walk 30 m east on a cut line and 30 m to northeast on a trail.

STOP 4 (UTM: 6073516N; 428973E): Stroud Lake felsic breccia

Introduction

The transition from the Anderson to Chisel sequences is characterized by an abrupt change from one dominated by subaqueous mafic flows (Stop 1 to 3; **Figure 8**) to one dominated by units composed of heterolithologic volcaniclastic detritus (Stops 4, 6 to 11, **Figure 14**). It is also marked by distinctive changes in geochemical character of associated mafic flows (discussed below). The Stroud Lake felsic breccia is both overlain by and locally intercalated with Snell Lake subaqueous mafic flows. These mafic flows display anomalously high Th contents and the highest apparent proportion of "old" Nd (-0.4 to +2.4 ε_{Nd}), of all the arc rocks in the Flin Flon belt. Stern et al. (1992, 1995a) attribute these features to intracrustal contamination.

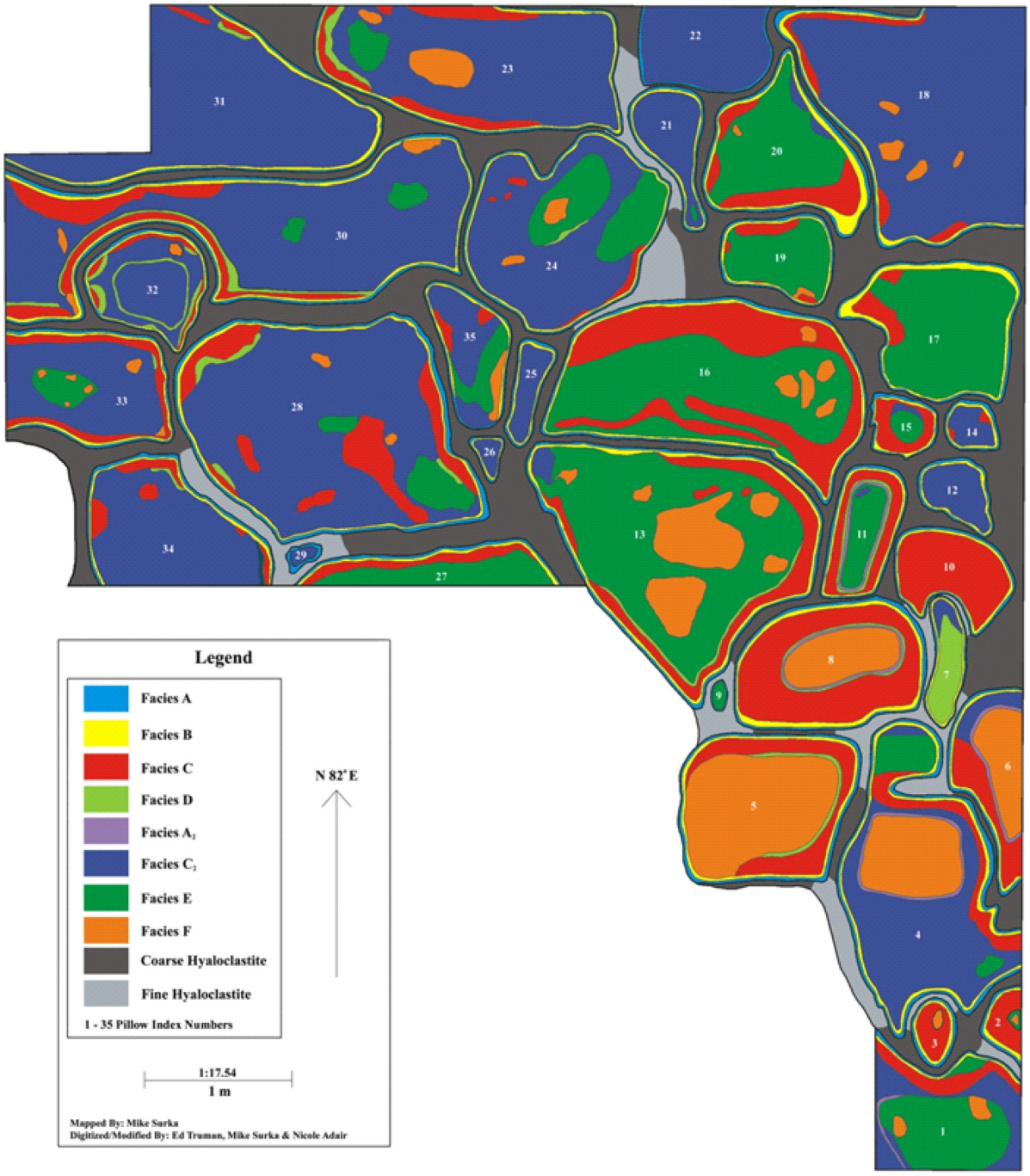

Figure 13: *Map of outcrop at Stop 3 detailing various types of alteration (from Surka, 2001). A – Dark green pillow rims containing abundant Mg-hornblende; B – Moderate hornblende abundance; C/C2 – Moderate/strong "silicification" and bleaching; D – Hornblende-biotite development; E/F – Weak/strong epidote-quartz development.*

David et al. (1996) analyzed zircons from a sample taken from a 1 m thick felsic wacke bed located at the southern end of the outcrop at Stop 4 (Location A, **Figure 15**). The sample yielded two zircon sample populations. One suite defined a discordia line with an upper intercept of 1892 ± 3 Ma, interpreted to be the age of crystallization of felsic material forming the felsic wacke. Within error this age is identical to that determined for the Sneath Lake (1886+17/-9 Ma) and Richard Lake (1889+8/-6 Ma) tonalite plutons, consistent with their interpretation as subvolcanic intrusions (Bailes et al., 1991). The second population yielded inversely discordant Pb-Pb ages of 2652 Ma and 2674, and Pb-Pb discordant ages of 2715 Ma, 2823 Ma and 2691 Ma that David et al. (1996) interpret as inherited. The *ca.* 2.7 Ga inherited zircons support the interpretation by Stern et al. (1992) that the high proportion of "old" Nd in the intercalated Snell mafic flows is due to intracrustal contamination, possibly through contamination by Archean crust in the basement to the Snow Lake arc segment or within an underlying subducting plate.

The coarsely porphyritic felsic blocks in the 18 m thick bed at this stop are texturally and geochemically indistinguishable from the megacrystic trondhjemite phase of the underly-

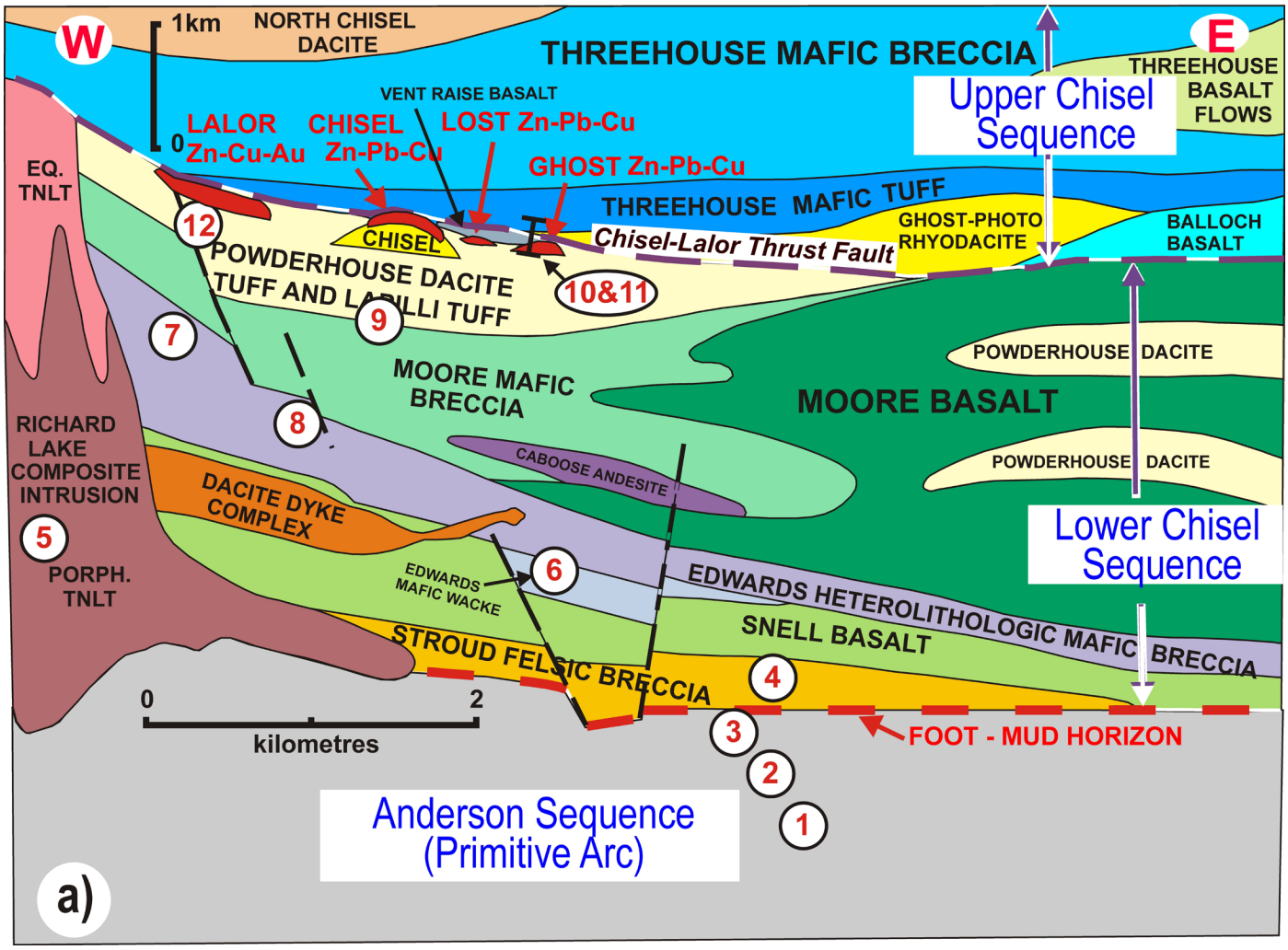

Figure 14: *Schematic cross section through the Chisel sequence showing a) stratigraphic units and b) domains of altered rocks. Note the Chisel-Lalor thrust fault at the contact between the Lower Chisel and Upper Chisel sequences. The large zone of alteration includes semi-conformable alteration focussed in the Edwards formation volcaniclastic rocks and a subconcordant Fe-Mg zone of alteration that merges with the cross-stratal disconformable zones of alteration. Circled numbers indicate field trip stops.*

ing Sneath Lake subvolcanic intrusion. This suggests that the Stroud Lake felsic breccia may have been derived by uplift and erosion of the underlying Anderson primitive arc sequence coincident with outpouring of the isotopically anomalous Snell Lake mafic flows.

Stop description

At this stop, located 50 m above the base of the Chisel sequence, a 29 m section of north-facing, well-bedded, monolithologic to heterolithologic felsic breccia and tuff is exposed (Figures 14 and 15). The southern 11 m consists of a series of <5 cm and up to 2.6 m thick intermediate to felsic tuff beds that display bed forms and sedimentary structures characteristic of turbidity and fluidized sediment flows. Normal size grading, scour channels, rip-ups, syn-sedimentary faults, load structures and beds with A, AB and ABD Bouma zonation are present. The northern 18 m of the outcrop consists of a single (?) felsic bed characterized by distinctive, large quartz and plagioclase phenoclasts. The lower 8.5 m of this bed is massive and texturally uniform with 10% quartz phenoclasts (2–15 mm), 15–20% plagioclase phenoclasts (2–5 mm) and possible fiamme in a fine grained matrix. The upper 9.5 m is clearly fragmental and includes a wide variety of over 30 cm diameter subangular to sub-rounded felsic blocks, including some that are texturally identical to the lower 8.5 m of the bed. The felsic blocks, as well as phenoclasts of quartz and plagioclase in the intervening detrital matrix, all display normal size grading. The top of the bed is fine grained felsic tuff.

Location A

The two heterolithologic felsic breccia beds at this location are matrix-supported and include subangular to sub-rounded quartz-plagioclase phyric rhyolite and trondhjemite clasts, as well as rip-up clasts of intermediate to mafic siltstone. The trondhjemite clasts are identical in texture and chemistry to the megacrystic trondhjemite phase of the underlying Sneath Lake subvolcanic intrusion. The matrix to these beds is composed of 1–4 mm quartz phenoclasts, 2–4 mm plagioclase phenoclasts, and 2–8 mm lithic felsic to mafic clasts. The detrital matrix of these beds is normally size graded.

The intermediate to mafic siltstone and wacke beds overlying the felsic breccia beds are 2–20 cm thick and display delicate

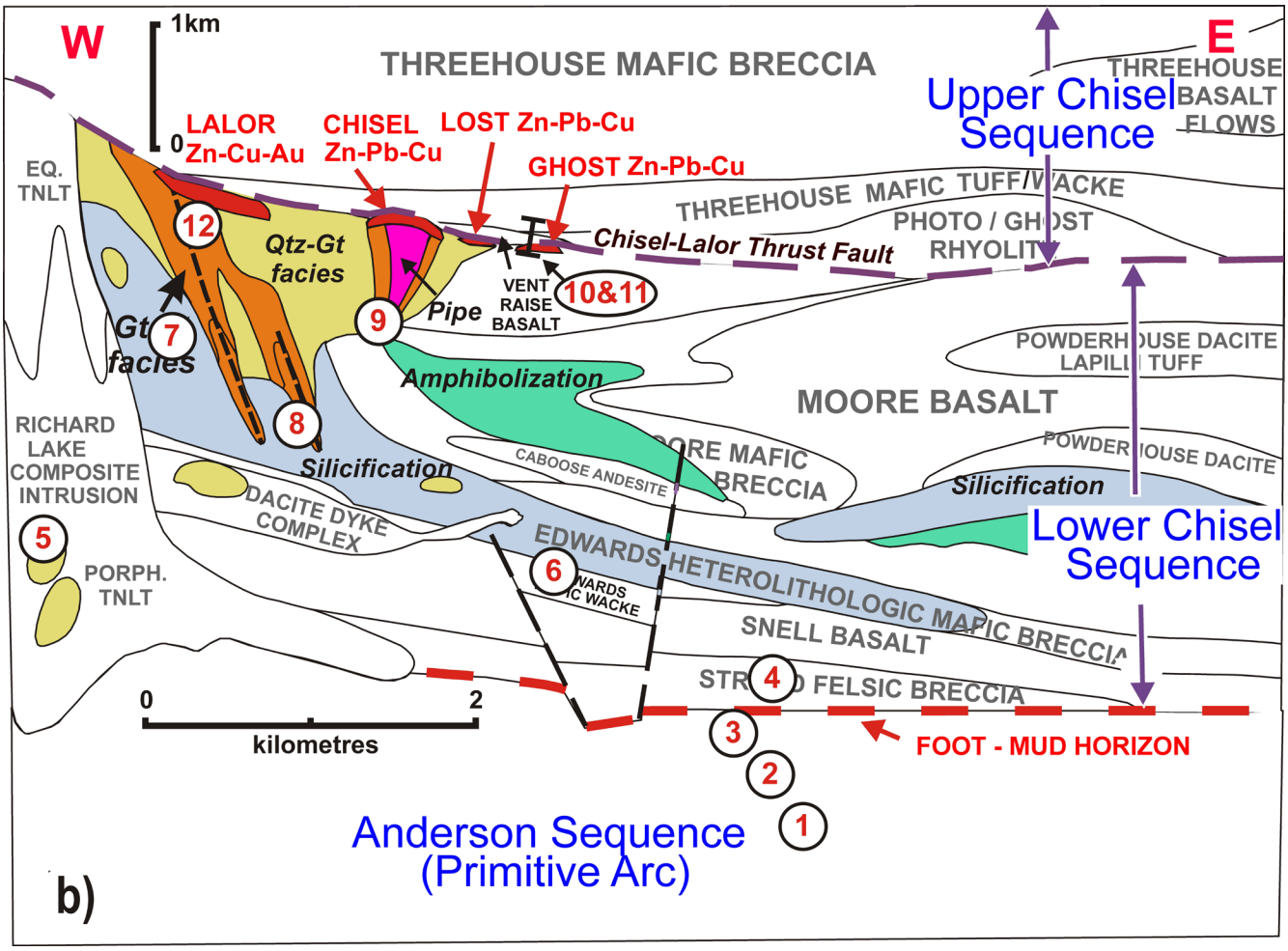

Figure 14 (continued): *Schematic cross section through the Chisel sequence showing a) stratigraphic units and b) domains of altered rocks. Note the Chisel-Lalor thrust fault at the contact between the Lower Chisel and Upper Chisel sequences. The large zone of alteration includes semi-conformable alteration focussed in the Edwards formation volcaniclastic rocks and a subconcordant Fe-Mg zone of alteration that merges with the cross-stratal disconformable zones of alteration. Circled numbers indicate field trip stops.*

layering, normal size grading, rip-ups, scour channels, and A and AB Bouma bed zonation. Disseminated pyrite in these beds has oxidized to produce a rusty weathered colour.

The 1 m thick AB Bouma zoned felsic wacke bed is composed of an 80 cm graded division composed of 1–4 mm felsic clasts and 2–6 mm mafic lithic clasts, and a 20 cm top of delicately laminated fine sand and silt. This bed contains rare, up to 4 cm cobbles of quartz megacrystic trondhjemite. This is the bed dated by David et al. (1996). The dating sample site is located at UTM: 6073521N; 428968E.

Location B

This 2 m thick unit of intermediate mafic wacke and siltstone is well bedded at a scale of 2–23 cm. Beds display A and AB Bouma zonation and normal size grading. Abundant delicate faults at high angles to the layering are interpreted as synsedimentary as they are discontinuous up section.

Location C

At this location the reverse graded 1 m base of a >18 m thick bed of felsic breccia is exposed. The reverse grading is displayed by both quartz phenoclasts in the matrix and by larger matrix-supported felsic blocks. Up section the felsic blocks, which are subtly defined by clusters of large quartz phenocrysts, are less obvious and the bed appears homogenous.

Location D

As the matrix fines, individual blocks of coarsely quartz-plagioclase phyric rhyolite and tonalite are increasingly evident in this thick bed. The felsic blocks are typically sub-rounded, matrix-supported and part of a distinctly heterolithogic felsic clast population. Clasts include aphyric rhyolite and a variety of quartz megacrystic and plagioclase porphyritic rhyolite and tonalite. A geochemical sample from one of the clasts at this locality displays identical geochemistry to that of the underlying Sneath Lake subvolcanic intrusion.

Return to vehicle and continue 1.2 km north on road to UTM: 6074231N, 428608E.

STOP 5: Richard Lake Intrusive Complex (virtual stop)

The *Richard Lake Intrusive Complex (RLIC)* is quite different from the Sneath Lake subvolcanic intrusion due to its large

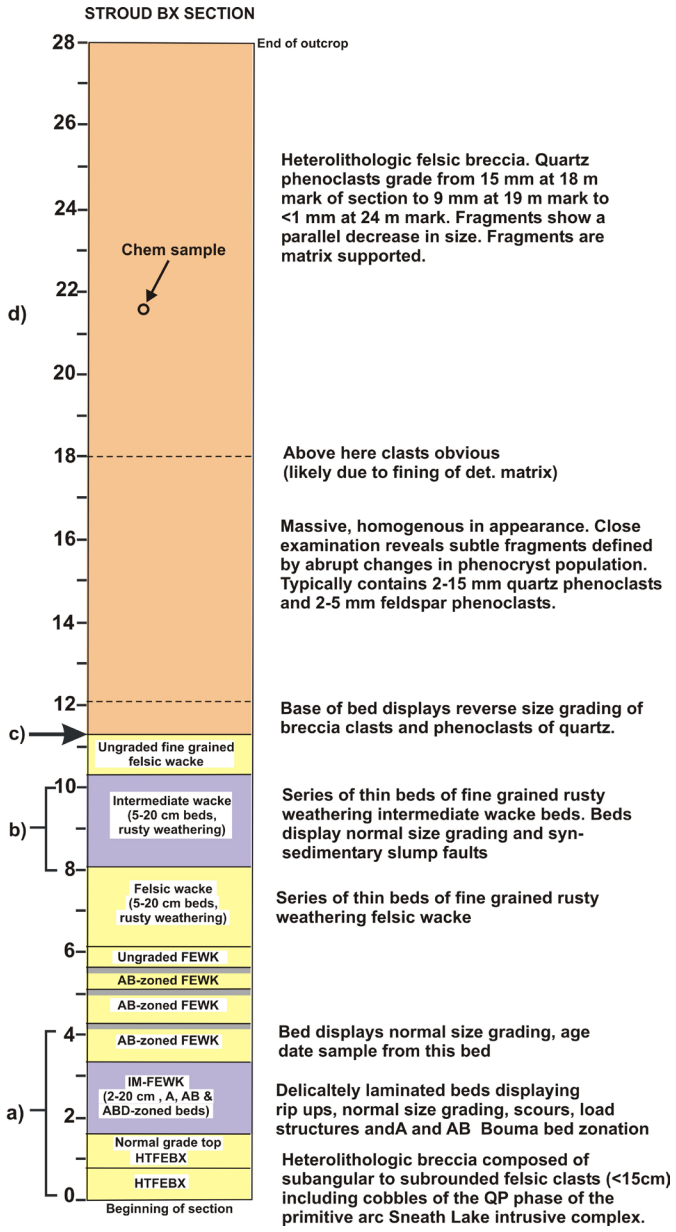

Figure 15: *Stratigraphic section of Stroud felsic breccia exposed at Stop 4. Letters indicate Stop locations.*

height to length ratio (**Figure 5**, **Figure 6** and **Figure 14**). It has had a complex intrusion history (Galley, 2003), much of which postdates VMS-related hydrothermal activity within the Chisel sequence (**Figure 16**). The intrusive complex is approximately 6500 m long, and up to 3000 m wide, with an average width of closer to 1000 m (**Figure 14**). The earliest RLIC-related intrusive activity consists of remnants of small stocks of hornblende porphyritic diorite along the margins of the composite intrusion and as xenoliths within early tonalite phases. These remnants are compositionally similar to andesite flows within the host volcanic succession (Bailes et al., 1996). The next phase is the 2 km long feldspar porphyritic dacite/tonalite Powderhouse sill-dike complex intruded along the contact between the Snell basalt formation and the overlying Edwards formation turbidite-debris flow succession. These dacite dikes continue upsection for nearly 1000 m and are feeders for the Powderhouse dacite that defines the immediate footwall to VMS-hosting rhyolite flow complexes. The composite dacite sill is up to 300 m wide, and thins to the east as it divides into a number of thinner sills. It is truncated to the west by later trondhjemitic phases of the RLIC. The presence of tonalite as infilling between pillows in basalt flows along the south contact of the RLIC suggests that this may have been the location for a feeder zone for the dacite/tonalite sill-dike swarm.

The main portion of the RLIC consists of a number of overlapping trondhjemite and aplite stocks and dikes. The southern (lower) half of the intrusion contains small bodies of medium to coarse-grained, equigranular trondhjemite within a larger stock of finer-grained, quartz phyric trondhjemite. A single U-Pb zircon date from a coarse-grained trondhjemite phase gives an age for the RLIC of 1889 Ma (Bailes et al., 1991). The quartz phyric trondhjemite stock is in turn intruded by dikes of aphyric to weakly quartz phyric, holocrystalline to granophyric trondhjemite. The trondhjemite phases are characterized by abundant miarolitic cavities that range from <10 mm in size near the margins of the intrusive complex to ovoids up to 15 cm in diameter. Some miarolitic cavities are elongate and form bubble "trains", particularly along the margins of aplite dikes.

Hydrothermal alteration

The RLIC is affected by various alteration types. The early phase Powderhouse dacite sill-dike swarm is commonly affected alteration manifest by chlorite-biotite-garnet ± staurolite metamorphic mineral assmeblages, with dike margins variously affected by silicification. The early phase trondhjemite along the west margin of the complex is crossed by rectilinear fracture patterns defined by quartz-chlorite-biotite-staurolite-kyanite-rich mineral assemblages. Miarolitic cavities within this trondhjemite phase contain a chlorite-quartz-garnet mineral assemblage. The core of the intrusive complex contains abundant veins and breccia zones filled with epidosite and silicified margins. Miarolitic cavities within the intrusion core are filled with epidote and quartz. Some of these cavities form pipe vesicles along the margins of late aplite dikes.

Emplacement history

The contact relationships between the RLIC and its host rocks, between different internal intrusive phases, and with alteration allow an emplacement history to be generated with respect to VMS mineralization (**Figure 16b**). The co-magmatic relationship between the early phase Powderhouse dacite sill-dike swarm and the footwall dacite formation to the Zn-Pb-Cu-Ag VMS deposits indicates emplacement before massive sulphide formation. The close spatial relationship between this sill-dike swarm and the large alteration system underlying the deposits suggests it initiated and sustained VMS-related hydrothermal activity. The first trondhjemite stocks to intrude and truncate the western margin of the dacite sill-dike swarm also truncate the alteration zones, but are they themselves affected by fracture-controlled Fe-Mg alteration. This suggests that they intruded the active hydrothermal system. The late trondhjemite and aplite phases cut through altered tonalite and trondhjemite and intrude into the alteration zone below the Cook Lake and Bomber VMS occurrences. They are affected by epidote-quartz

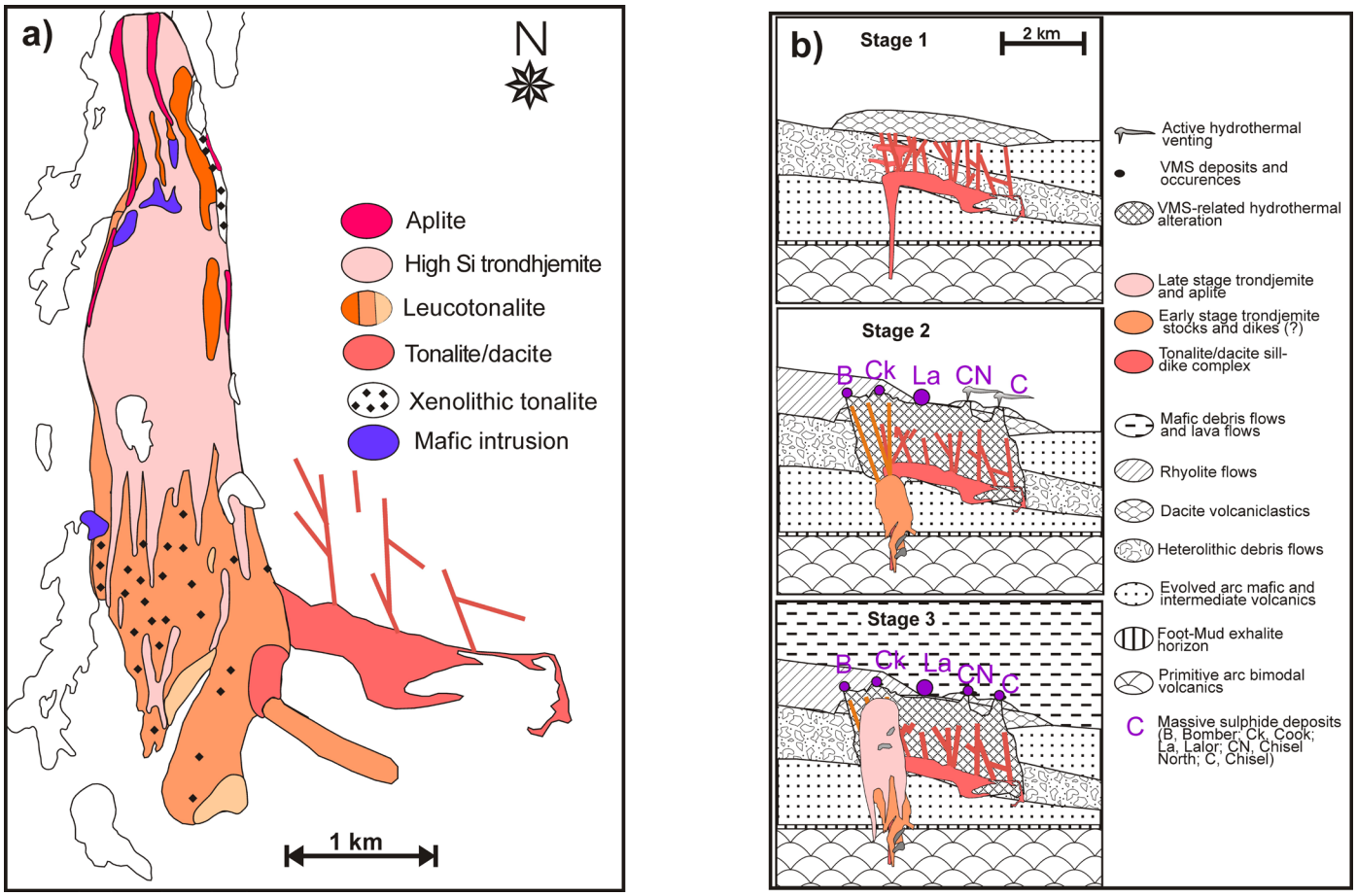

Figure 16: *Geology (a) of the Richard Lake Intrusive Complex (RLIC) and "cartoon" (b) showing possible stages (1–3) in evolution of the RLIC.*

alteration that increases in intensity towards the core of the intrusive complex. This suggests a magmatic-hydrothermal derivation brought on by volatile exsolution that took place during late stage crystallization. The majority of the RLIC was therefore emplaced after VMS formation. Only the early dacite/tonalite phases were coeval with the Chisel-Lalor VMS-forming hydrothermal system.

Leave vehicles and follow cut trail 30 m to north of the road and then a further 30 m to the northwest.

STOP 6: Silicification/feldspathization associated with dacite dikes in the Edwards Lake formation (UTM: 6074287N; 428607E)

The Edwards Lake formation consists of up to 1200 m of fine grained mafic bedded tuff and heterolithologic mafic volcanic breccia (**Figure 14a**). The lower 550 m consists of fine grained mafic tuff (observed at this Stop). The upper 650 m consists of heterolithologic mafic breccias (Stop 7). Because much of this volcaniclastic formation is altered (**Figure 14b**) it has been interpreted to have been a hydrothermal aquifer (Skirrow, 1987; Bailes and Galley, 1996, 2007; Bailes et al., in press; Skirrow and Franklin, 1994). The alteration is spatially associated with an array of subvolcanic mafic to felsic sills, dikes and plugs that intrude both the Edwards Lake heterolithologic mafic wacke/breccia and the underlying Snell Lake mafic flows (Galley and Scoates, 1990). Most prominent among the syn-volcanic intrusions is a large swarm of aphyric and plagioclase phyric dacite dikes (**Figure 6**c and **Figure 14**a) interpreted to be the initial phase of the Richard Lake subvolcanic intrusive complex. The dacite dikes are identical in texture and chemistry to the Powderhouse dacite tuff (**Figure 14**a), the unit that directly underlies the Chisel-Lost-Ghost-North Chisel-Lalor Zn-Cu-Pb-Ag sulphide deposits (Bailes and Galley, 1999; 2007).

At this stop we will examine silicified/feldspathized fine grained mafic bedded tuff of the Edwards Lake formation. This tuff is typically massive and featureless, such that altered varieties are difficult to distinguish from the dikes. However, at this stop the dacite intrusions are sheetlike bodies, cross-cut bedding, and have sharp, commonly flow-banded margins. They are creamy white in colour and are plagioclase-phyric with a fine grained groundmass of quartz, plagioclase and minor biotite. Plagioclase phenocrysts are commonly enveloped or partially replaced by biotite giving dikes a spotted appearance. Adjacent to dacite dikes the host mafic volcanic wacke is weakly to intensely silicified/feldspathized (**Figure 17**). The feldspar-quartz altered rocks are mottled shades of grey in colour, are composed of plagioclase, quartz and hornblende, and are slightly darker in colour than the adjacent dacite dikes. More than one age of dacite dikes have intruded the mafic tuff at this stop (**Figure 17**).

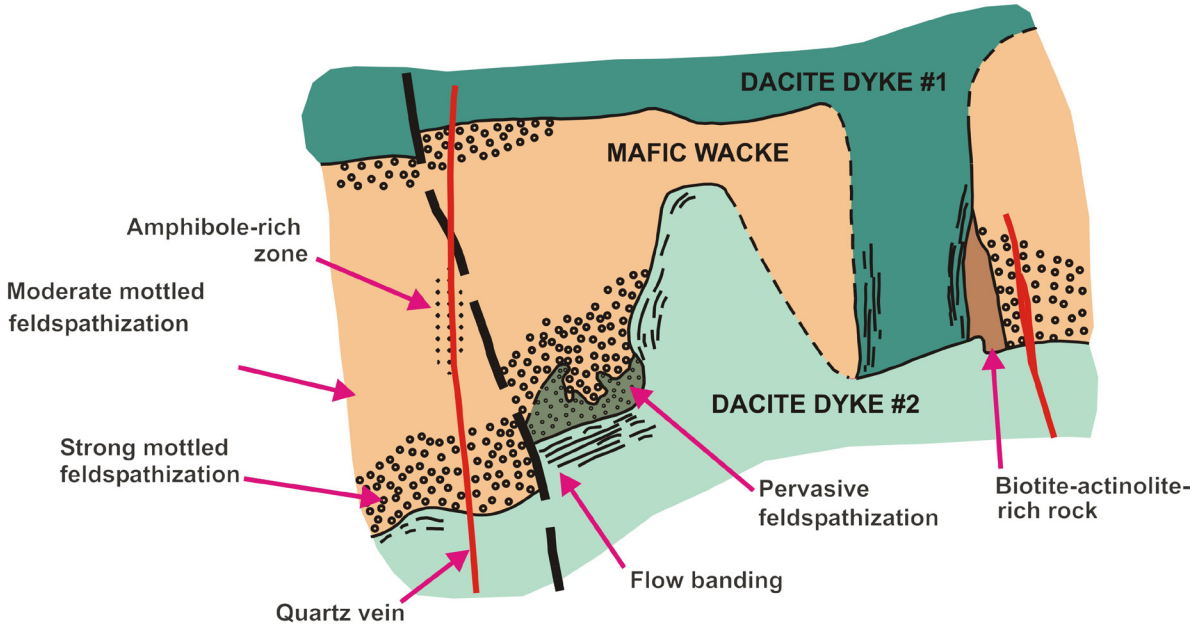

***Figure 17**: Sketch of two dacite dikes at Stop 6 that display flow banded margins and have silica-feldspar rich alteration domains developed in the adjacent mafic tuff.*

Mass balance calculations were completed on both the dikes and wallrocks by Skirrow (1987) and Galley and Bailes (2002) to determine elemental gains and losses in silicified/feldspathized rocks. These indicate that with an increase in alteration intensity of the dacite dikes there is an overall increase in Fe^{+2}, MnO, MgO and K_2O, and decreases in Cu, Fe^{+3}, CaO, Na_2O and BaO. Small variations in silica suggest very little addition or subtraction of this element from within the dikes. Bleaching of the surrounding mafic tuff resulted in a corresponding increase in Cu, Zn, SiO_2, Na_2O, and Rb, and a decrease in Fe (T), MnO, MgO, CaO and H_2O. Skirrow (1987) suggested that felsic dikes at this outcrop were emplaced into a SiO_2-rich hydrothermal system, locally heating the fluids to >350° C, resulting in Si-Na metasomatism and resultant silicification and feldspar addition. Fluid interaction with the cooling dike resulted in metal leaching from the latter.

The bleaching of the mafic wackes in the presence of the dacite feeder dikes is an example of another type of silicification/feldspathization present within the Snow Lake alteration systems (**Figure 7** and **Figure 9**). As opposed to the bleaching at the top of the Welch Lake primitive arc flows as viewed at Stops 2 and 3, the alteration we observe here is a product of deep sub-seafloor fluid-rock interaction. The dacite dikes are the intrusive equivalent of the Powderhouse dacite, and this implies that the alteration at this outcrop took place at depths of up to 2 km below the paleo-seafloor (**Figure 14**). Another difference is that this silicification/feldspathization event forms at the base of a layered, semi-conformable alteration system in which a number of stacked alteration zones represent a series of seawater-rock interactions that took place more than 2000 m below the seafloor. This is evidence for the generation of a mature convective hydrothermal system rooted at the top of the Powderhouse dacite sill-dike swarm that produced the Chisel-Chisel North-Lost-Ghost-Lalor Zn-Pb-Cu-Ag VMS deposits.

Evidence for the maturity and higher temperatures involved in the generation of this semi-conformable zone of silicification and feldspathization is the $\delta^{18}O$ values obtained for this alteration system (Taylor and Timbal, 1998; **Figure 10**). Whereas the alteration zone affecting the upper part of the Welch Lake mafic flows shows an increase in $\delta^{18}O$ values relative to unaltered volcanic strata (**Figure 10**), the silicification/feldspathization observed at Stop 6 lies within a zone of <6 per mil $\delta^{18}O$ values. This indicates that the alteration processes are due to high temperature (>350°C) seawater-rock interactions. This is the temperature range expected for the development of a robust, metal-producing convective hydrothermal system (Seyfried and Bishoff, 1977; Rosenbauer and Bischoff, 1983; Seyfried et al., 1988, Alt, 1995; Galley, 1993).

Return to vehicles and drive north and back to the Chisel mine site. Proceed west down ramp into open pit and at UTM: 6075601N; 427900E turn south and follow road beside buried water line. At UTM: 6076283N; 427651E turn west at T junction and then immediately to south and follow road on east side of drainage ditch to abandoned gravel pit (UTM: 6075866N; 427406E). Proceed on foot to the west and cross the drainage ditch (UTM: 6075884N; 427169E) by canoe. Stop 7 is reached by a 1 kilometre hike along a rough trail marked by flagging tape.

Permission is required from HudBay Minerals Ltd. to access the Chisel Open Pit. Roads used to access this outcrop are in poor repair and caution is advised.

STOP 7: Alteration of the Edwards Lake mafic tuff and heterolithologic breccia: Roots of a VMS hydrothermal system

The extensive 9 x 2km alteration system within the Lower Chisel sequence below the Chisel-Chisel North-Lost-Ghost-Lalor Zn-Pb-Cu-Ag VMS deposits is rooted within the Edwards Lake formation (**Figure 6**, **Figure 9** and **Figure 14**).

This wedge-shaped formation consists of a basal unit of turbiditic mafic tuff overlain by 550 m of heterolithologic mafic boulder, cobble and pebble breccias intercalated with mafic tuff. The breccias are composed mainly of plagioclase- and plagioclase-pyroxene–phyric mafic fine-grained fragments with lesser amounts of other mafic and felsic volcanic clasts. Most breccia beds in the Edwards Lake formation are 1–20 m thick; Skirrow (1987) reports one 60 m bed. Organization of breccia beds is consistent with deposition by subaqueous debris flows (Bailes, 1986; Skirrow, 1987).

At Stop 6 we saw the effects of the intrusion of the early phase dacite sill-dike swarm of the RLIC upon the mafic tuff near the base of the Edwards formation. Moving west along the Edwards formation the underlying dacite sill-dike complex becomes thicker, with a corresponding increase in the degree and complexity in alteration of the host epiclastic strata (**Figure 14**). At Stop 7 (**Figure 14** and **Figure 18**) the relationship between various alteration facies and their host rocks are well exposed. A large outcrop exposes mafic tuff with turbidite bed forms overlain by intercalated units of Edward breccia. Over 20% of the outcrop at Stop 7 consists of narrow (~1–4 m) dikes that range from mafic to felsic in composition, and are co-magmatic with overlying dacite and basalt units (Bailes et al., 1996). Many of the dikes have irregular shapes with some displaying pillow-like, amoeboid protrusions into the host volcaniclastic rocks of the Edwards Lake formation. The dikes are interpreted to be synvolcanic, an interpretation consistent with their morphologies and with their intimate spatial relationship to alteration phenomenon in the Edwards Lake formation both regionally and at an outcrop scale.

The turbidite deposited mafic tuff is affected by varying degrees of silicification and feldspathization in proximity to the dacite dikes (as seen previously at Stop 16). The tuff also contains layer-controlled zones of coarse-grained chlorite-amphibole-alteration (**Figure 18**). With increasing intensity of this alteration type, there is a corresponding increase in Cu, Zn, Fe^{+3}, MnO and MgO, and decreases in Fe^{+2}, CaO, Na_2O, K_2O, P and Sr. The overlying mafic breccia units are affected by varying degrees of silicification and feldspathization and patchy epidote -rich alteration (**Figure 18c**). This involves the replacement of the mafic detritus by varying amounts of fine grained quartz and feldspar to produce a white or grey weathering rock. The silicification is intense along dike margins, with the mafic dikes displaying abundant silica-feldspar-rich patches, whereas the clasts within the breccia display various intensities of bleaching, and some act as loci for epidote-rich alteration patches. These patches are decimetres in diameter, and when fully developed completely obliterate the form of the host clast. The alteration "egg-shaped" most commonly have an epidosite core, followed by an oligoclase-quartz-amphibole-rich margin, followed by an actinolite-rich rim. Zones with abundant epidote "eggs" are spatially associated with synvolcanic dikes (typically <5m from these dikes).

The mafic breccia units and transecting dikes are cut by a number of semi-conformable to discordant fracture systems (**Figure 18b**). These fractures vary in mineralogical zonation, but most commonly have epidote-rich cores with actinolite-garnet-rich margins and garnet-actinolite-rich rims. The epidosite cores are commonly host to syn-kinematic quartz veins. Mass balance calculations indicate that these fractures contain anomalous concentrations of Fe, Mg, Cu and Zn, with Zn to 5040 ppm and Cu to 778 ppm. It is proposed that the alteration facies observed at this stop represent the roots of the Chisel-Lalor VMS hydrothermal system. Injection of the Powderhouse dacite sill-dike complex at approximately 2000 mbsf (metres below seafloor) resulted in an overall increase in the thermal gradient within the water-rich Edwards formation. The criss-crossed injection of dikes into the breccia pile rapidly increased the temperature of connate seawater resulting in a rapid loss of permeability through secondary mineral formation. The silicification of 30–40% of the Edwards formation resulted in the remobilization of metals from the mafic volcaniclastic precursor. Dike injection and resultant silicification/feldspathization essentially sealed the underlying mafic tuff against the main dacite sill complex, resulting in the formation of a relatively closed system, high temperature reaction zone. This is manifested by the presence of the coarse-grained amphibole-garnet alteration, which is the metamorphosed equivalent to a high temperature, hydrous reaction zone enriched in metals. Periodic overpressuring of this reaction zone, or seismic activity, resulted in fracturing of the silicified breccias and associated dikes. This allowed escape of metal-enriched fluids along the adiabatic pressure gradient. The high temperatures, at which these hydrothermal processes took place, is reflected by their low $\delta^{18}O$ signatures (**Figure 10**). The alteration zone at this outcrop, which can be traced to the north into gahnite-bearing rocks, is considered to be part of the footwall hydrothermal system for the Lalor VMS deposit.

Location A (UTM: 6076208N; 426441E): Synvolcanic dikes intruding heterolithic mafic breccia

In general the level of alteration is less pronounced at the northwest end of the outcrop area, such that the original features of the volcaniclastic rocks are locally preserved. The breccia is composed of framework supported subangular to sub-rounded boulders up to 1.5 m in diameter. Most of the large boulders are porphyritic mafic blocks.

At location A the heterolithologic mafic breccia is intruded by a dark grey green weathering mafic (basalt?) dike that displays amoeboid margins and thermal contraction cracks, features that are consistent with intrusion of this dike into the breccia while it was still unconsolidated and water-saturated. The mafic dike both cuts and is cut by dacite dikes, indicating a complex chronology of dike emplacement. Adjacent to the mafic dikes the heterolithic breccia displays both pervasive and orbicular domains of epidotization; the latter are spatially associated with the mafic dikes (typically only occurring with 2–5 m of dike margins). This dike is a feeder for the overlying Moore formation basalts (**Figure 14**).

Location B (UTM: 6076111N; 426456E): Multiple episodes of dike emplacement and alteration

At this location >60% of the outcrop is composed of various mafic to felsic synvolcanic dikes. Both the dikes and the host mafic pebble wackes display considerable alteration. The

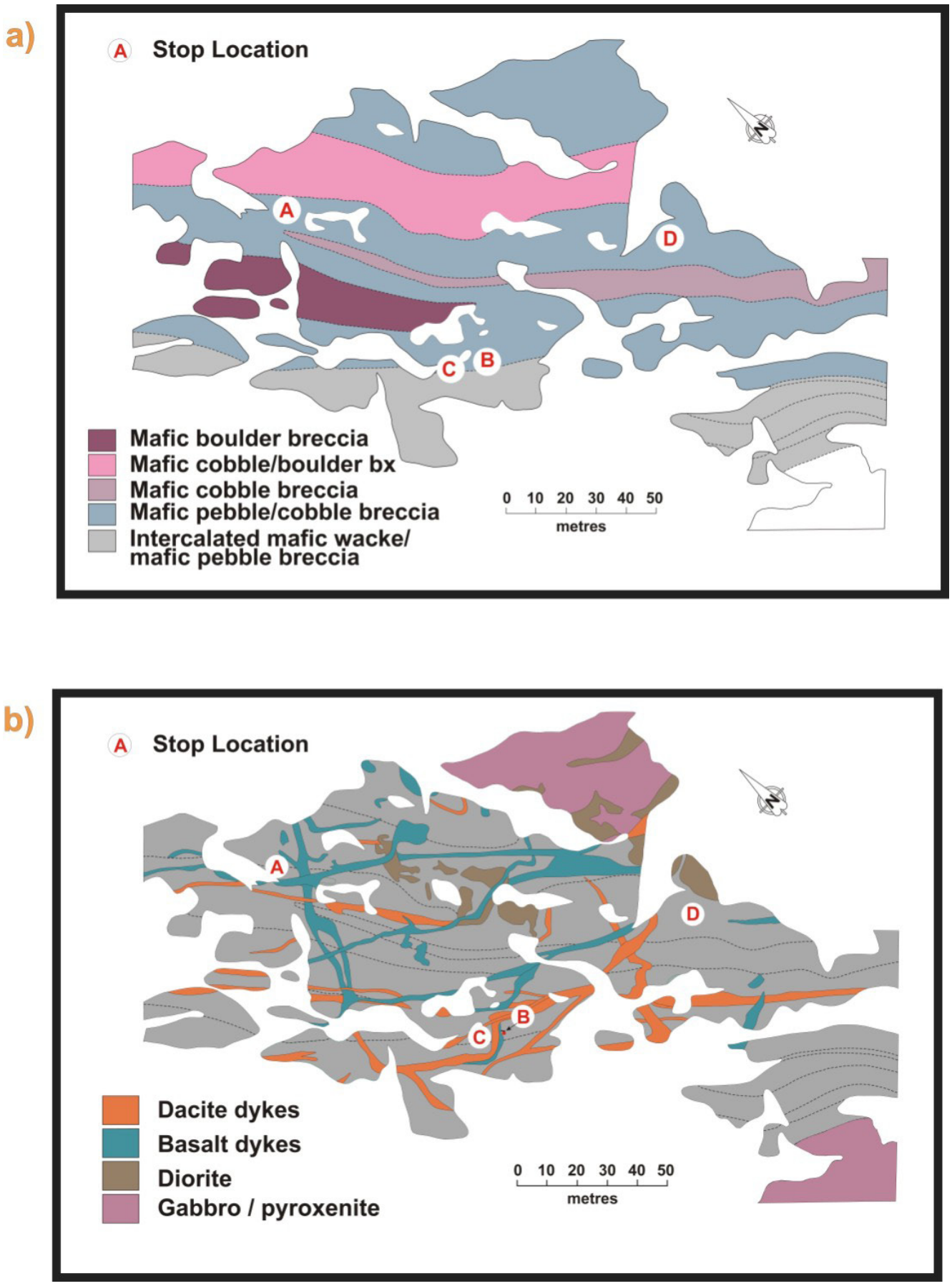

Figure 18: *Stop 7 is an example of Edwards formation volcaniclastic rocks that were altered within the high temperature hydrothermal reservoir 1.5–2 km below the Chisel-North Chisel-Lalor VMS deposits:* ***a)*** *Main supracrustal units with intrusive rocks removed;* ***b)*** *main intrusive units and* ***c)*** *distribution of altered rocks. Figure from Galley and Scoates (1990).*

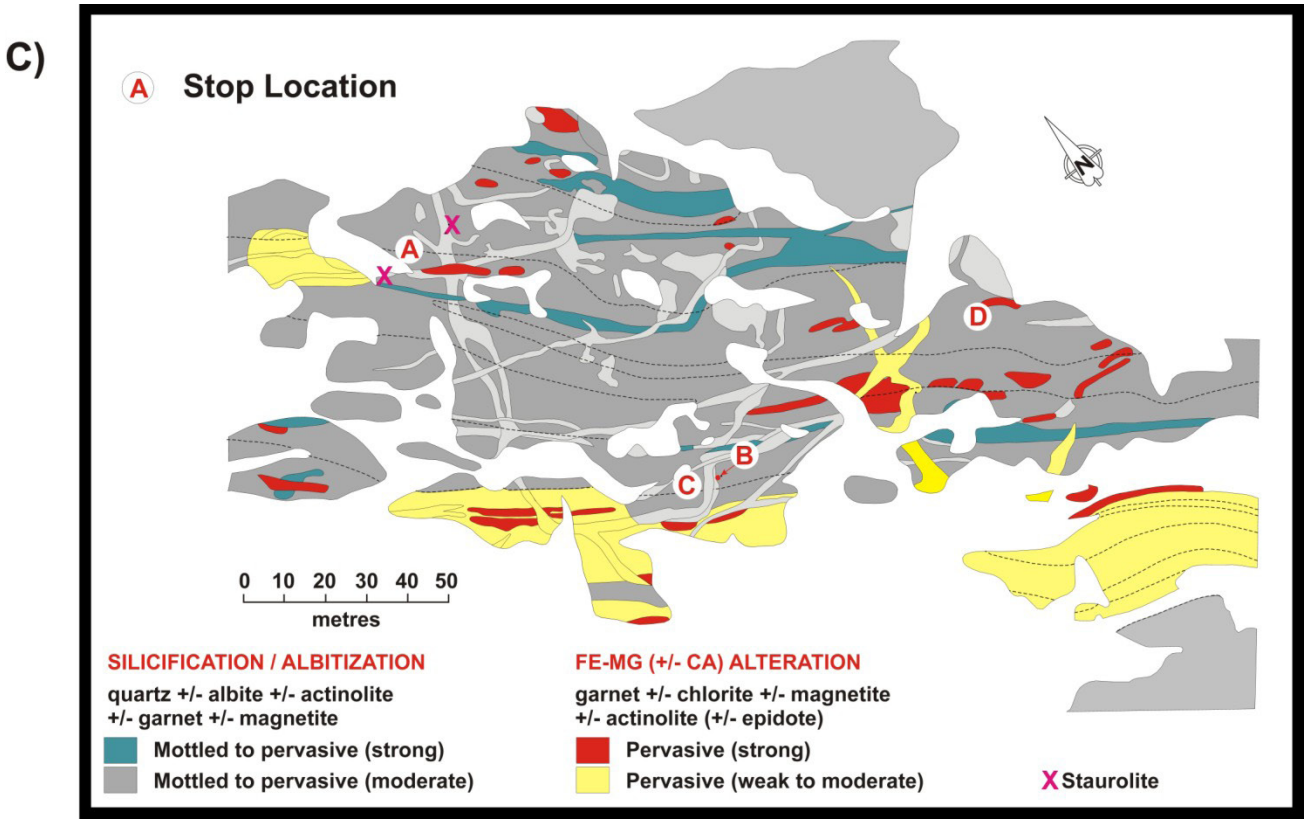

Figure 18 (continued): *Stop 7 is an example of Edwards formation volcaniclastic rocks that were altered within the high temperature hydrothermal reservoir 1.5–2 km below the Chisel-North Chisel-Lalor VMS deposits:* ***a)*** *Main supracrustal units with intrusive rocks removed;* ***b)*** *main intrusive units and* ***c)*** *distribution of altered rocks. Figure from Galley and Scoates (1990).*

relationship between the alteration and the dikes is most evident where a narrow mafic dike intruding well bedded mafic wacke displays an adjacent 1 to 3 cm zone of pervasive feldspathization-silicification (UTM: 6076108N; 426442E). In addition, the adjacent mafic tuff at this location is characterized by numerous small oval domains of fine grained quartz and plagioclase up to 50 cm from the dike margin. Feldspathization/silicification adjacent to the mafic dike is interpreted to be due to decreased silica solubility caused by rising temperature generated by dike intrusion, identical to the mechanism described for this type of alteration adjacent to the dacite dikes at Stop 6.

Location C (UTM: 6076107N; 426436E): Orbicular quartz-plagioclase rich domains overprinting both matrix and fragments

Orbicular quartz-plagioclase alteration structures overgrow both fragments and inter-fragment areas at this location conclusively demonstrating that alteration took place after deposition of the breccia. The orbicular alteration structures occur in two size ranges, 0.2 to 0.4 cm and 1 to 4 cm, but are otherwise identical. The small and large alteration structures, which occur together, are developed in irregular domains that cut across fragment boundaries.

Location D (UTM: 6076091N; 426511E): Zoned alteration in breccia fragments

Pervasively altered breccia fragments at this location display a wide variety of compositional zoning. Fragments typically have an epidosite-rich core surrounded by a quartz-feldspar-rich rim, but some fragments show a more complex zoning that can include actinolite rich cores, actinolite-garnet rich margins or, in some instances, both. In one fragment an amphibole-rich zone overprints earlier formed silica-rich and epidote-rich zones suggesting a complex interplay between the altering hydrothermal fluids and individual fragments. The breccia is cut by altered fractures filled and replaced by garnet-actinolite-chlorite.

Return along trail to canoe crossing and retrace steps to abandoned gravel pit (UTM: 6076601 N/0427900E). Proceed to the large outcrop south of the road.

STOP 8: Highly altered Moore Lake mafic breccias (UTM: 6075801N; 427304E)

The permeable nature of volcaniclastic rocks of the Edwards and Moore formations probably played an important role in the hydrology of the hydrothermal system that formed the semi-conformable alteration zone observed previously at Stops 6 and 7. Alteration in the eastern portion of the semi-conformable zone at Stop 6 is associated exclusively with volcaniclastic rocks of the Edwards Lake formation, but to the west it also affects the overlying Moore and Powderhouse formations. This is interpreted to be due to: (1) increasing primary permeability of the overlying Moore formation, accompanying a westerly facies change from massive and pillowed flows to more permeable flow breccia and debris flow deposits; and (2) the presence of a series of north-trending and crosscutting

synvolcanic faults that may have focussed hydrothermal fluid discharge (Bailes and Galley 1996). At this stop we will examine Moore Lake formation mafic breccias which have been affected by both semi-conformable alteration and focussed, fault-controlled (?) disconformable alteration. Synvolcanic faulting likely focused discharge of metal-enriched fluids from the underlying high temperature reaction zone in the Edwards formation and resulted in transport of the metals to the seafloor to form the Chisel Zn-Pb-Cu-Ag VMS deposit.

At Stop 8 an east-trending unit of variably feldspathized/silicified monolithologic Moore Lake formation mafic volcanic breccia (**Figure 5**, **Figure 14a** and **Figure 14b**) is cross-cut, at a high angle, by a prominent zone of chlorite-rich altered rocks characterized by abundant porphyroblasts of staurolite and garnet in a chlorite-biotite-rich groundmass. The crosscutting chlorite-rich alteration zone at this stop is likely related to a synvolcanic fault. In other places these faults host dacite feeder dikes to the overlying Powderhouse formation, along with localizing intense Fe-Mg metasomatism.

Least altered breccias at this stop include complete pillows as fragments and broken pillow pieces, and are interpreted to be pillow fragment breccias derived from cold fragmentation and slumping of Moore Lake basalt flows. Chemical analyses of pillow fragments from this breccia display the prominent light REE enrichment that characterizes Moore Lake basalt flows. We will first examine the least altered breccias in the centre of the outcrop (location A) and then proceed to the most altered portion at the east end of the outcrop (location B).

Location A (UTM: 6075801N; 427304E): Silicified/feldspathized and chlorite-rich altered mafic monolithologic breccia

The breccia at this location is coarse with many fragments up to 40 cm in diameter and rare blocks up to 1 m in size. It is composed of medium grey, light grey and white weathering blocks which appear to be a heterolithologic mixture of mafic to felsic fragments but which are actually variably feldspathized/silicified aphyric mafic fragments. The primary mafic composition of fragments is manifest by their morphology; most are broken pieces of pillows, some are complete pillows, and one large block comprises a piece composed of several intact pillows. Many fragments contain quartz amygdales. Rare slabby fragments of altered laminated mafic tuff (interflow sediments?) are present; they must have been lithified prior to incorporation into the breccia.

Pillow fragment pieces vary from relatively unaltered medium grey blocks to white weathering completely altered clasts composed almost entirely of quartz and feldspar. Many fragments are zoned with a less altered core (composed of amphibole, garnet, quartz, and fine grained plagioclase) and a 1–3 cm wide, white-weathering rim (composed of quartz, feldspar, minor amphibole and magnetite). Inter-fragment matrix is a completely recrystallized mixture of black amphibole, anhedral garnet, plagioclase, quartz and minor euhedral magnetite.

The alteration of breccias at location A probably occurred in two stages. The early stage involved feldspathization/silicification during which Fe and Mg were removed and SiO_2 was added. This stage of alteration is represented by replacement of mafic pillow fragments by quartz and feldspar. Zones of feldspathization/silicification completely rim margins of broken pillows indicating that this alteration post-dated deposition of the breccia. The second stage of alteration consisted of addition of Fe and Mg and is represented by garnet, amphibole and chlorite-rich rocks. This stage of alteration began with the overgrowth of permeable interfragment domains, and proceeded to alter the previously silicified pillow fragments. The zone of Fe-Mg metasomatism becomes more intense towards location B. Proceeding east towards the crosscutting zone of intensely altered rocks at location B, the breccia is gradually overprinted by Fe- Mg-rich minerals such as garnet, chlorite and amphibole. Initially, the garnet-chlorite-amphibole alteration-assemblage is confined to the interfragment domains (i.e., zones of high permeability) but as location B is approached the fragments themselves are also affected. The altered breccia just west of the staurolite-bearing zone is a garnet-amphibole-biotite-rich rock with numerous white quartzo-feldspathic fragments. The inter-fragment domains are composed amphibole, biotite, garnet and plagioclase. The fragments contain up to 5% garnet but virtually no other ferromagnesian minerals.

Location B (UTM: 6075801N; 427304E): Staurolite-garnet-chlorite-biotite-rich altered rocks

The strongly altered staurolite-rich rocks at location B form a cross-cutting north-trending zone. The contact of this zone of alteration is rapidly gradational to the west into the less altered equivalents exposed at location A. The most strongly altered rocks are characterized by subhedral to euhedral honey brown to dark brown staurolite porphyroblasts (up to 5 cm long). In this zone, fragments are much less conspicuous than to the west, and where preserved are composed of quartz and feldspar with up to 50% anhedral garnet. The remainder of this zone is composed of 20% subhedral to euhedral staurolite, anhedral to euhedral garnet, biotite, chlorite, and 50% fine grained quartz and plagioclase. It is not surprising that this rock was misidentified as pelitic schist by early geologists (Harrison, 1949).

Return to vehicles and retrace route to first junction. Continue past junction for 50m (UTM: 6076279N; 427656E). Location A of Stop 9 is just west of road.

STOP 9: Distal part of the discordant Chisel Mine footwall alteration zone (in Powderhouse dacite)

A 100–250 m thick unit of plagioclase phyric dacite tuff and lapilli tuff forms the stratigraphic footwall to the Chisel Lake, Lost Lake and Ghost Lake Zn-Cu massive sulphide deposits. The dacite tuff is typically a massive, pale buff weathering unbedded rock with 5–15% tablet shaped plagioclase phenocrysts and glomerophenocrysts (0.5 to 2mm). It locally contains angular white weathering plagioclase phyric lithic felsic fragments and is occasionally well-bedded. The dacite tuff is identical in texture and chemical composition to the dacite dike complex observed previously at Stop 6. At this stop relatively unaltered dacite tuff (Location A) is compared to altered equivalents (Location B). The altered rocks at location B can be traced to the north (with a minor break) into the footwall alteration zone below the main Chisel Mine orebody.

Location A: Relatively unaltered Powderhouse dacite (UTM: 6076332N; 427628E)

Massive, homogeneous dacite tuff typical of the Powderhouse unit occurs at this outcrop located just west of the road. The characteristic plagioclase phenocyrsts and small white lithic felsic fragments of the Powderhouse formation are present, as well as local scoria lapilli. Minor alteration of the dacite has occurred and this is indicated by the presence of scattered, small porphyroblasts of garnet and actinolite.

Location B: Altered Powderhouse dacite (UTM: 6076263N; 427748E)

One hundred and fifty metres east of location A on the other side of the access road, the same rocks are intensely altered; the alteration is patchy in development and comprises 30–35% garnet, 25–30% quartz, 15–20% biotite, 10–15% staurolite and 2–5% sericite. Textures of the original rock are generally obliterated. Whole rock analyses indicate a depletion of CaO and Na_2O and an increase in total iron content relative to the rock at location A.

Return to vehicles and retrace route to beginning of the ramp at the Chisel Lake open pit. Proceed 1.2 km to the south along the abandoned rail bed and then follow the short trail east to join up with the Edwards Lake trail/road. Follow this road to the north (left) to the Chisel Lake minesite. Park vehicles where access to an east-trending road is blocked by mine waste (UTM: 428550E/ 6076498N). Proceed approximately 500 m down the road to the east by foot.

STOP 10 (UTM: 6076471N; 429000E): Surface expression of the Ghost Lake "mine horizon"

The Ghost lake orebody is within 100 m of surface at Stop 10.The surface expression of the Ghost Lake mine "horizon" is a 30–60 cm thick unit of coarse heterolithic felsic fragmental rocks (Figure 19). In the Ghost Lake Mine, this felsic fragmental unit may be up to 10 m thick where it commonly occurs adjacent to the massive sulphide zone (N. Provins, pers. comm., 1987). At Stop 10, the felsic fragmental unit is matrix-supported and consists of quartz-feldspar phyric felsic fragments up to 45 by 18 cm in size. Fragments have highly irregular of sub-rounded shapes, some with silicic margins up to 1 cm thick. A thicker unit of the felsic breccia is exposed on the southwest shore of Lost Lake (UTM: 6076514N; 428476E). The felsic fragmental unit is interpreted to be part of the Powderhouse tuff-breccia bed that 1.4 km to the west southwest (**Figure 19**) is up to 100 m thick and occurs at the base of the Powderhouse formation.

At Stop 10, the felsic breccia is underlain to the east by laminated (bedding stikes 340° and dips 83°), weakly altered and gossaned intermediate volcaniclastic rocks of the Powderhouse formation. These rocks are well layered and display many primary sedimentary structure including size grading, parallel lamination, convolute lamination, scours, and flame

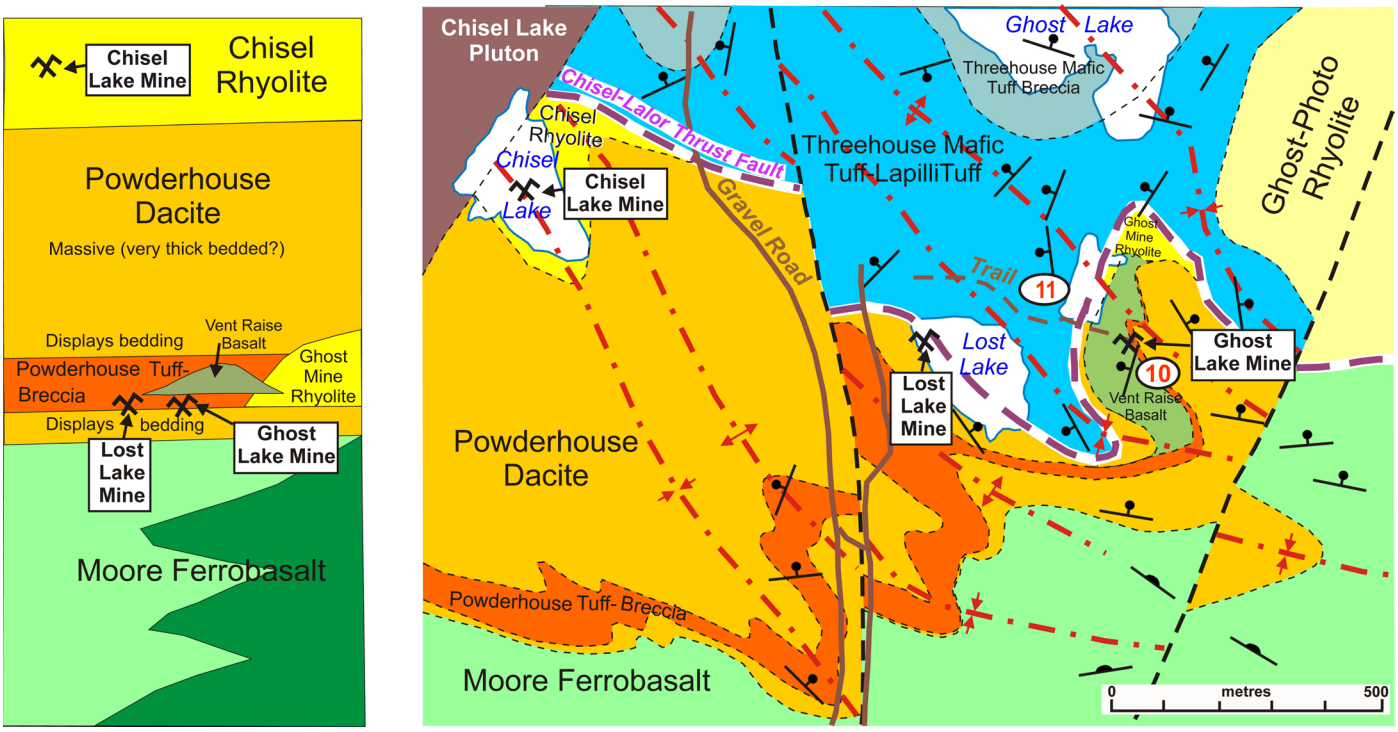

Figure 19: *Plan view of the distribution of rock units hosting the Chisel, Lost and Ghost lakes VMS deposits. Note the angular discordance between the Chisel rhyolite, Powderhouse dacite and Moore ferrobasalt (of the Lower Chisel Sequence) with the Threehouse Formation and Ghost-Photo rhyolite (of the Upper Chisel Sequence) along the interpreted trace of the Chisel-Lalor thrust fault (Bailes et al., 2009). Note the truncation of the Powderhouse tuff breccia unit at the fault surface, with the tuff breccia occurring 600m south of the Chisel Lake VMS deposit and directly underlying the contact and the Ghost Lake VMS deposit to the east. The sulphide deposits and host rocks are deformed by northwest- trending F_2 folds and north-northeast trending open F_3 folds. The folding of the Chisel-Lalor thrust fault by F_2 folds suggest that it is a D_1 structure. A simplified stratigraphic section to the left shows the important units in the Lower Chisel sequence and location of VMS deposits interpreted to occur at two stratigraphic levels.*

structures. Bed thickness is from 15 cm to 1.2 m. Bouma B and AB bed zonation predominates.

To the west the felsic breccia is overlain by a narrow unit of altered bedded intermediate tuff followed by a 75 m thick unit of aphyric basalt (Vent Raise basalt, **Figure 19**). The overlying basalt, which is mainly massive, with local faint "pillow" selvages, contains quartz amygdales up to 1 cm in diameter. The basal 2 m of the basalt is intensely brecciated (blocky pepperite) with interfragment epidotized tuff and quartzofeldspathic cement. This breccia zone is up to 11 m thick at a locality 60 m to the north. The upper several metres of the flow is exposed in small outcrops in a low area to the west (south of the road). Here the flow comprises mainly flow-top amoeboid breccia. The upper contact of the basalt with the overlying intermediate volcaniclastic rocks (Powerhouse dacite?) is unfaulted with local pepperite, but the latter can only be observed at the water's edge when water levels are low. The basalt is likely a cryptoflow (shallow synvolcanic intrusion; H. Gibson, pers com., 2012).

The contact between the rocks observed at Stop 10 and 11 is interpreted to be a fault (Chisel-Lalor thrust fault) for reasons presented in the discussion of the virtual Stop 12.

Proceed west (back) on the road and climb the first outcrop north of the road beyond the swampy area.

STOP 11: Threehouse mafic volcaniclastic rocks

Introduction

The Threehouse formation consists of an approximately 50 m thick unit of well-bedded, mafic tuff and lapilli tuff followed up section by several hundred meters of poorly bedded, scoria-rich mafic tuff-breccia and heterolithologic mafic breccia. Discrete beds of heterolithologic mafic breccia up to 30 m thick are present in the upper poorly bedded part of the unit. These tuff breccia beds are debris flow deposits composed of a lithologically diverse suite of matrix supported mafic bombs and clasts, with rare rhyolite fragments (e.g., UTM: 6077035N; 428288E). Although many of the rocks stratigraphically below the Threehouse formation volcaniclastic rocks are intensely altered (e.g., in the Chisel Open Pit and elsewhere), the Threehouse formation rocks everywhere are remarkably unaffected by alteration. The Threehouse mafic volcaniclastic rocks exposed at Stop 11 are part of the 50 m interval of well-bedded, mafic tuff that forms the base of the Threehouse formation (**Figure 14**a).

Proceed north from the trail/road along the cliff face for approximately 30 m to location A of Stop 11.

Location A (UTM: 6076584N; 428868E): Large scour channel and bomb sag in mafic tuff

The outcrop at location A is best observed on a ledge part way down the cliff face and looking west. Here well-bedded mafic tuffs display excellent graded bedding, a large scour channel, load structures and a bomb sag with lee side cross bedding. The bomb sag indicates explosive volcanism was contemporaneous with turbidity current transport and deposition of the bedded mafic tuff. The mafic tuff dips shallowly to the west (strike 060° and dip 15°) in sharp contrast to the steep dip of bedding (>60°) in the underlying Powderhouse dacite at Stop 10.

Proceed up stratigraphy (to the west and slightly south) for approximately 30 m. Note thick beds of graded mafic tuff and lapilli tuff on route to Location B

Location B (UTM: 6076580N; 428831E): Cross bedded mafic tuff and lapilli tuff

This outcrop is composed of well-bedded, laminated and normally graded mafic tuff and lapilli tuff characterized by prominent trough cross bedding. The bed forms and primary sedimentary structures for this outcrop are sketched in **Figure 20**. Bed bases are typically composed of granular mafic tuff and lapilli tuff composed of phenoclasts of plagioclase and amphibole-replaced pyroxene. Pebble lags of coarse pyroxene (pseudomorphed by amphibole) phenoclasts occur along foreset laminae in some cross bed sets. Bed tops are typically fine grained and epidotized. Mafic mud tops to beds, which are commonly completely epidote-replaced, locally display asymmetrical ripples with mud drapes. Orbicular feldspathic domains, which resemble accretionary lapilli, are interpreted to be alteration features because elsewhere zones of these structures crosscut bedding. Besides phenoclasts the lapilli tuff is composed of dark angular shards, abundant scoria, and local cored bombs and accretionary lapilli.

The bed forms at this outcrop suggest deposition occurred in either a fluviatile and/or inter-tidal environment coincident with a shoaling active volcano. In either interpretation, the environment of deposition was subaerial or very shallow marine. This is in sharp contrast to the subaqueous environment displayed by the underlying Lower Chisel sequence. Heterolithic, matrix-supported, mafic breccias higher in the Threehouse formation (not exposed here) form beds up to 30 m thick that likely represent debris flow deposits triggered by wave undercutting of the emergent portions of the volcano and deposition in basin areas surrounding the central edifice(s).

Stop 12: Drill cross section, Lalor VMS deposit (virtual stop)

Although only partially addressed by Bailes and Galley (2007, 1999, and 1996), the contact between the Lower and Upper subdivision of the Chisel sequence has been problematic for years. This is because a satisfactory explanation for a number of features associated with this contact has been elusive. Some of the puzzling features associated with this contact are:

1. different rocks directly underlie the contact (e.g., Anderson sequence rocks at the Anderson Lake VMS deposit and Lower Chisel rocks at the Chisel Lake VMS deposit);
2. variable rocks occur in the hanging wall to this contact (e.g., the change in hanging wall rocks directly along this contact from the Chisel Lake to the Chisel North deposits; **Figure 5** and **Figure 21**; Galley et al., 1993; Bailes et al., 1997);
3. different stratigraphy north and south of the Threehouse formation rocks north of the Chisel Lake deposit (Map 2007-1; Bailes and Galley, 2007); and

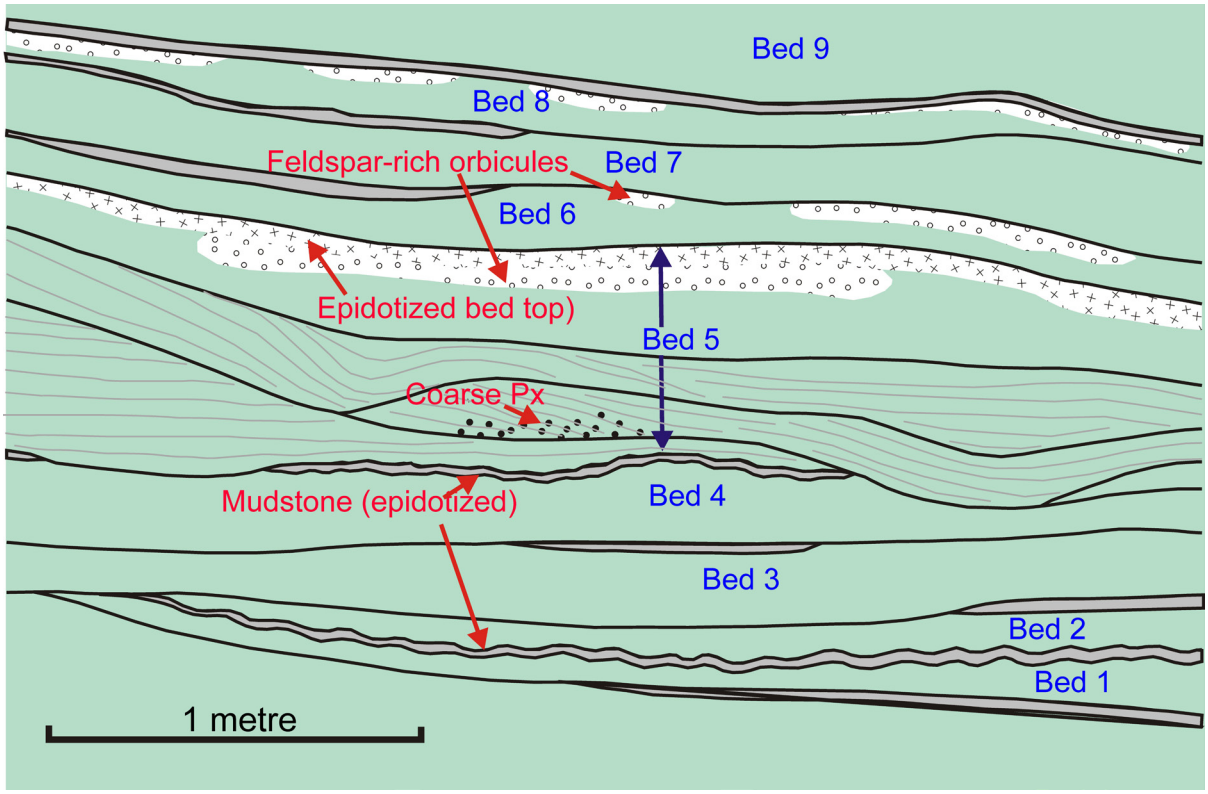

Figure 20: *Sketch of outcrop at Stop 11 showing well bedded Threehouse mafic volcaniclastic rocks with numerous primary features. Beds are typically normally size graded.*

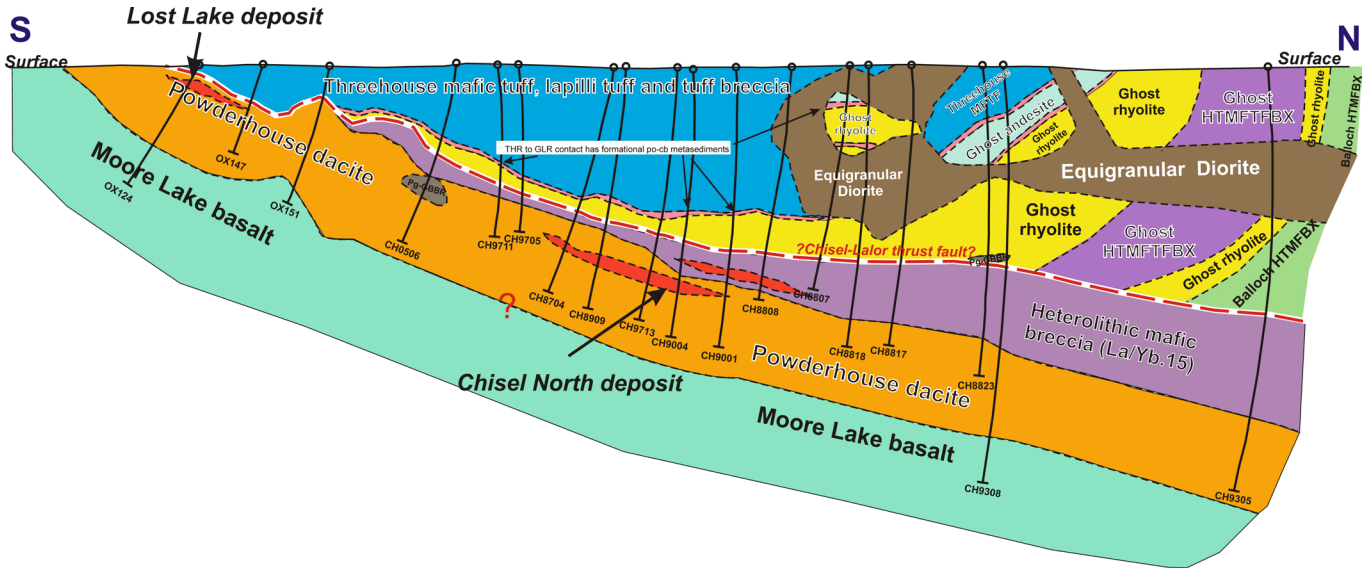

Figure 21*: Vertical cross section (UTM 428650E) looking west showing the Lost Lake and Chisel North VMS deposits (from Bailes, 2012b). Note the discontinuity between units of the Upper Chisel Sequence and those of the VMS-hosting Lower Chisel Sequence and the continuation of the mineralization to depth to the north.*

4. folds localized below and above the contact in the Chisel Lake area that cannot be traced laterally and, in many instances, have truncated fold limbs (**Figure 21**).

A number of different interpretations have been entertained over the years to explain the above features. The one adopted by Bailes and Galley (2007) was that the sequence is conformable and along strike variations are due to a combination of facies variations in volcanic constructs (e.g., local effusive centres) and unrecognized volcano-tectonic depressions (e.g., caldrons). Other possibilities considered, but eliminated in favour of the above explanation, included the contact being a disconformity along which significant erosion occurred (Bailes and Simms (1994) or a thrust fault that disrupted the sequence

(Bailes et al., 1996). The interpretation of the contact as a disconformity was dropped as a less elegant interpretation than the facies variation explanation. The thrust fault interpretation was considered unlikely as no fault surface was ever identified in outcrop despite careful examination of the contact area at several well exposed localities. In addition synvolcanic feeders for the Threehouse formation volcanic rocks (Upper Chisel rocks) are abundant in the underlying Lower Chisel rocks, consistent with it being a structurally intact section.

Exploration diamond drill holes at the Lalor deposit were examined by Bailes (internal reports, HBED, 2008, 2010). In the hangingwall to the Lalor deposit, the drilling intersected a steep-dipping, southwest-facing sequence of units identical to those mapped at surface by Bailes et al. (1997) but, below the deposit, they intersected an entirely different sequence (**Figure 22**). Rocks intersected in the footwall resemble rocks that occur in the footwall to the Chisel and Chisel North deposits (e.g., Powderhouse and Moore formations). An angular discordance of 60–45° exists between the orientation of rocks in the structural hangingwall and the dip of Lalor ore zone. This strongly suggests that the top of the Lalor deposit is a structural discontinuity, most likely a thrust fault.

The presence of a thrust fault in the hanging wall of the Lalor-Chisel North-Chisel Zn-rich VMS deposits requires a fundamental shift in the way in which the geology of the Snow Lake area is viewed and interpreted. In the past the volcanic rocks of the Snow Lake arc assemblage have been considered to be part of a structurally intact section in which a succession of discrete geochemically identifiable sequences occurs: Anderson sequence (primitive arc), Chisel sequence (lower and upper subdivisions, mature arc) and Snow Creek sequence (arc rift). A thrust fault in the structural hanging wall to the Chisel-Chisel North-Lalor VMS deposits means that the Snow Lake arc assemblage is not structurally intact and there is a fundamental break at the contact between the Lower and Upper Chisel subdivisions. Is the sequence above the structural break is in anyway related to the underlying rocks? The presence of synvolcanic Threehouse formation intrusions in the footwall to the deposits that cut hydrothermally altered rocks suggests that the upper side of the thrust may be fairly local in origin. Although this may be valid, the volume of syn-Threehouse intrusions in the footwall to the thrust is an order of magnitude less than in the structural hanging wall and this allows the two structural panels to be structurally far travelled.

Stop Descriptions 13 to 16: Geology and hydrothermal alteration features in the Anderson Lake-Stall Lake mine area

Introduction

The 1 by 12 km Anderson rhyolite body is the largest of three felsic extrusive complexes in the upper 1 km of the

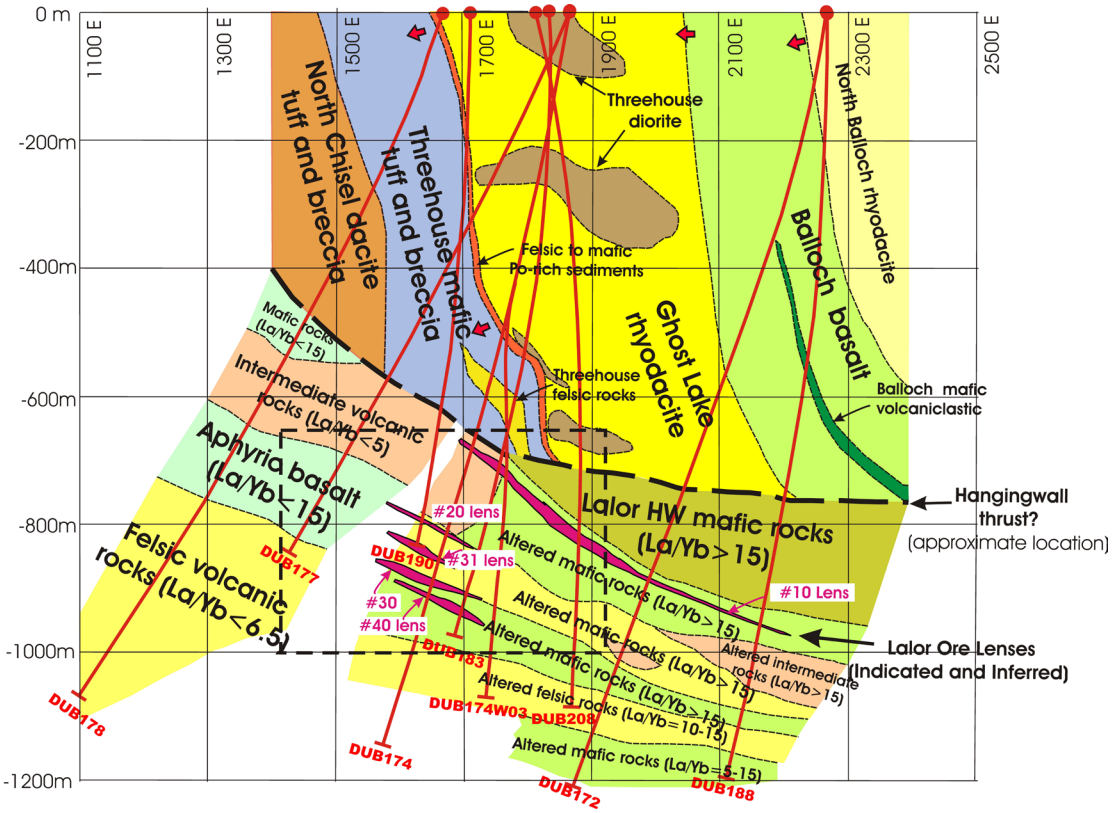

Figure 22: *Vertical section of the geology on S5200N based on re-logging of drill holes by Bailes (2008, 2009). Note the steep dipping southwest facing sequence of rocks in the hangingwall to the Lalor deposit and the 40–60° angular discordance between the footwall and hangingwall rocks that is most logically interpreted as a structural break (thrust fault). Rocks above a proposed hangingwall thrust fault belong to the Upper Chisel Sequence and all display La/Yb <5. Rocks below the thrust fault belong to the Lower Chisel Sequence and display variable La/Yb ratios, but many are above 15 similar to the values shown by the Powderhouse and Moore "formations". The rectangle shows the area shown in* ***Figure 43****.*

Anderson sequence at Snow Lake (**Figure 8**, **Figure 9**, **Figure 10** and **Figure 23**). Near the Stall Lake deposit, the basal 750 m of the Anderson rhyolite is aphyric and massive, and is overlain to the north by 100 m of quartz-phyric and 150 m of quartz megacrystic varieties (**Figure 24**). The aphyric unit shows very little in the way of texture variation, whereas the quartz phyric unit has distinct examples of lobe-hyaloclastite flow facies and associated autoclastic flow breccia. The quartz megacrystic unit is characterized in places by coarse, monolithic breccias. The change with time from aphyric through quartz phyric to quartz megacrystic is typical for a rhyolite flow complex that was built through eruption from a fractionating magma chamber.

The Anderson rhyolite hosts three mined-out Cu-rich deposits (Anderson, Stall and Rod) that originally contained a total of 11.0 Mt with an average grade of 4.27% Cu, 0.56% Zn and 1.5g/t Au (Bailes and Galley 1996). It also hosts the low-grade 13 Mt Linda deposit grading 0.3% Cu and 0.79% Zn (Zaleski et al., 1991), and two sub-economic, stockwork-type zones (Joannie and Ram). The original character of the Anderson rhyolite is obscured by intrusion of the synvolcanic Sneath Lake intrusive complex, by large areas of hydrothermal alteration, by tight folding about the F_2 Anderson Bay anticline, and by recrystallization to lower almandine amphibolite facies mineral assemblages during regional metamorphism. Recrystallized lithologies are composed of fine-grained granoblastic mosaics of quartz, feldspar and biotite, with varying amounts of amphibole, garnet, sericite, chlorite, staurolite and kyanite that increase in amount with degree of hydrothermal alteration. Both the Anderson and Stall are located at the contact between the lower aphyric member of the Anderson rhyolite complex and the overlying quartz phyric phases.

The complex pattern of metamorphosed alteration assemblages in and around the Anderson rhyolite complex can be divided into a series of stacked, sub-concordant alteration zones. In the footwall stratigraphy to the VMS deposits the sub-concordant alteration zones represent seawater-related hydrothermal alteration developed along a thermal gradient centered on the underlying Sneath Lake intrusive complex. These zones are cut by a number of discordant, metamorphosed, aluminosilicate-rich alteration zones that can be spatially related to overlying VMS deposits (**Figure 18b**). Quartz-plagioclase-rich alteration of basalt flows in the hangingwall stratigraphy to the VMS deposits is related to the same low temperature (200–300°C), shallow sub-seafloor event observed at Stops 2 and 3 of the fieldtrip. The thermal history of the Anderson-Stall-Rod hydrothermal system is elucidated by oxygen isotope mapping (**Figure 23a**). Shifts in oxygen isotope defined during synvolcanic fluid-rock interaction indicate that the semi-conformable alteration directly overlying, and including, the Sneath Lake subvolcanic intrusive complex, was formed at high temperatures (>350°C). The discordant pipes below Anderson and Stall VMS deposits also define high temperature alteration zones. The lack of an appreciable oxygen isotope shift (<6 or >9 per mil $\delta^{18}O$) for much of the Anderson rhyolite suggests that the chlorite-biotite-staurolite-rich alteration originally formed at relatively low fluid-rock ratios, i.e. rock-dominated reactions, at low temperatures, or that there may have been a magmatic component to the hydrothermal fluid. The >9 per mil $\delta^{18}O$ zones within the hangingwall strata to the VMS deposits indicates that quartz and feldspar addition took place in a temperature range between 200 and 300°C.

During this part of the field trip the role played by the Sneath Lake intrusive complex in generating hydrothermal activity and the VMS deposits will be presented at Stop 13. This will be followed by examination of hydrothermally altered rocks in the Anderson rhyolite at Stops 14 and 15, part of the stratigraphic footwall alteration zones to the Stall Lake and Anderson Lake Cu-Zn VMS deposits respectively. At Stop 16, a zone of silicification/albitization in the hanging wall to the Stall Lake mine will be examined. Rocks at the latter stop will be readily recognized as the more strongly deformed and recrystallized equivalent of the alteration zone examined at Stops 2 and 3. Also to be observed at Stop 16 is the potential trace of the thrust fault at its contact with an overlying Upper Chisel sequence rhyolite flow.

On Highway 392, proceed 3 km south past the intersection with Highway 393 and turn vehicles around on a small access road on the east side of the highway. Stop 13 is a poorly exposed small outcrop exposed on the east side of highway 392 approximately 0.7 km north of the access road. Because highway 392 is busy, park vehicles well off the road on its east side and progress with caution from the car to the outcrop.

STOP 13: Sneath Lake Synvolcanic Intrusive Complex (UTM: 6077921N; 439143E)

The SLIC is very well exposed in many localities in the Snow Lake area but none are readily accessible. Stop 13, which consists of hydrothermally altered quartz phyric leucotonalite containing abundant garnet and staurolite porphyroblasts produced during 1.81 Ga regional metamorphism, is an opportunity to observe a typical altered variety of the SLIC and, more importantly, to discuss the geology of the SLIC and its place in the generation of the VMS deposits within the Anderson sequence.

The SLIC is part of the Anderson sequence which is a flow-dominated dominated basalt-rhyolite volcanic succession near the base off the Snow Lake arc assemblage (**Figure 6**, **Figure 7** and **Figure 8**).The SLIC is 18 km long and up to 2500 m thick, with an average thickness between 1000 and 1500 m. There is an asymmetric distribution of internal phases, which proliferate within the two ends of the intrusion (**Figure 6**). Remnants and xenoliths of equigranular massive tonalite occur along the upper contact of the SLIC. This xenolithic phase contains abundant angular to sub-rounded inclusions of amphibolite, gabbro and quartz diorite up to 2 m in diameter. The xenoliths are the only evidence that there may have been an early mafic phase to the composite intrusion. The tonalite is characterized by up to 15% hornblende. The restriction in distribution of the multiple tonalite phases to either end of the SLIC suggests their emplacement as stocks or small sills directly below a volcanic eruptive centre. This conclusion is supported by the fact that the two largest rhyolite flow complexes within the host volcanic rocks lie directly above the two ends of the composite intrusion.

A series of hornblende-biotite to biotite-bearing trondhjemite stocks overprint the tonalite at the two ends of the composite intrusion. A number of quartz phyric trondhjemite stocks

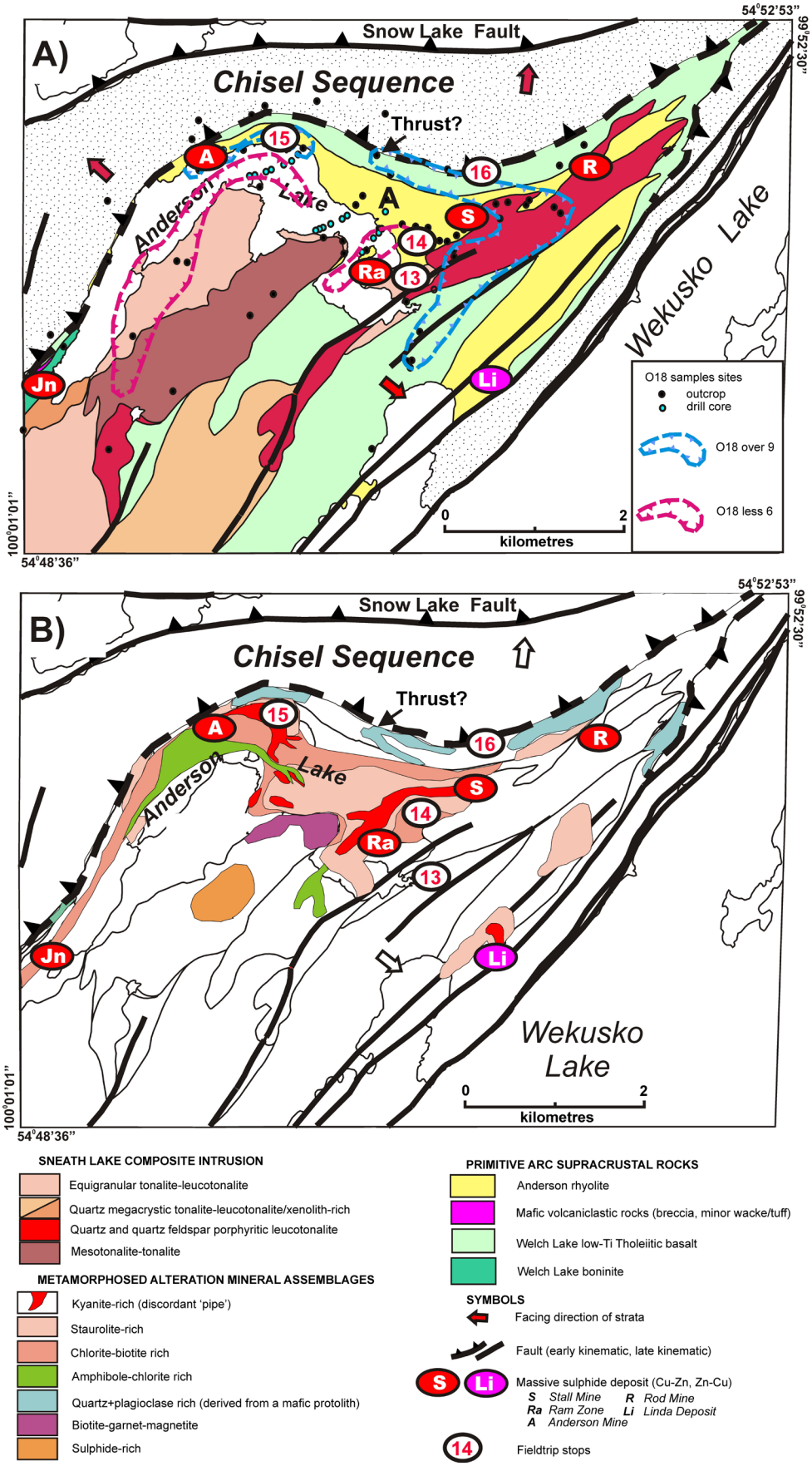

Figure 23: a) *Generalized geology of the Anderson sequence, which hosts the Anderson, Stall, Rod and Linda VMS deposits, overlaid by anomalous whole rock isotope patterns defining both high T (< 6 per mil) and low T (>9 per mil) portions of the alteration system.* ***b)*** *Distribution of mineralogically defined alteration facies associated with the Anderson-Stall-Rod-Linda hydrothermal system (after Galley and Bailes, 2002).*

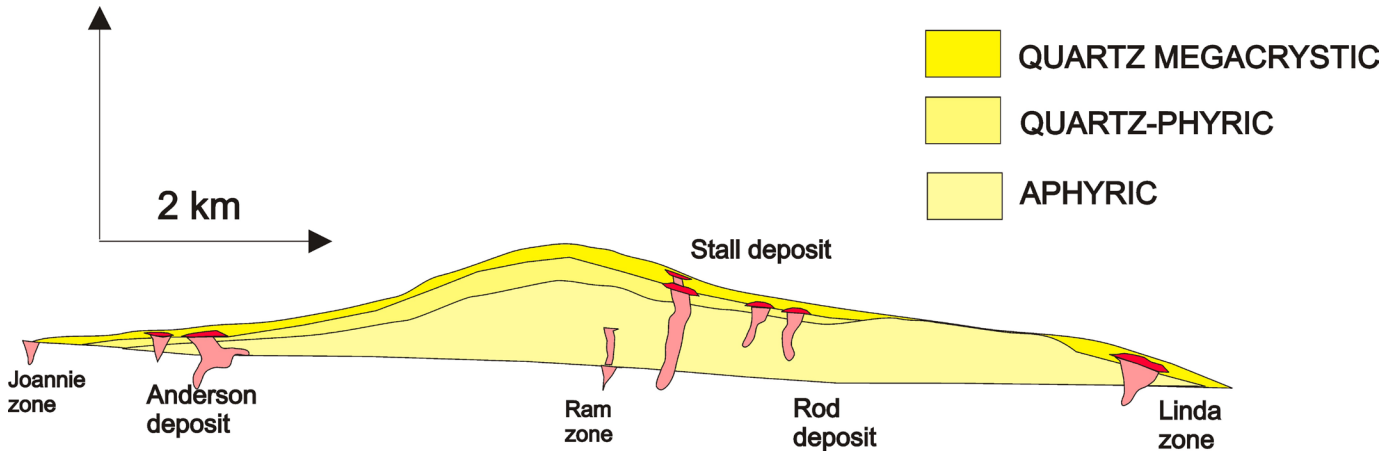

Figure 24: *Reconstruction of the Anderson rhyolite in cross section to illustrate the different flow units and the position of the VMS deposits and major base metal sulphide occurrences.*

are enveloped by at least two pulses of quartz megacrystic trondhjemite. At the western end of the SLIC the quartz phyric stocks remain as pendants within the first phases of quartz megacrystic trondhjemite. The western margin of this body contains well-developed columnar joints. The second quartz megacrystic phase occupies the core of the SLIC as a sill 5 km long by up to 2000 m thick. Sharp-sided dikes of the quartz megacrystic trondhjemite cross the earlier formed tonalite phases, but contacts between the different trondhjemite phases are gradational over centimetres to tens of metres. Convincing evidence that the central, quartz megacrystic sill is younger than the quartz phyric stocks is the presence of altered pendants of the latter.

At the east end of the SLIC a quartz phyric trondhjemite stock transects all previous phases and intrudes the overlying rhyolite complex and envelops the rhyolite-hosted Rod VMS deposit. Dikes associated with this phase intrude into the basaltic andesite overlying the VMS-hosting rhyolite complex. Both ends of the SLIC are transected by mafic dike swarms that are co-magmatic with basaltic flows in younger volcanic successions.

The rocks in the Snow Lake arc assemblage are inadequately dated due to low HFSE concentrations resulting in little zircon (Stern et al., 1995b). A discordant U-Pb zircon crystallization age of 1886 Ma is reported for the SLIC (Bailes et al., 1991). The only U-Pb date from the host volcanic succession comes from a felsic volcaniclastic bed within the overlying Stroud formation at 1892 Ma (David et al., 1996). The Stroud formation contains many clasts that are texturally and compositionally identical to the quartz megacrystic phase of the SLIC.

The SLIC also shows evidence that at least part of its emplacement history took place after formation of the Anderson sequence Cu-Zn VMS deposits (**Figure 6**, **Figure 8**, **Figure 9** and **Figure 25**). Only the tonalite and trondhjemite stocks clustered at either end of the composite intrusion are hydrothermally altered to any extent. These stocks lie directly beneath, and in some cases intrude the VMS-mineralized rhyolite that has been demonstrated to be co-magmatic with the SLIC (Bailes and Galley, 1999). The quartz megacrystic trondhjemite sill that forms the centre of the SLIC is not only unaltered, but contains chlorite-staurolite-garnet-rich xenoliths and pendants of previously altered trondhjemite. The quartz phyric trondhjemite stock at the far east end of the SLIC is clearly represents a post-VMS intrusive phase as it has enveloped the Rod VMS deposit. It appears then that only the quartz diorite (?)-tonalite-trondhjemite stocks directly below the VMS hosting rhyolites were present at the time of VMS-related hydrothermal alteration.

Much of the SLIC may have been involved in hydrothermal activity that post-dated VMS mineralization and took place at the end of the Anderson sequence volcanism. The top of the Anderson sequence is defined by the Foot-Mud horizon, a unit of sulphidic mudstone-chert and felsic epiclastic units that is metres thick (**Figure 6**, **Figure 8**, **Figure 9** and **Figure 25**). This sulphidic unit has almost the identical strike length as the underlying SLIC (except at the east end where it has been removed by a later thrust fault). Furthermore, it is underlain along its entire strike length by several hundred metres of variably silicified basaltic andesite (Skirrow and Franklin, 1994). The high $\delta^{18}O$ values (> 9 per mil) for the silicified mafic volcanic rocks (Figure 18a) suggest that the alteration was a product of relatively low temperature sub-seafloor seawater-rock interaction. The entire SLIC may have therefore acted as a heat source to generate a shallow, diffuse, but areally extensive hydrothermal event which resulted in the hydrothermal component of the Foot-Mud horizon.

Stop 14 is located on the east side of the highway, 800 m south of intersection with Highway 393 and approximately 500 m north of Stop 13. Park vehicles as far off the road surface as possible, and proceed with caution to the outcrop. This is a busy section of road with rapidly travelling vehicles.

STOP 14 (UTM: 60798509N; 438915E): Altered Anderson rhyolite adjacent to Stall alteration pipe

Aphyric rhyolite at this outcrop is approximately 300 m stratigraphically below the Stall Lake orebody. It displays a pervasive and characteristic alteration mineralogy that is typical of the lower semi-conformable alteration zone (**Figure 23b**). The disconformable Stall Lake alteration "pipe" is poorly exposed 200 m to the north in small outcrops east of the road. The Stall Lake alteration "pipe" will not be examined at this locality as the similar and much better exposed disconformable alteration zone to the Anderson orebody will be examined at the next stop

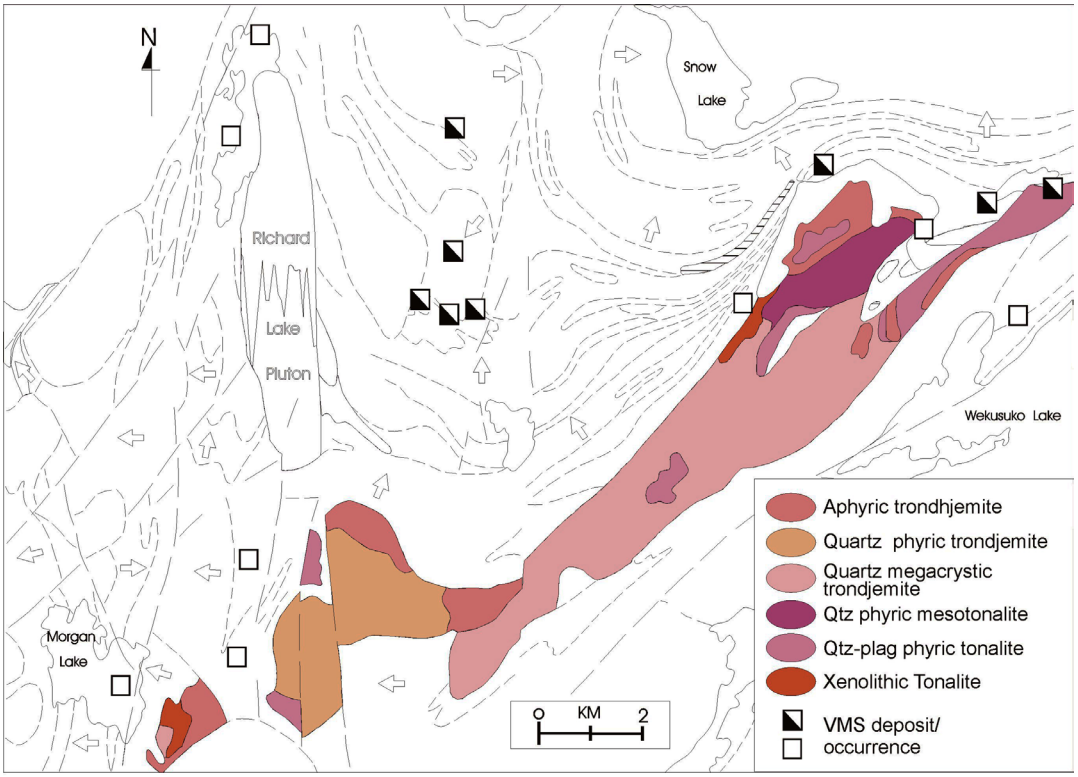

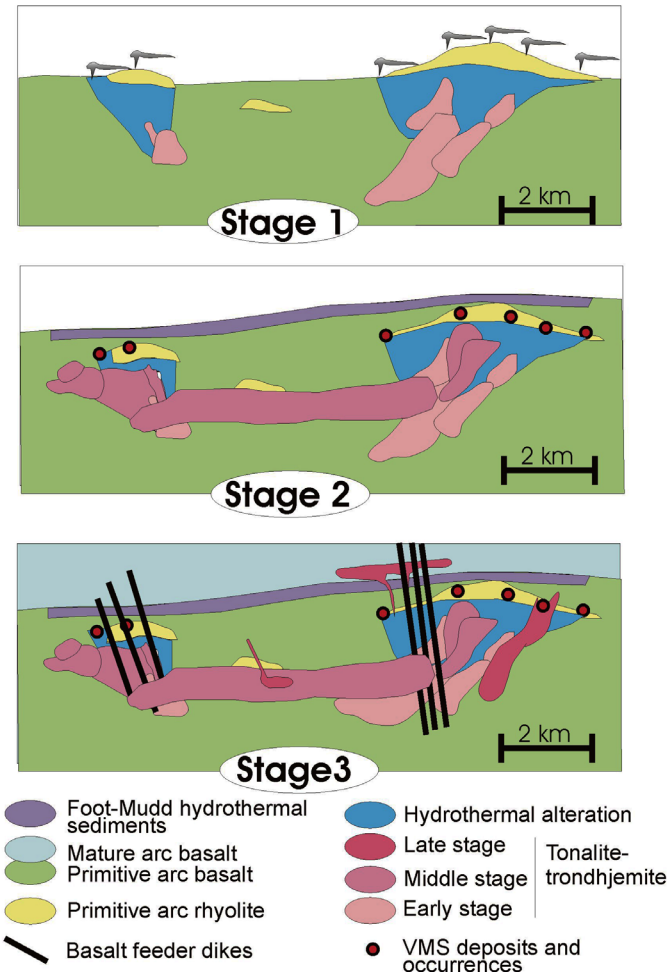

Figure 25: *Cartoon illustrating the evolution of the Sneath Lake intrusive complex in relation to the development of the Anderson-Stall hydrothermal system within the Anderson sequence (from Galley and Bailes, 2002).*

(Stop 15). Altered rhyolite at Stop 14 has a "bleached" appearance and locally contains wavy, discontinuous, sub-parallel fractures which meet every 5–30 cm along strike and are spaced 1–5 cm apart. Origin of the fracture set, which is subparallel to stratigraphy, has been a source of controversy for many years. The fractures are defined by staurolite, garnet, magnetite, chlorite and biotite. Bleached, silicified zones up to 3 cm wide are adjacent to some fractures. Additional alteration phenomena include a patchy, coarse staurolite blastesis and "washed out", silicified zones containing amphibole or chlorite with magnetite. Many zones of the wavy, fracture-controlled alteration, similar to those at Stop 14, exist in the highly altered Anderson rhyolite. Trembath (1986) interpreted the fracture structures at this outcrop to be primary. He suggested that they were produced by self-sealing of the venting hydrothermal system, with reduced flow rate and consequent fluid over-pressuring causing semi-horizontal fracturing in overlying rocks. A more likely explanation is that they are secondary and represent a premetamorphic solution cleavage produced during the F_2 folding that formed the Anderson Bay anticline. Their selective occurrence in altered rocks is due to the availability of mobile elements already present in the alteration zone. This implies some mobility of elements during deformation and metamorphism but the original synvolcanic alteration is still the major cause of their anomalous chemistry and mineralogy.

Proceed 0.6 km north on Highway 392 and turn left on a mine property access road about 200 m south of the intersection with Highway 393. The road is gated and you will require a key and permission from HudBay Minerals Ltc. to enter the mine property. Proceed down road for 0.37 km, turn right at intersection and travel an additional 1.4 km along the road to a small outcrop on the south side of the road. The road is not maintained and can be rough and may locally be washed out.

STOP 15 (UTM: 6079683N; 437009E): Anderson alteration pipe

Discordant zones of more completely altered rocks (**Figure 9**, **Figure 24** and **Figure 25**) transect the Anderson rhyolite in the immediate footwall to the Anderson, Stall and Linda VMS deposits (Bailes and Galley, 1996). These planar zones of highly altered rocks are interpreted by Walford and Franklin (1982) and Bailes and Galley (1996) to be hydrothermally-modified up-flow zones following the trace of synvolcanic faults. They are characterized by chlorite- and sericite-rich rocks containing varying amounts of staurolite, garnet, biotite, magnetite and kyanite. They also contain disseminated blebs, veinlets and stockworks of sulphide minerals, mainly pyrite, within 10–20 m of the main sulphide lenses, as well as local areas of anhydrite-, carbonate- and anthophyllite-rich domains in proximity to the ore bodies. The discordant alteration zones terminate up section at the massive sulphide lenses, which display only minor, metres-wide zones of intensely altered rocks in their immediate hanging wall. The Anderson and Stall discordant alteration zones are truncated at depth by the late, mesotonalite phase of the synvolcanic Sneath Lake intrusive complex (**Figure 25**). The Stall VMS deposit has vertically stacked massive sulphide lenses, linked by its discordant alteration zone (Studer, 1982).

Stop 15 is in the disconformable footwall alteration "pipe" to the Anderson Lake orebody. The most intensely altered zone consists of chlorite-biotite-kyanite schist and subordinate sericite-kyanite schist. Less intensely altered rocks contain staurolite and magnetite. The Anderson alteration "pipe" cross-cuts the footwall rocks at approximately 30° to strike (Walford and Franklin, 1982; Bailes and Galley, 1993, 1996) and can be traced in surface exposures over 1400 m east and east-southeast of the now abandoned mine site (**Figure 23**). At Stop 15 the alteration "pipe" consists of chlorite-biotite- kyanite schist containing minor stringer chalcopyrite. Also of note is the preferential development of kyanite crystals along planar surfaces. These kyanite rich fractures are likely of the same origin, but different mineralogy, as those previously observed at Stop 14. Again they are interpreted to represent a metamorphically recrystallized solution cleavage that was preferentially developed during D2 deformation of hydrothermally altered rocks.

Additional exposures of the Anderson alteration "pipe" can be observed adjacent to the abandoned rail bed (UTM: 6079594N; 437253E), located 50 m through the bush to the north of the road.

Return to vehicles and retrace route to Highway 392. Turn north on Highway 392 and then east on Highway 393. Proceed 0.55 km and turn north and park on small access road to hydro terminal.

STOP 16 (UTM: 6079347N; 439327E): Hangingwall alteration above Stall Lake VMS mine

Welch Lake basalts in the hangingwall to the Anderson, Stall and Rod VMS deposits are locally characterized by anomalous zones of amphibole blastesis and local prominent zones of silicification/albitization. The latter are common near the upper contact of the Anderson sequence basalts with overlying volcaniclastic rocks of the Upper Chisel sequence. Oxygen isotope studies by Holk (1998) and Taylor (1998) indicate that the exchange between seawater and basalt during silicification/albitization occurred at <250°C (**Figure 23**a). They interpret the alteration to have been produced by post mineralization, waning hydrothermal activity, and its presence above the mineralization to be a diagnostic feature, in conjunction with high temperature $\delta^{18}O$ footwall signatures, of robust VMS-producing hydrothermal systems.

Location A is the first outcrop area west of the access road.

Location A (UTM: 6079365N; 439290E): Relatively unaltered Welch Lake pillowed basaltic andesite

The outcrop south of the hydro station is an aphyric pillowed basaltic andesite with well formed 0.5 to 1.5 m diameter pillows. The pillows contain local quartz-filled thermal contraction cracks and display draped shapes indicating tops to the north. They are variably, but weakly altered with local 5 to 10 cm bleached (silicified/albitized) outer margins. The bleached domains are themselves enveloped in darker 1–2 cm amphibole-enriched domains. Irregular domains of yellow to orange-green epidosite are common in this pillowed flow.

Follow power line northwest for approximately 200 m from location A to outcrop preceding low lying area.

Location B (UTM: 6079445N; 439240E): Strongly silicified/albitized Welch Lake pillowed basaltic andesite

Strongly silicified/albitized pillowed basaltic andesite at this stop occurs within 30 m of the upper contact of the Anderson primitive arc sequence. Silicified/albitized pillows at this outcrop are readily recognizable as the more deformed equivalent of the altered Welch Lake basalts at Stop 1–3. Both occur at the same stratigraphic position.

Location C is located approximately 200 m east southeast of location A. It is an isolated outcrop in the middle of an area of waste rock that formed the base for a now removed bunkhouse complex.

Location C (UTM: 6079383N; 439429E): Contact between Anderson and Upper Chisel sequences

This stop, the main features of which are sketched in **Figure 26**, comprises the contact between highly silicified/albitized Welch pillowed basalt from the top of the primitive arc sequence and an overlying lobe and tongue facies rhyolite flow of the Upper Chisel mature arc sequence. Because bleached silicified/albitized mafic flows are commonly mistaken for rhyolite flows, this outcrop is useful for directly comparing the two in one locality. The southern 5 m of the outcrop consists of a tectonically flattened, silicified/albitized pillowed, aphyric, quartz amygdaloidal Welch Lake basaltic andesite flow. The pillow shapes are still readily recognizable but the selvages are no longer preserved. The pillow margins, which were selectively bleached, are preserved as flattened "doughnut" shapes. The white weathering bleached domains are composed mainly of a fine grained mosaic of quartz and feldspar, with minor porphyroblasts of amphibole and garnet. Interiors of pillows are brown grey and composed of 35–40% amphibole (0.5–1mm) and 60–70% feldspar (0.5 mm) with local 1–5 mm garnet porphyroblasts.

The contact between the bleached, pillowed basaltic andesite and the overlying rhyolite is sharp with a 1–2 cm zone of more strongly schistose rocks striking 285° and dipping 67° north (**Figure 20**). The contact is most likely the lateral extension of the Chisel-Lalor hangingwall thrust. The northern 18 m

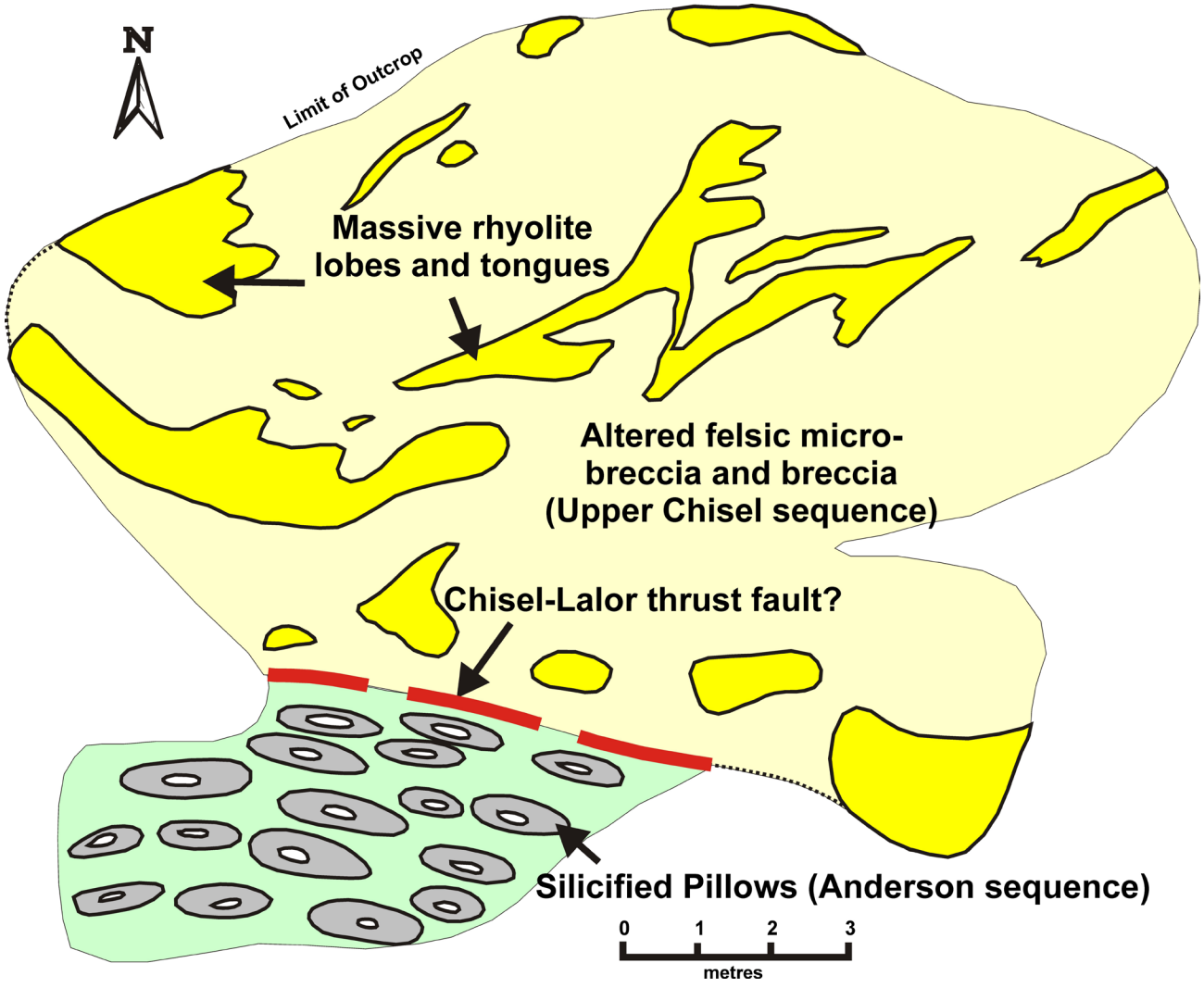

Figure 26: *Sketch of outcrop at Stop 16, Location C, showing contact between strongly silicified Welch pillowed basalt of the Anderson sequence and overlying weakly altered lobe-hyaloclasite rhyolite of the Upper Chisel sequence.*

of the outcrop is a quartz phyric lobe and tongue facies rhyolite flow.

Massive rhyolite lobes, which form 15% of the unit, are white weathering and 0.15 by 1 m to 3 m by 10 m in size. The interlobe material is a grey weathering, strongly recrystallized microbreccia with up to 15–20% rhyolite blocks. Both the massive rhyolite lobes and the intervening microbreccia contain the identical phenocryst population consisting of 5% quartz phenocrysts (0.5 –1.5 mm). The microbreccia has been selectively altered, probably due to its greater permeability. It contains 12–15% anhedral to euhedral garnet (1–6 mm), 10–15% biotite and 1–2% magnetite (4–5 mm). The rhyolite is crossed by some rusty weathering quartz-filled fractures along which there may have been some late remobilization of sulphides from the Stall Lake VMS deposit. Location C is 500 m stratigraphically above the Stall Lake VMS orebody.

Part 2: Stratigraphy, structure and orogenic lode gold mineralization within the McLeod Road–Birch Lake thrust panel (by Kate Rubingh and Simon Gagné)

Introduction

The McLeod Road–Birch Lake thrust panel (MB panel) is a fault-bounded package of mafic to felsic volcanic and volcaniclastic rocks, which are consistently north-dipping, as defined by Bailes and Schledewitz (1998). The panel is bounded to the south by the McLeod Road Thrust (MRT) and to the north by the Birch Lake Fault (**Figure 27**). Recent lithostratigraphic mapping and lithogeochemistry has further defined the internal geometry of the MB panel and recognized potential early thrust fault repetition of stratigraphic units within the panel (Rubingh et al., 2012a; **Figure 27** and **Figure 28**). Identification of early thrust faults has implications for our understanding of the stratigraphic and structural setting of gold mineralization. The purpose of this portion of the field trip is to review our current understanding of the stratigraphic and structural setting of gold mineralization within the MB panel. We will do this by examining outcrops that elucidate the structure of the area and by visiting the surface expression of three of the four gold deposits at Snow Lake: the Boundary zone; the No. 3 zone, and the Nor-Acme deposit of the New Britannia mine.

The New Britannia mine has been renamed 'Snow Lake mine' by QMX Minerals Corporation in 2012; however, for consistency with earlier publications, this field trip guide book will continue to use 'New Britannia mine'.

Stratigraphy

Lithostratigraphic mapping of the MB panel (Rubingh et al., 2012a, b) has identified a potential repetition of lithostratigraphic units that we interpret to be a product of early thrusting. This thrusting has repeated packages of units (e.g., units1–2 and units 3–5) as depicted in **Figure 28**. No repetition of units 6 and 7 has been identified within the MB panel. This repetition of stratigraphic packages suggests that early thrust faults follow the upper contact of unit 2 as well as the upper contact of unit 5 (Rubingh et al., 2012a).

Description of stratigraphic units

A brief description of the stratigraphic units of the MB panel is summarized below from Rubingh (2011) and Rubingh et al. (2012a). Lithogeochemistry of samples collected in 2011 indicates that units 3, 4, 5 and 6 are comparable to the upper part of the Chisel sequence of the Snow Lake arc assemblage. These results are preliminary with confirmation waiting on geochemisty from rocks collected in 2012.

Unit 1: Mafic volcaniclastic rocks

Unit 1 comprises a single lithofacies of moderately well-bedded heterolithic lapillistone to tuff breccia composed of felsic and mafic volcanic fragments. Fragments are typically matrix- to clast-supported and subangular to subrounded, with a crystal-rich (pyroxene- and plagioclase-phyric) matrix. This unit, which displays prominent tectonic flattening of fragments, is repeated together with unit 2 in the lower part of the MB panel (**Figure 27** and **Figure 28**).

Unit 2: Felsic volcaniclastic rocks

Unit 2 comprises two lithofacies: quartz- and plagioclase-phyric felsic volcaniclastic rocks and aphyric to plagioclase-phyric flows/sills. Plagioclase-phyric (5–8%) and quartz-phyric (3–5%) volcaniclastic rocks form a crudely bedded sequence of lapillistone and tuff breccia. Clast populations are typically monolithic and the same composition as the matrix. This unit is repeated together with unit 1 of the MB panel (**Figure 27** and **Figure 28**).

Unit 3: Heterolithic felsic volcaniclastic rocks

Unit 3 comprises three lithofacies: dacitic volcaniclastic rocks, with distinctive wispy mafic shards that are interpreted as flattened pumice fragments (Rubingh, 2011); amygdaloidal plagioclase-phyric felsic volcanic flows/sills; and heterolithic felsic volcaniclastic rocks (dominantly quartz-feldspar–phyric clasts, with minor plagioclase-phyric and aphyric to plagioclase-phyric mafic clasts). This unit is repeated together with units 4 and 5 of the MB panel (**Figure 27** and **Figure 28**).

Unit 4: Felsic volcanic and volcaniclastic rocks

Unit 4 is characterized by its plagioclase-phyric composition. It comprises two lithofacies: dominantly plagioclase-phyric (1–5%) rhyolite flows and less abundant felsic volcaniclastic rocks. Coherent rhyolite in the flows displays flow banding, well-preserved flow lobes, flow-top breccias and local quartz-filled amygdules. This unit is repeated together with units 3 and 5 of the MB panel (**Figure 27** and **Figure 28**). There is also apparent duplication of unit 4 above unit 5, possibly also resulting from thrust repeation of unit 4 at the base of unit 6.

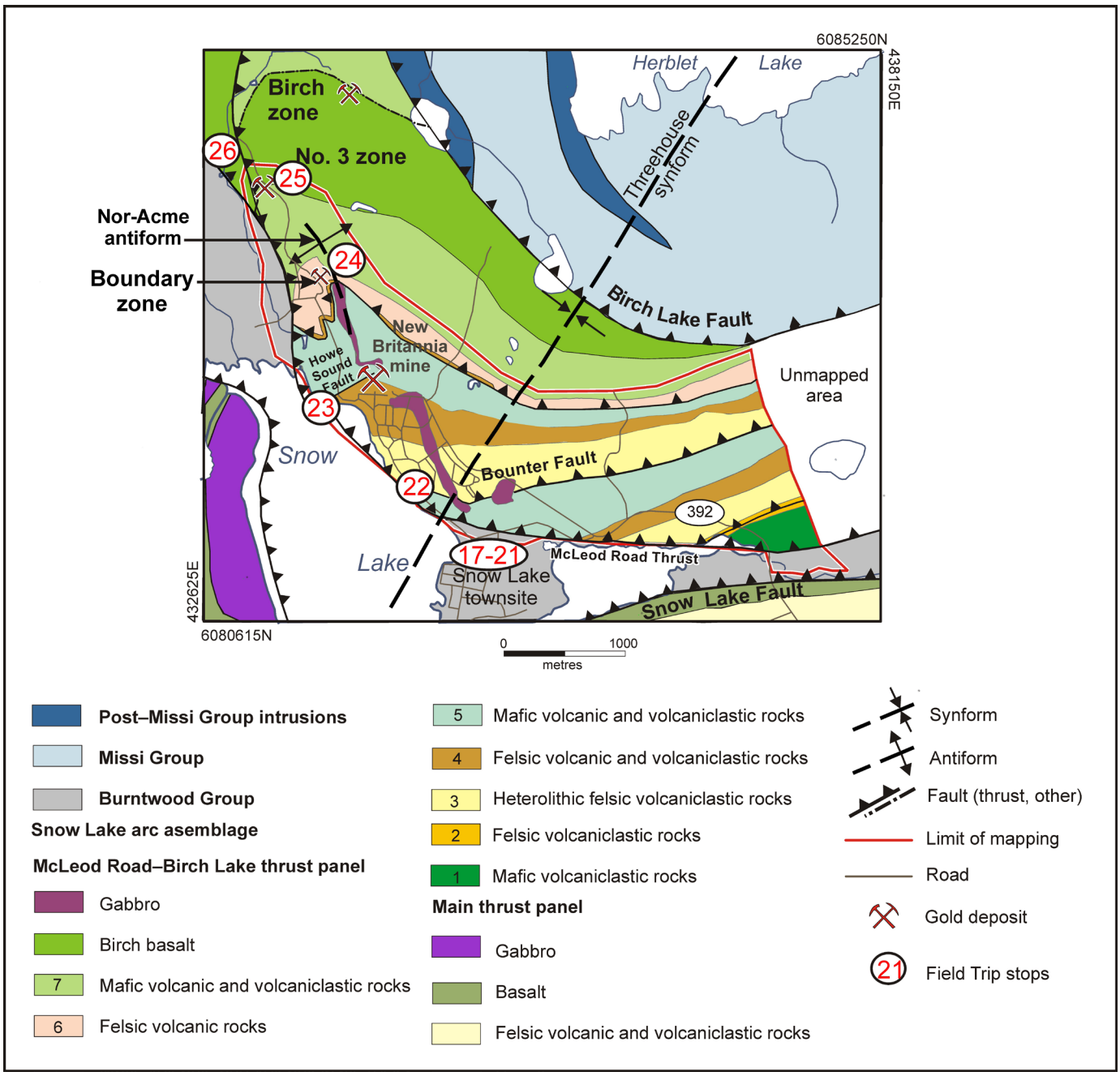

Figure 27: *Simplified geological map of the McLeod Road-Birch Lake thrust panel showing main units and structures, as well as bounding successor arc sedimentary rocks (Burnwood and Missi Groups). Unit numbers (supracrustal rocks only) in legend correspond to the units shown in the simplified stratigraphic column in Figure 28.*

Unit 5: Mafic volcanic and volcaniclastic rocks

Unit 5 consists mainly of well-bedded, heterolithic, mafic volcaniclastic rocks with minor plagioclase-phyric pillowed flows. Clasts include aphyric to plagioclase-phyric mafic, aphyric to plagioclase-phyric felsic, scoriaceous and plagioclase- and pyroxene-phyric mafic lithologies. The matrix is crystal rich with abundant pyroxene and plagioclase phenoclasts. Individual lithofacies within unit 5 include some with monolithic clast populations, but heterolithic clast populations are more typical. Clast size varies from lapilli tuff to lapillistone to tuff breccia. This unit is repeated together with units 3 and 4 of the MB panel (**Figure 27** and **Figure 28**).

Unit 6: Felsic volcanic rocks

A description of this unit was previously given in Rubingh (2011, as unit 9). It comprises a single lithofacies: a massive, aphyric, aphanitic rhyolite flow with flow banding and rare quartz-filled amygdules. No repetition of this unit has been observed within the MB panel (**Figure 27** and **Figure 28**).

Unit 7: Mafic volcanic and volcaniclastic rocks

Unit 7 comprises two lithofacies: mafic volcaniclastic rocks and pillowed flows. A distinguishing characteristic of this unit is the ubiquitous presence of large pyroxene phenoclasts and phenocrysts, which range from 0.5 to 1 cm in diameter.

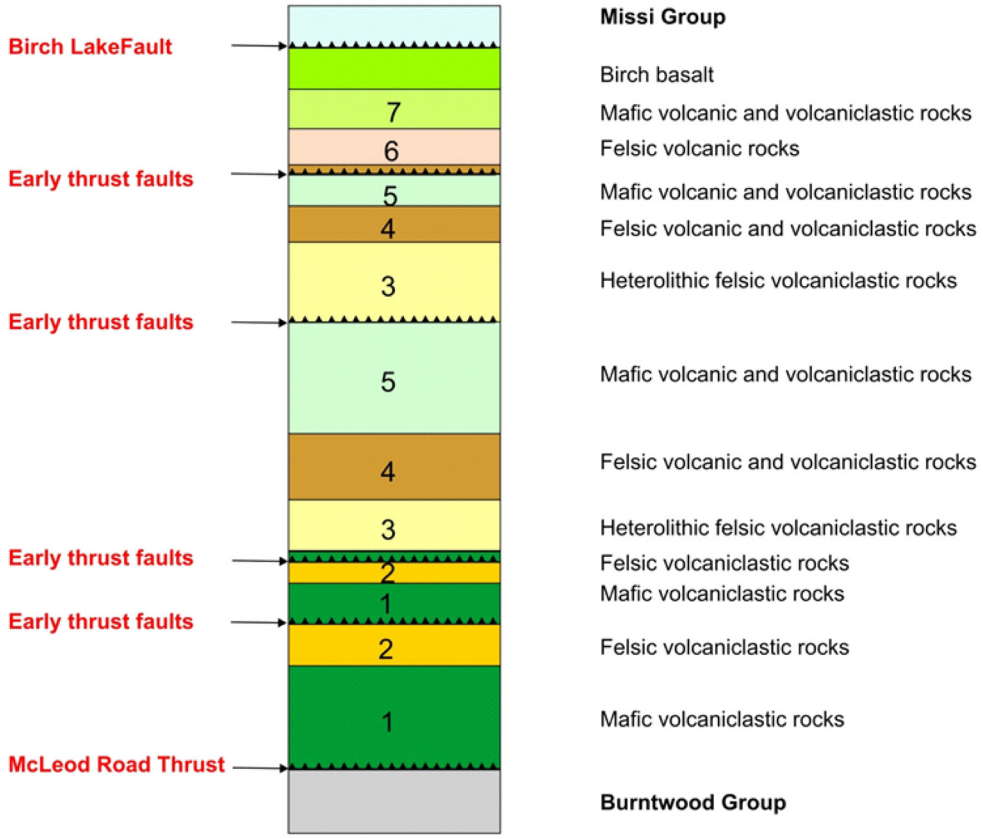

Figure 28: *Simplified "stratigraphic" column for the McLeod Road-Birch Lake thrust panel. Note thrust repetition of units in the MB thrust panel by early faults that predate the bounding McLeod Road and Birch Lake faults.*

The mafic volcaniclastic rocks, which vary from lapillistone to tuff breccias, are distinguished from those belonging to unit 5 because they have a pyroxene-plagioclase–phyric crystal-rich matrix and contain a monolithic clast population with phenocrysts similar to those in the matrix. Pillowed and massive flows in this unit display a similar coarse-pyroxene-crystal–rich character with the pillowed lithofacies characterized by thin, indistinct selvages. Unit 7 is not repeated within the part of the MB panel that has been mapped (**Figure 27** and **Figure 28**).

Structural geology

A series of field trip stops within the Town of Snow Lake and on the New Britannia mine property will highlight the importance of particular structures and how they relate to the structural history as defined for the Burntwood Group. Previous studies have documented four main deformational events in the Burntwood Group (Kraus, 1998; Kraus and Williams, 1999). Structural analysis focused on the volcanic rocks of the MB panel and correlation of those fabrics with the Burntwood Group recognized at least three deformational events (Beaumont-Smith and Lavigne, 2008). Therefore the deformational events described by Kraus and Williams (1999) have been simplified into D_1–D_3 events for correlation between authors, and are presented together with recent field work by Rubingh et al. (2012a) in **Table 2**.

The recent lithostratigraphic mapping by Rubingh et al. (2012a, b; **Figure 27**) has recognized that the main macroscopic fabric in the MB panel is an S_1 foliation, which is not correlative with the macroscopic S_2 foliation in the Burntwood Group, as was previously interpreted. This S_1 foliation in the MB panel is defined by the flattening of the clasts, which also have a consistent strong stretching lineation (L_1) plunging moderately to the northeast. The S_1 foliation is axial planar to the Nor-Acme anticline (F_1 fold) and its orientation changes throughout the study area so that it remains parallel to the MRT (late D_1 thrust) contact. The early thrust faults described previously (Rubingh et al., 2012a) appear to be truncated by the MRT and may represent a much earlier thrusting event, but have been currently included within D_1 deformational event for simplification and subject to further investigation during the 2013 field season.

The D_1 deformation is attributed to south- to southwest-directed thrusting of the MRT, causing early thrust imbrication and formation of the Nor-Acme fold, a drag fold related to thrusting. These D_1 structures are overprinted by a spaced cleavage (S_2), which overprints the Howe Sound Fault, the MRT and the Nor-Acme anticline. This fabric is correlative with the regional S_2 fabric in the Burntwood Group, and it is inferred that the S_2 fabric in the MB panel may be related to sinistral reactivation of the MRT. These structures were subsequently folded around the northeast-trending D_3 Threehouse synform, and the S_3 fabric elements identified in the MB panel correlate with those of Kraus and Williams (1999), Beaumont-Smith and Lavigne (2008) and Gagné (2009).

Table 2: Comparison of deformational events identified by various authors in the McLeod Road-Birch Lake thrust panel. Bold face indicates principle structures formed during each deformational event.

Kraus and Williams (1999)	Beaumont-Smith and Lavigne (2008)	Rubingh et al., (2012)
D3	**D3**	**D3**
F3 fold (Macroscopic North-northeast- trending Threehouse synform) chevron folds; S3 spaced fracture cleavage	**F3 fold (Macroscopic northeast-trending Threehouse synform)** S3 foliation is a weak to penetrative axial planar foliation and spaced fracture cleavage	**F3 fold (Macroscopic northeast-trending Threehouse synform)** S3 foliation is northeast - to east-northeast trending, steeply dipping, axial - planar, weakly spaced fracture cleavage
D2	**D2**	**D2**
F2 folds (Nor Acme)isoclinal south verging. S2 is a weakly spaced differentiated foliation and is associated with preferential alignment of staurolite porphyroblasts ; **F2 thrust fault (McLeod Rood Thrust Fault, MRT)**(north to northeast - trending, moderately dipping, a down dip stretching lineation and sinistral, transcurrent shear sense indicators indicate oblique slip) **Howe Sound Fault** (sinistral offset of the MRT.	**F2 folds (Nor-Acme)** shallow to moderately inclined, open to close, north east trending. Axial planar S2 foliation which is a north dipping, penetrative, slaty to spaced cleavage; **F2 thrust fault (McLeod Rood Thrust Fault, MRT)**(north to northeast - trending, moderately dipping, a down dip stretching lineation and sinistral, transcurrent shear sense indicators indicate oblique slip) **Howe Sound Fault** (sinistral offset of the MRT.	**F2 folds (s - asymmetric north east plunging shallowly inclined folds)** these folds fold the S1 shear foliation along the McLeod Road Thrust Fault (MRT) and indicate sinistral reactivation of the MRT. S2 in the volcanic rocks is defined by hornblende mineral alignment as a northwest- to north - north east trending spaced cleavage. S2 in the Burntwood Group is a spaced cleavage defined by biotite and aligned staurolite.
D1	**D1**	**D1**
F1 isoclinal south-verging folds S1 is preserved as a mesoscopic pervasive fabric as microlithons in staurolite porphyroblasts	**F1 isoclinal folds** S1 only preserved as a layer parallel fabric at stratigraphic contacts	**McLeod Road Thrust Fault;** **Howe Sound Fault;** **F1 Nor-Acme fold** S1 foliation is a macroscopic fabric defined by the flattening of the clasts, which is axial planar to the Nor - Acme fold **Early thrust repetition pre - McLeod Road Thrust fault**

Mineralization

The characteristic features of gold mineralization at the New Britannia mine are consistent with those recognized in all other deposits on the mine property. The gold deposits are all spatially associated with the hangingwall of the MRT and they are located where a fault intersects the hinge of the Nor-Acme F_1 fold at stratigraphic contacts between units of contrasting competency. Gold mineralization is associated with quartz–albite–iron carbonate veins and fine-grained acicular arsenopyrite (Fieldhouse, 1999; Beaumont-Smith and Lavigne, 2008; Galley et al., 1991).

Although considerable work has been undertaken to examine the regional geology of the MB panel and identify the main controls on gold mineralization (Harrison, 1949; Hogg, 1957; Russel, 1957; Galley et al., 1988; Bailes and Schledewitz, 1998; Fieldhouse, 1999; Fulton, 1999; Gale, 2002; Beaumont-Smith and Lavigne, 2008), the structural history and controls on gold mineralization are not fully understood. Preliminary investigations from field mapping in 2011 and 2012 suggest that gold mineralization is associated with D_1 structures and there is evidence to suggest that emplacement was late D_1 with later remobilization during D_2.

Stop descriptions 17 to 22: structural features in post-accretion sedimentary rocks

In addition to the older volcanic rocks of the Snow Lake arc assemblage (ca. 1.89 Ga), the Snow Lake area also comprises significant amounts of younger (1.85–1.83 Ga) sedimentary, plutonic and volcanic rocks that post-date the 1.88–1.87 Ga intra-oceanic accretion events of the Amisk Collage. These younger rocks, which occur as thrust imbricated panels between slices of 1.89 Ga Snow Lake arc assemblage rocks, can be traced

continuously to the north into the higher metamorphic grade Kisseynew domain (Bailes and McRitchie, 1978). Understanding the nature and deformation history of these post-accretion rocks provides essential information on the nature of the tectonic relationship between the dominantly volcanic rocks of the Flin Flon Belt and the mainly metasedimentary rocks of the Kisseynew domain.

Stops 17 to 22 (**Figure 29**) will examine exposures of Burntwood Group metaturbidites that display some of the characteristic primary sedimentary features of these post-accretion rocks. At each stop special attention will also be given to structural and metamorphic features that bear important information to unravelling the tectonostratigraphic events at Snow Lake. Another major suite of post-accretion rocks in the Snow Lake area are the Missi Group fluvial-alluvial metasedimentary rocks. These rocks, which can also be traced into the Kisseynew Domain, are at Snow Lake typically monotonous biotite-bearing quartzo-feldspathic gneisses locally containing pebble beds and fluviatile cross bedding. The Missi Group arkosic gneiss will not be visited during this field trip.

Deposition of the Burntwood Group metaturbidites is bracketed between 1835 Ma (cross cutting plutons) and 1842 Ma (age of the youngest detrital zircon; Machado and Zwanzig, 1995). The fluvial-alluvial arkosic and conglomeratic gneisses of the Missi Group have been interpreted at ca. 1845 Ma (Ansdell, 1993). Southward coarsening of Burntwood Group metaturbidites (Bailes, 1980; Syme et al., 1995) and northward fining of conglomeratic Missi Group rocks (Harrison, 1951; Bailes, 1971; Ansdell et al., 1995) suggests that the two units were, at least locally, sedimentary facies equivalents. This interpretation is supported by the presence of local turbidite bedforms in ca 1.84 Ga Missi Group arkosic sediments

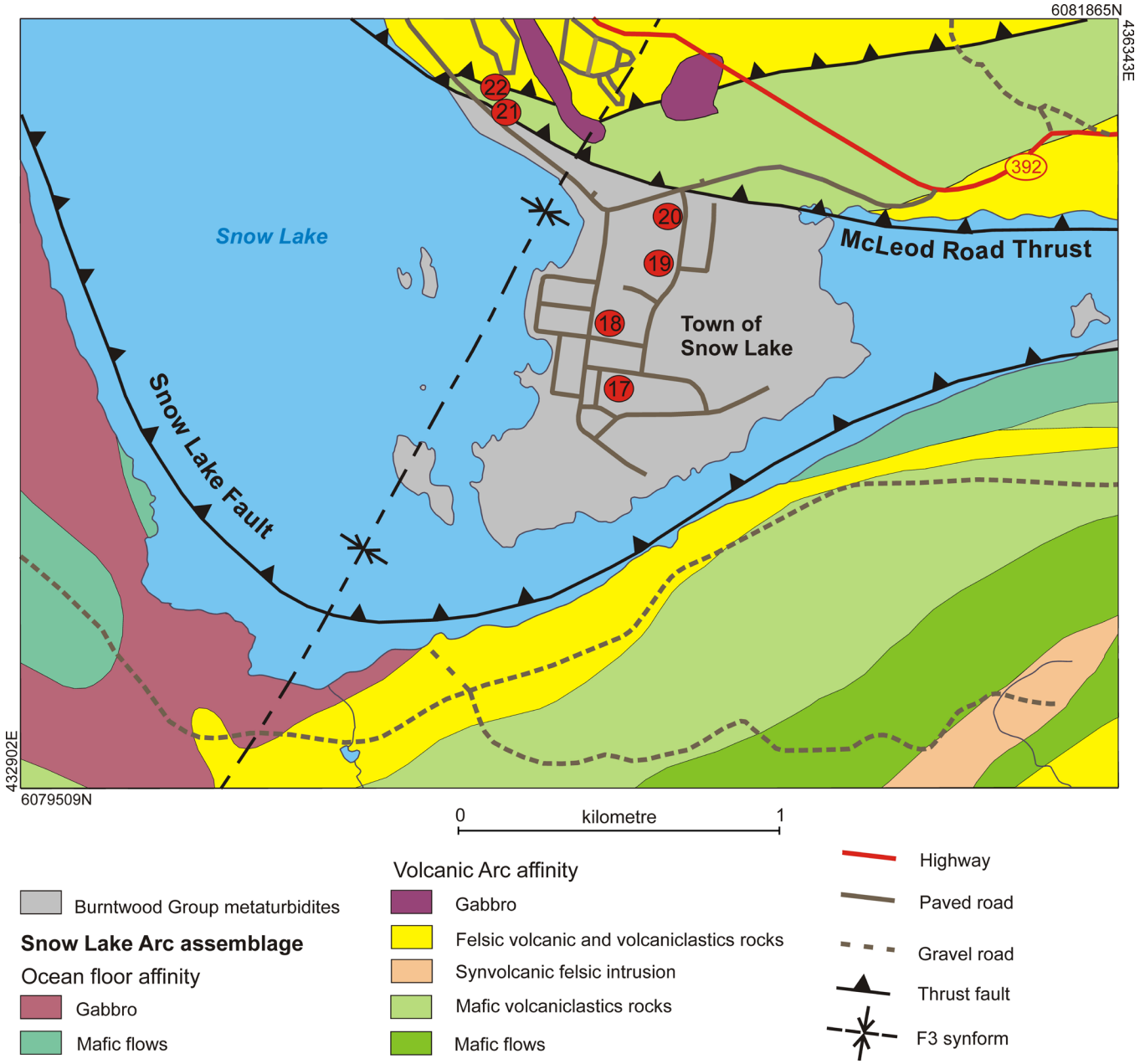

Figure 29: *Simplified geological map showing the location of Stops 17 to 22 (modified after Bailes and Galley, 2007, and Rubingh et al., 2012b).*

on Tramping Lake and well rounded, 'Missi-type' clast populations in pebble- and cobble-rich Burntwood Group metaturbidites on Reed Lake (Syme et al., 1995).

U-Pb dating of Burntwood Group detrital zircons from Wekusko and File lakes by David et al. (1996) revealed three main age populations: 1874–1859 Ma, 1890–1885 Ma and 2429–2362 Ma. The 1874–1859 Ma and the 1890–1885 Ma detrital zircon age populations are consistent with derivation of detritus by unroofing of accreted intraoceanic volcanic and intrusive rocks of the Amisk Collage, as well as subsequent successor arc calc-alkaline plutons and extrusive equivalents. The 2429–2362 Ma detrital zircons in the Burntwood Group at Wekusko Lake suggest that a cratonic terrane, younger than the bounding *ca*. 2.7–2.8 Ga Archean Superior craton, was present in the source area of the turbidites. There is no evidence to date of input of detritus from the bounding *ca*. 2.7–2.8 Ga Superior craton, suggesting that juxtaposition of the Flin Flon and Kisseynew domains with the Superior craton occurred later than 1.845–1.835 Ga. Ansdell et al. (1995) have suggested a back arc tectonic setting for the Burntwood Group and the Kisseynew Domain. They suggest that the post-accretionary sediments likely reflect significant uplift across the Trans-Hudson orogen at ca. 1.86–1.85 Ga, possibly from the arc-arc and arc-continent (Sask Craton?) collisions (e.g. Bickford et al., 1990; Lucas et al., 1996).

To get to Stop 17, from the Diamond Willow turn east (left) onto Lakeshore Drive, continue for 100 m and take a right (south) on Crystal Street (Esso gas station and grocery at the corner). Drive 650 m south on Crystal Street until T-junction with Olson Street. Park the vehicles along side of the road. Near the intersection, on the south side of Olson Street is a small water substation with green metal siding. Walk south for 100 m following a small trail on the left (east) side of green building and then turn right and walk west (~50 m) until you reach UTM: 6080710N; 434760E. The outcrop is located behind a private residence, so please be respectful of the private property and do not collect samples without the owner's permission.

STOP 17 (UTM: 6080710N; 434760E): Burntwood Group, Snow Lake

Stop 17 consists of thin to thick bedded Burntwood Group metaturbidites which have experienced peak regional metamorphic conditions of the lower amphibolite facies. The metamorphosed turbidites in the Snow Lake area are characterized by a metamorphic mineral assemblage consisting of large porphyroblasts of staurolite (up to 8 cm), garnet (up to 5 mm), and biotite (up to 5 mm). Despite recrystallization these metaturbidites preserve many primary sedimentary features such as normal size grading and local mudstone rip-ups.

Garnet-biotite thermometry using the calibration of Kleeman and Reinhardt (1994) indicates a temperature of 536 ± 11^0 C for a population of 24 garnet-biotite pairs from a sample of the Burntwood Group at Snow Lake (Kraus and Menard, 1997). A pressure of approximately 4 kb for the same sample was determined by Kraus and Menard (1997) using the garnet-biotite-muscovite-plagioclase barometer of Ghent and Stout (1981). Sparse geothermal and geobarometric data from metamorphic minerals in altered volcanic rocks south of the Snow Lake fault (Zaleski et al., 1991; Menard and Gordon, 1995) suggest fairly constant peak temperatures of approximately 550^o C in conjunction with a northward increase in pressure across strike of tectonostratigraphic units. Kraus and Menard (1995) suggest that this is consistent with a uniform metamorphic regime for the volcanic rocks to the south of the fault and for the Burntwood Group slice at Snow Lake. Peak metamorphic conditions were reached in the Snow Lake area at *ca*. 1.81 Ga according to U-Pb age dates of metamorphic zircon and titanite reported by David et al. (1996).

The effects of successive episodes of deformation in the Snow Lake area are recorded in these well-bedded metaturbidites by minor folds, cleavage relationships, and fabrics formed during porphyroblast growth and deformation. As part of a Ph.D. study at the University of New Brunswick, Jurgen Kraus studied the Burntwood Group rocks in the Snow Lake area and established the presence of four phases of folding (F_1–F_4). The framework for describing the deformational history of the Burntwood Group rocks in the Snow Lake area is based on Kraus` work.

The outcrop at Stop 17 displays north-younging graded beds (striking 245° and dipping 85° north). In the Snow Lake area the penetrative development and preservation of S_1 is rare. Generally, F_1 folds in the Burntwood Group lack an axial-planar foliation, with S_1 largely transposed into a bedding-oblique, weakly differentiated S_2 foliation. Kraus (1998) and Kraus and Williams (1999) reported the widespread preservation of S_1 as internal foliations in the microlithons of crenulation cleavage in staurolite porphyroblasts, suggesting an early pervasive S_1 development in the Burntwood Group. The dominant S_2 fabric at this stop is well-developed and strikes oblique to bedding. In the Burntwood Group, D_3 fabric elements consist of chevron folds developed in the more pelitic portions of beds. These folds generally lack a true axial-planar foliation, but rather a spaced fracture cleavage is locally developed. Moderately to well-developed crenulation of S_2 defines the S_3 fabric at this location. The relationship between S_2 and S_3 is best shown in a small saw cut near the top, along the southwest side of the outcrop. Cleavage refraction between psammitic and pelitic layers is locally well-developed and large syn-sedimentary calcareous concretions up to 30 cm can be observed in the more psammitic horizons.

To reach Stop 18, return to vehicle and drive 150 m north on Crystal Street, then turn left (west) on the back alley immediately north of McGilvray Avenue and continue (100 m) until the end of the back lane at a T-junction. Stop 3 is a flat-lying outcrop on the northeast side of the intersection.

STOP 18 (UTM: 6 080 953N; 434781E): Burntwood Group, Snow Lake

Stop 18 is also characterized by thin to medium beds of biotite-staurolite-garnet bearing Burntwood Group metaturbidites. At this outcrop, an early S-asymetrical isoclinal F_1 fold can be observed. The beds are north-younging, generally east trending and are steeply dipping. The fold lacks a true axial-planar foliation and is overprinted by an oblique well-developed S_2 fabric. A weakly developed S_3 spaced cleavage can be seen in places.

To reach Stop 19, drive back to Crystal Street and drive 200 m to the north (left turn). At the intersection with Gowan Avenue turn left (west) on a small gravel extension of Gowan Avenue and park your vehicle. Stop 19 is an outcrop in a small clearing along the side of the bush.

STOP 19 (UTM: 6081099N; 434929 mE): Burntwood Group, Snow Lake

Structural and tectonic analysis (Connors and Ansdell, 1994; Kraus and Williams, 1994a, b, 1995; Connors, 1996; Kraus and Williams, 1999) and recent mapping (Syme et al., 1995; Bailes and Galley, 2007) indicate that the present distribution of Burntwood Group rocks in the Snow Lake area reflects thrusting that occurred during southwest-directed convergence between the Kisseynew domain and Flin Flon domain. During this deformation, the Burntwood Group (and other KD lithologies) were thrust onto and imbricated with volcanic rocks of the Flin Flon domain. Thus, slices of Burntwood Group metaturbidites commonly mark the location of tectonic boundaries between various thrust panels.

Stop 19 consists of isoclinally folded and metamorphosed Burntwood Group greywacke, siltstone and mudstone turbidites. Similar to other outcrops of the Snow Lake area, the metaturbidites at Stop 19 contain almandine-amphibolite facies metamorphic mineral assemblages, including prominent porphyroblasts of staurolite, garnet and biotite. Differentiation of the S_2 crenulation cleavage into muscovite septae and quartz-rich microlithons has formed a penetrative schistosity or a domainal cleavage that anastomoses around porphyroblasts. The presence of S_2-crenulated S_1 inclusion trails in porphyroblasts suggest that porphyroblast growth was coeval with early stages of isoclinal F_2 folding (Kraus and Williams, 1994a). Continued F_2 deformation is suggested to be responsible for curvature of S_2 muscovite septae around porphyroblasts, as well as prominent pressure shadows and quartz-filled pull-aparts displayed by large staurolite porphyroblasts. The S_2 fabric is refracted across the relatively incompetent pelitic layers (**Figure 30**). Open crenulations of the S_2 fabric, occurring selectively in pelitic layers, are interpreted by Kraus and Williams (1994a) to be related to large-scale F_3 folds (e.g., Threehouse synform). At the north end of the outcrop, a small, Z-asymmetrical, F_3 minor fold overprints a minor F_1 fold and the S_2 cleavage. Bedding-parallel, quartz-filled faults locally offset F_1 fold limbs and place beds with opposite facing directions together. These faults are early as they are crenulated by S_2. Refraction of the S_2 differentiated cleavage in incompetent layers (pelitic beds), is suggested to reflect bedding-parallel shear

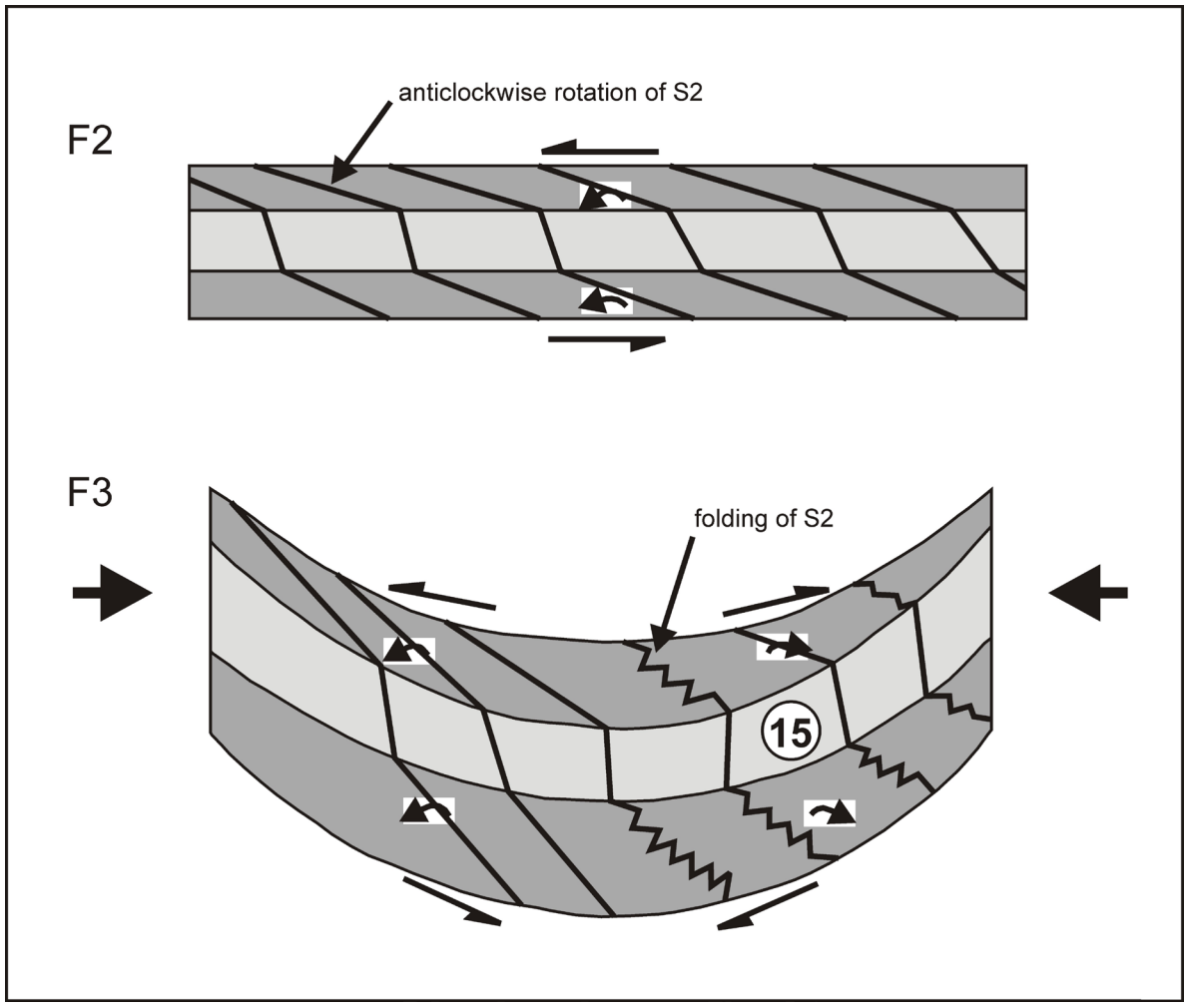

Figure 30: *Two layer model illustrating the modification of S_2 during F_2 and F_3 from Kraus and Wiliams (1994b). Note the partitioning of deformation in competent (light grey) and incompetent (dark grey) layers.*

(Figure 30; Kraus and Williams, 1994a). Recent structural work in the Snow Lake area by Beaumont-Smith and Lavigne (2008) supports this structural interpretation and proposes that rocks of the McLeod Road-Birch Lake thrust panel to the north are also isoclinally folded by D_2 deformation.

To access Stop 20, return to vehicle and drive another 200 m north on Crystal Street. Just before the intersection with Lakeview Drive and across from the grocery store, there is parking lot along the west side of Crystal Street. Follow the trail into Crystal View Park to visit outcrop exposed at Stop 20.

STOP 20 (UTM: 6081255N; 434924E): Burntwood Group, Crystal View Park

At this Stop, well-bedded greywacke-siltstone-mudstone metaturbidites display prominent staurolite porphyroblasts and well developed beds that average 10–30 cm thick. Many beds have leucocratic sandstone-siltstone bases that grade rapidly upward into dark grey mudstone tops. The mudstone is preferentially overgrown by 2–10 cm euhedral to subhedral dark brown staurolite porphyroblasts and 1–4mm booklets of brown biotite. The largest and most abundant staurolite and biotite porphyroblasts are concentrated in mudstone-siltstone bed tops giving a reverse (metamorphic) size grading.

An early F_1 isoclinal fold passes through this outcrop. Careful observation of the bedding younging directions and attitudes allows recognition of the fold trace. Bedding on the south side of the outcrop strikes 295–305° and dips 70–75° to the north and faces south, whereas bedding on the north side of the outcrop strikes 275–285° and dips 85–90° to the north and faces north. Bedding along the axial trace of the F_1 fold is contorted but does not display the prominent fold closures present at Stop 19. S_1 is not prominent and largely obliterated by a strong S_2 crenulation/domainal cleavage. S_1 is locally preserved in microlithons between the S_2 cleavage planes and within porphyroblasts. The S_2 crenulation cleavage is strongly refracted between competent sandstone and less competent mudstone-siltstone layers (**Figure 30**). S_2 is oriented 005–020° with a dip of 70–80° in sandstone beds and 340–350° with a dip of 60–70°: in mudstone layers. In the mudstone layers S_2 is locally S-asymmetrically folded (F_3 of Kraus and Williams, 1999), whereas in the sandstone layers short quartz-filled tension-gash veinlets parallel S_2. Staurolite and biotite porphyroblasts overgrow S_1 and S_2, and are weakly aligned with S_2. Staurolite porphyroblasts are boudinaged with quartz occupying the pull-aparts between boudins.

To reach Stop 21, take a left (west) on Lakeshore Drive, keep right at T-junction and continue for 800 m until you reach the stop coordinates. The stop is a set of 1 m high outcrops on the north side of the road about 100 m south-east of the RCMP station.

STOP 21 (UTM: 6081614N; 434355E): Corley Lake member of the Burntwood Group

A distinctive unit of well-bedded, coarsely garnet-porphyroblastic metasedimentary rocks (the Corley Lake member of Bailes, 1980) outcrops in the immediate structural footwall of the MRT, on surface and at the 915 m (3000 ft.) level in the New Britannia mine. In addition, Ian Fieldhouse (pers. comm., 1998) reports that mine site exploration drill holes penetrating the structural footwall of the MRT fault also intersected this garnet-porphyroblastic metasedimentary rock.

At File Lake (25 km to the west) the Corley Lake member is a 50 m thick. It can be traced along strike for over 60 km (from its type locality at File Lake area) to Squall Lake, north of Snow Lake. It has also been observed at the upper contact of the Burntwood Group metapelites southwest of Cleaver Lake. Bailes and Schledewitz (1998) suggest that the MRT follows the southeast shore of Squall Lake and extends over the Squall Lake dome, rather than projecting through Cleaver Lake to Angus Bay on Herblet Lake, as previously suggested (Russell, 1957; Froese and Moore, 1980). However, detailed structural work (Kraus and Williams, 1999) suggests that the fault is in fact more likely to project through Cleaver Lake. The Corley Lake member is an important and distinctive marker unit that been observed in a number of fault-bounded slices of the Burntwood Group, including as far east as Roberts Lake, 27 km east of Snow Lake.

At this outcrop we can observe the well-bedded turbidites and the S_2 fabric defined by preferential alignment of staurolite porphyroblasts (Kraus and Williams, 1999). Recent mapping by Rubingh et al. (2012a, b) identified in outcrop the implied thrust contact between the Burntwood Group and the volcanics of the MB panel. This outcrop (Stop 22) is located on the hill above this location (**Figure 29** and **Figure 31**).

To reach Stop 22, walk 50 metres to the north-northeast and hike up a small ridge.

STOP 22 (UTM: 6081670N; 434365E): McLeod Road Thrust; examination of the contact between the Burntwood Group and the volcanics of the MB panel

Introduction

Improved understanding of the volcanic stratigraphy and structural history of the MB panel during field mapping in 2012 and 2011 has resulted in the identification of early structural repetition within the panel and thrust faults which appear to be younger than the MRT. This stop reviews the fabric relationships in the Burntwood Group metasedimentary rocks and the MB panel volcanics rock at the inferred location of the MRT. It also highlights the importance of another fault, the Bounter fault, which appears to offset the MRT. The Bounter fault was described by Galley et al. (1991) and Fieldhouse (1999) as a series of anastomosing shear zones that are associated with the Bounter gold occurrences. The Bounter fault has a strike length of 3 km and occurs at the contact between the felsic and mafic volcanic rocks; the contact appears to be the site of the early thrust faults described previously. Gold mineralization occurs intermittently along the structure; the most important occurrence is the Bounter showing, with gold values > 2000 ppb (Galley et al., 1991). This structure was considered either as a splay of the MRT or to be truncated by the MRT.

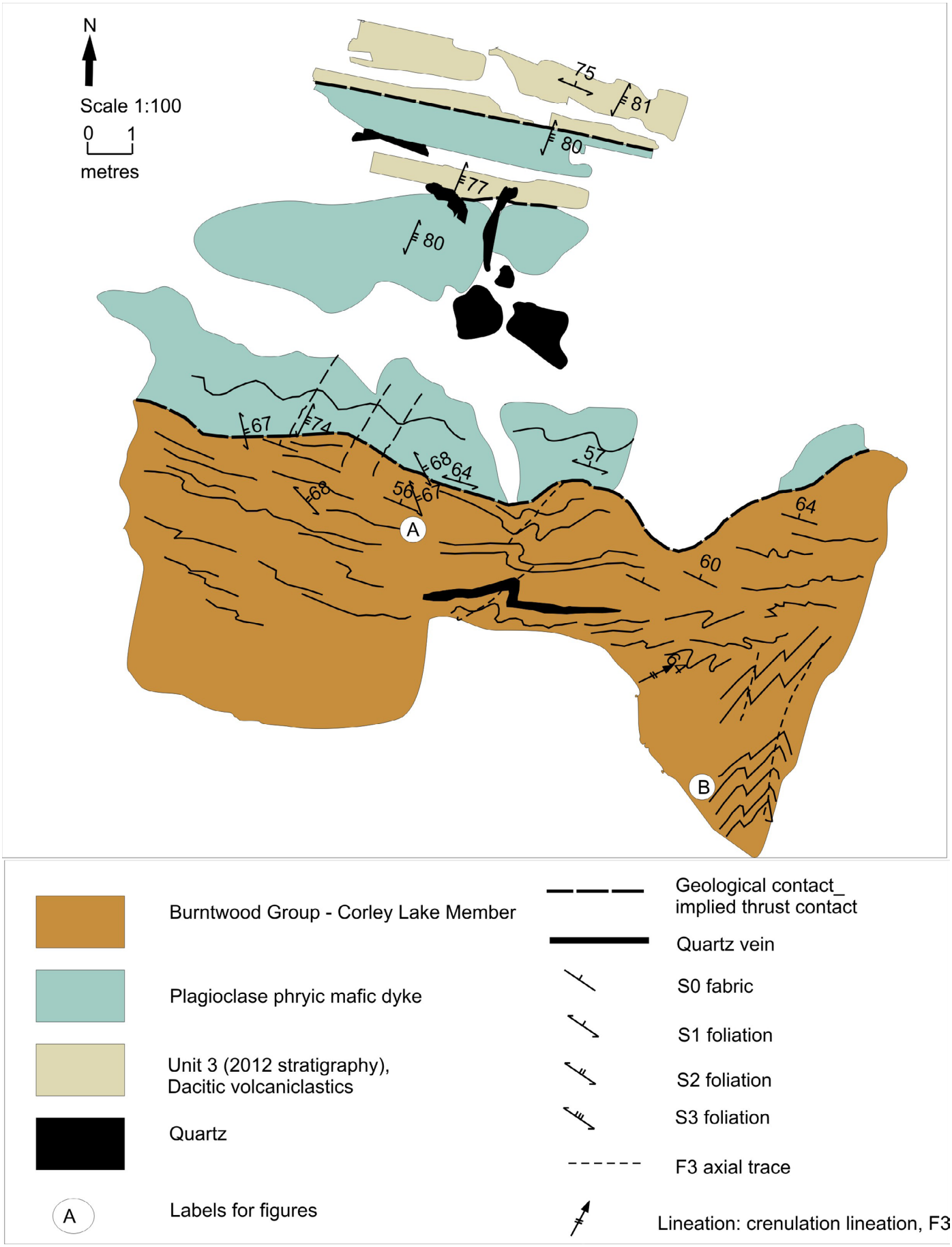

Figure 31: *Sketch map showing the inferred MRT contact between the Burntwood Group metasedimentary rocks and the metavolcanic rocks of the McLeod Road-Birch Lake thrust panel at Stop 22.*

Stop Description

At this stop we will examine a newly-exposed outcrop which is interpreted as a structural repetition of the Burntwood Group within the MB panel. We can observe the fabric relationships along the inferred thrust contact between the Burntwood Group and the felsic volcanics of unit 3, with a mafic dike intruding the contact (**Figure 31**). The Bounter occurrence is along strike from this stop.

The Burntwood Group, which at this locality is represented by the Corley Lake member due to its position in the footwall of the inferred MRT, is juxtaposed with the heterolithic felsic volcanics (unit 3) of the MB panel (Rubingh et al., 2012a). The lithofacies observed here are dacitic volcaniclastic rocks, containing 8–10% feldspar and 1% quartz phenocrysts and phenoclasts. A distinctive characteristic of these rocks is wispy mafic shards that are interpreted to be flattened pumice fragments (Rubingh, 2011).

The Burntwood Group at this stop displays narrow beds 3–8 cm wide which become disrupted and discontinuous towards the contact with the mafic dike. The bedding and S_1 (microscopic fabric preserved as microlithons) are truncated along the inferred MRT by an early mafic dike. The S_2 fabric in the Burntwood Group (**Figure 32a**) is a spaced cleavage which overprints the S_0/S_1 fabrics and the MRT, therefore implying that the S_2 regional fabric observed in the Burntwood Group is post D_1, as recognized in the MB panel (Rubingh, et al., 2012).

The S_2 fabric in the Burntwood Group is itself folded by Z-asymmetric F_3 folds related to the Threehouse syncline. These F_3 folds lack a true axial-planar S_3 cleavage but the S_3 fabric is parallel to the axial planes of Z-asymmetric folds (**Figure 32b**). The F_3 open folds deform the mafic dike, as indicated by the axial plane of the S_3 fabric. The S_3 fabric in the MB panel is typically weakly developed; however, at this outcrop—located in the hinge of the Threehouse syncline—it occurs as a moderate to strong, northeast- to east-northeast-trending, steeply southeast- dipping, spaced fracture cleavage in the dacitic volcaniclastic rocks (unit 3) and in the mafic dike.

The structural observations seen at this outcrop will be further reviewed at Stop 23, where the relationship of the S_2 fabric of the Burntwood Group and the volcanics of the MB panel can be examined at the MRT.

Stop Descriptions 23 to 26: Structural relationships observed in the volcanic rocks of the MB panel and the implications for the setting of gold mineralization

Introduction

The purpose of Stops 23 to 26 is to present the MB panel, relate it to the Snow Lake arc assemblage and discuss the characteristics of the gold deposits within the panel.

At Stops 23 to 25 we will examine three of the main showings on the New Britannia Mine property. At each of these stops we will discuss the structure, stratigraphy and how it relates to the mineralization. At Stop 26 (an optional stop), the S_1 shear foliation along the base of the MRT is well exposed. At Stop 26, S_1 has been folded and this is interpreted to represent sinistral reactivation of the MRT.

Following the recent mapping in 2011 and 2012 for the MB panel, as discussed previously, two distinct packages of rocks are recognized within the MB panel (**Figure 27** and **Figure 28**).

To reach Stop 23, return to vehicles. Drive 1.0 km on Lakeshore drive heading northwest. Then, turn left towards the golf course as indicated by road signs. About 100 m after turning left, there is a junction to the left that leads to a water pumping station by the lake shore. Park your vehicle here. About 30 m north of the water pumping station there is a small path heading west into the bush. Walk 40 m along this path and you will come to a clearance. This is the site of an old vent raise.

STOP 23 (UTM: 6082438N; 433614E) Howe Sound Fault

Introduction

The Nor-Acme deposit is the largest gold deposit within the Trans Hudson Orogen, and since production commenced in 1949 the New Britannia mine has produced 1,404,950 oz. (43 699 kg) of gold. The Nor-Acme deposit consists of four zones—Toots, Dick, Ruttan and Hogg—which lie over a 2.7 km interval along the Howe Sound Fault (Galley et al., 1991). The Howe Sound Fault is hosted within the mafic volcaniclastic rocks (unit 5) and is subparallel to the contact with the felsic rocks (unit 4; Rubingh, et. al. 2012a). The fault cuts across the Nor-Acme anticline but is also slightly folded. The mineralized zones, which are located at the contact with the Howe Sound Fault and the fold hinge (D_1 fold), plunge northeast to north-northeast at 40–80° and are 3–30 m wide (Galley et al., 1991).

The relationship and timing of the Howe Sound Fault with respect to the MRT and gold mineralization is not well defined. Several interpretations have been advanced : i) the Howe Sound Fault is interpreted to cut the MRT and mineralization is considered syn-D_2, or older and subsequently remobilised during D_2 (Beaumont-Smith and Lavigne, 2008); ii) Galley et al., (1991) interpreted the Howe Sound Fault to be a secondary splay of the MRT which cuts the MRT, with mineralization attributed to late D_2 structures such as the Howe Sound Fault; iii) Fieldhouse (1999) interpreted the Howe Sound Fault to precede the MRT, with mineralization related to late brittle reactivation of an earlier ductile shear zone.

Stop description

This outcrop is the surface exposure of the Toots zone, which is the smallest of the New Brittania gold ore bodies associated with the Howe Sound Fault. It is located at the intersection between the Howe Sound Fault and the MRT, and extends for 900 m down plunge. The main lithologies observed at this outcrop are heterolithic mafic volcaniclastic tuff breccias of unit 5, which are cross cut by amphibolite dikes (see **Figure 33**) and display an intense carbonate-biotite alteration. In the northwest portion (Figure 33), unit 4 felsic volcanic rocks are observed. The mineralization is hosted by east trending fault breccias, massive to brecciated quartz carbonate vein system and the adjacent wall rock (Galley et al., 1991), none of which

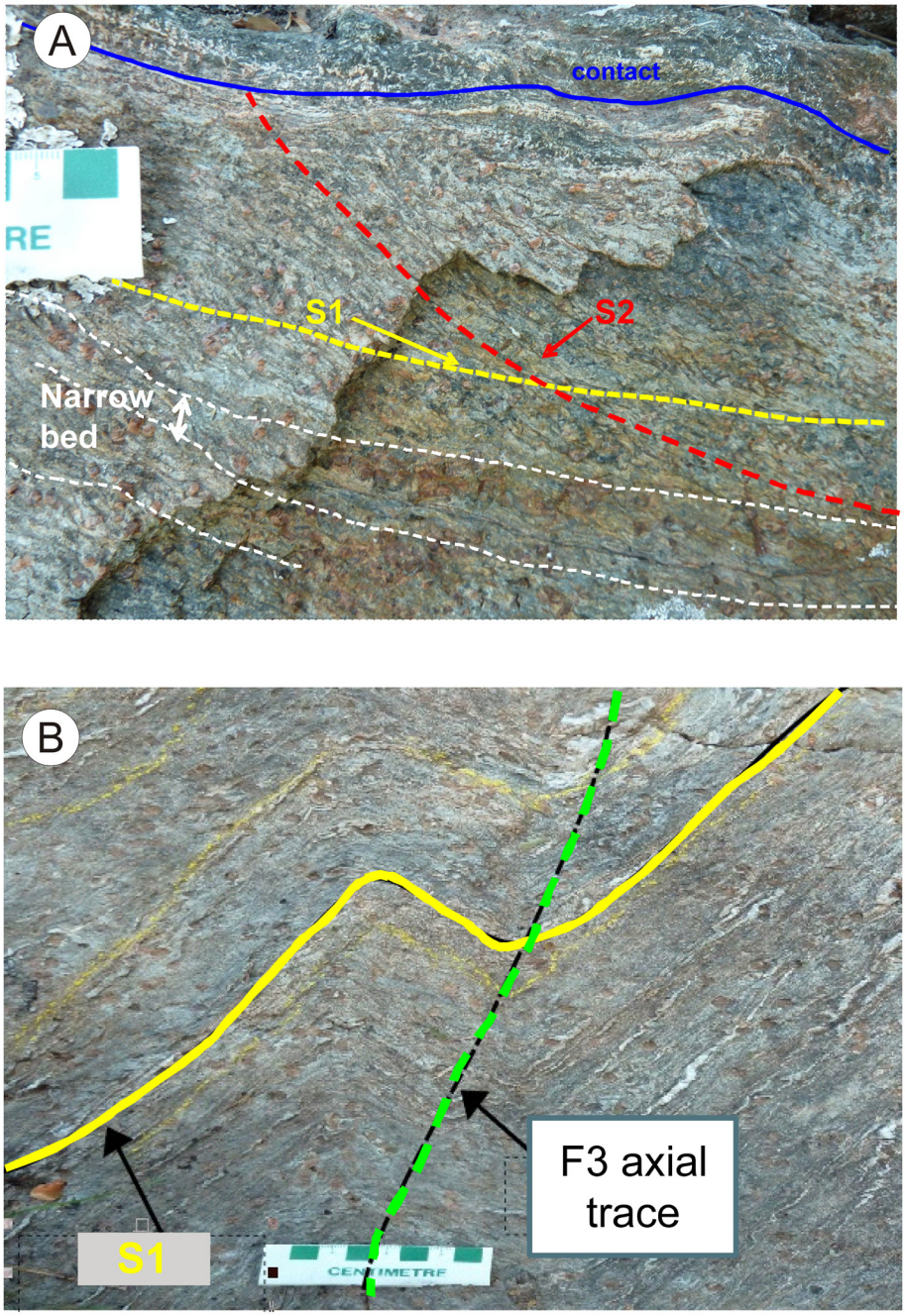

Figure 32: *a) S_2 fabric in the Burntwood Group overprinting the S_0/S_1 fabric; b) S_2 fabric in the Burntwood Group is folded and the S_3 fabric is axial planar to the Z asymmetric folds.*

are observed *in situ* at this outcrop. However large remnant blocks of the brecciated quartz carbonate veins and wall rock can be observed, which are considered to represent this rock type.

The regional north-northwest trending S_1 foliation, which is defined by flattening of clasts, is observed along the Howe Sound Fault east of Stop 23 to be rotated towards the Howe Sound Fault in an anticlockwise sense, implying a sinistral movement on this structure. Along the bedding-parallel contact of the Howe Sound Fault preliminary interpretations infer S-asymmetric drag folds due to rotation of the S_1 foliation as illustrated in **Figure 34**. This is consistent with an interpretation of the Howe Sound Fault as having sinistral offset. The fault also cuts the MRT and is interpreted to be pre D_2 because on a map scale the S_2 fabric overprints the fault (**Figure 34**). These preliminary field observations imply that the Howe Sound Fault is a late D_1 structure. One interpretation is that the Howe Sound Fault could have formed as a result of a transfer fault during thrusting and formation of the Nor Acme fold. The typical mineralogical assemblage of the altered and mineralized mafic wall rock is quartz, albite, actinolite, biotite, calcite arsenopyrite and other minor sulphides (Fieldhouse, 1999).

At this outcrop we can examine a shear zone which is interpreted to be representative of movement along the MRT, and not related to the Howe Sound Fault. The S_1 fabric defined by flattened clasts is observed, together with a strong stretching

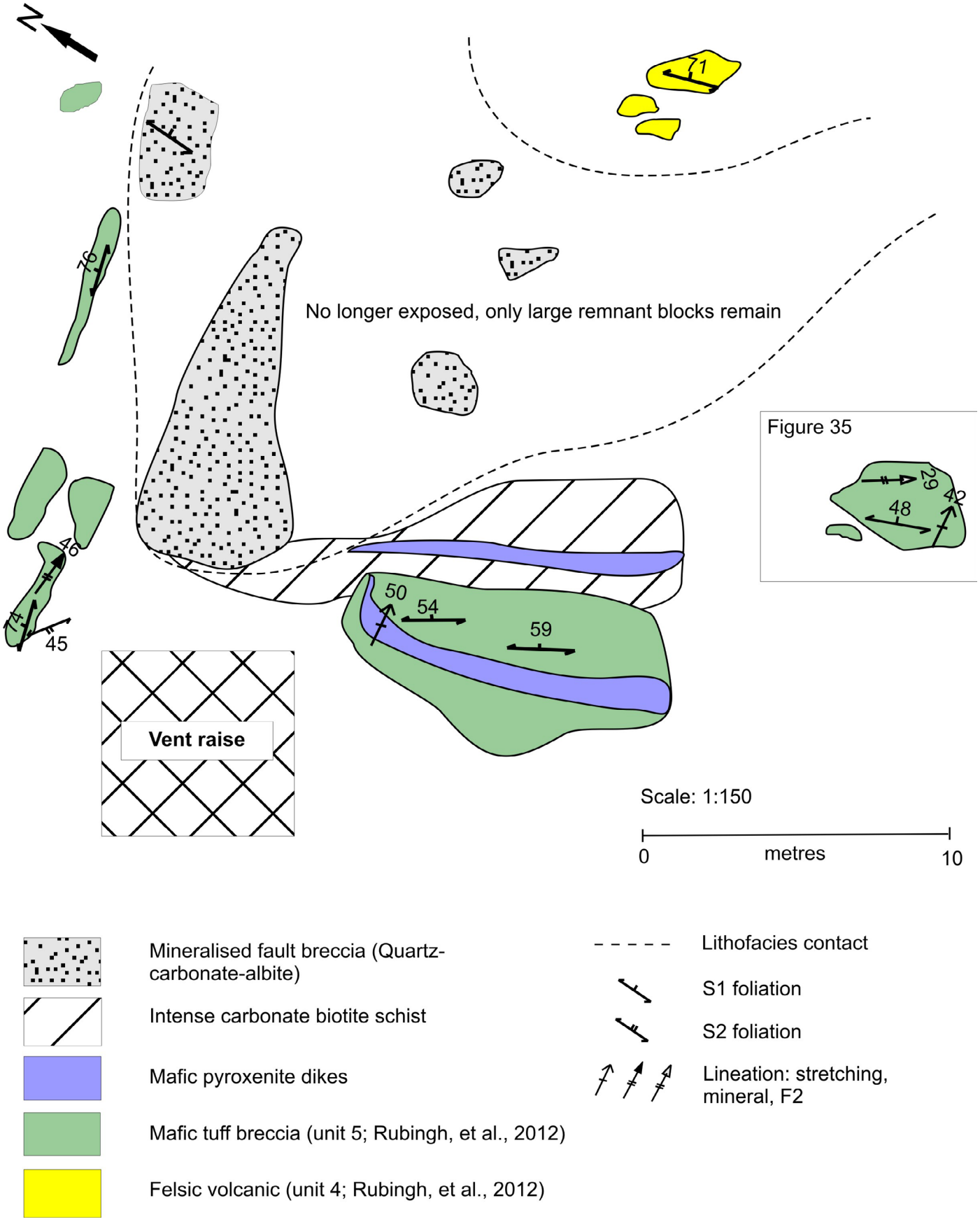

Figure 33: *Surface geology of the Toots zone, modified from Galley et al. (1991).*

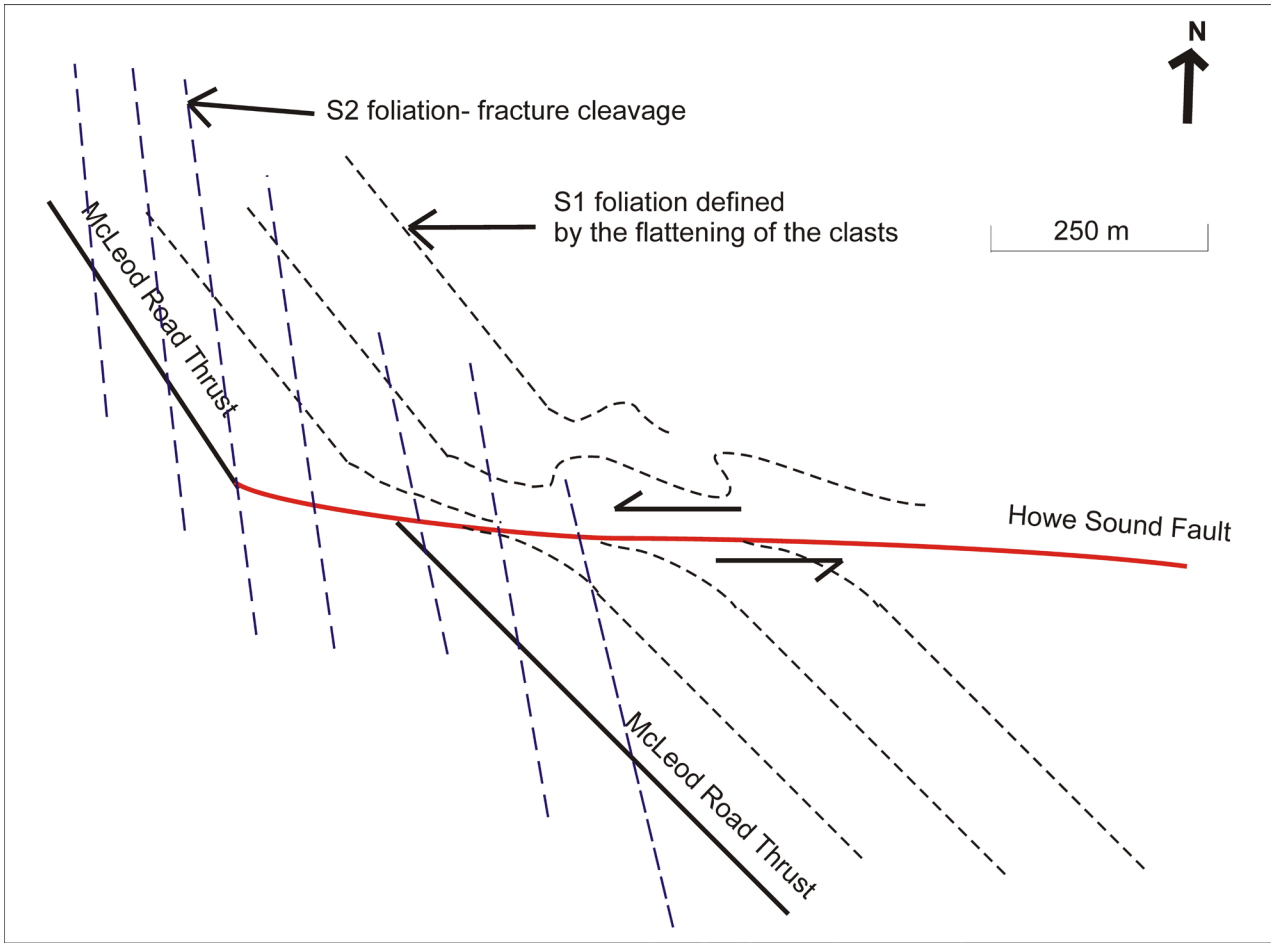

Figure 34: *Simplified map to show the regional fabric relationships of the Howe Sound Fault and the MRT.*

lineation. The S-C fabric relationship observed implies sinistral movement consistent with the latest movement (reactivation) on the MRT (**Figure 35**). Three sets of iron carbonate veins can also be observed, which display sinistral offset and are also folded with their axial planes parallel to the main S_1 foliation.

Stops 24-26 are located on QMX's New Britannia Mine property. To enter the property, participants must report to the company`s main office and get permission to access the mine property. To get to the main office from Stop 23, return to vehicles and back track the last 100 m to then turn left (north) on Lakeshore drive. After 100 m Lakeshore Drive makes a sharp turn to the right (east) and becomes Cedar Avenue. Follow Cedar Avenue for 500 m. As you go up a small hill, the New Britannia mine complex will be to the left (north side of the road). Report yourself to the front desk. Enter mine complex and drive north until junction with gravel road. Turn left (west) on gravel road and and drive 1.2 km. Stop 24 is about 30 m off the north side of the road. Park vehicles along the road.

STOP 24 (UTM: 6083561N; 433511E): Boundary zone

Introduction

The Boundary zone mineralization is located in close proximity to the fault at the contact between the mafic volcaniclastic and felsic volcanic rocks. The mineralization is focused where the fault truncates the nose of the F_1 Nor-Acme antiform. Gold mineralization is hosted by both quartz carbonate and quartz veins (Beaumont-Smith and Lavigne, 2008). Galley et al. (1991) classified the Boundary zone as a vein breccia system that failed to fully develop, as gold mineralization is focused within a series of thin north striking breccia zones that parallel the regional foliation within the felsic volcanic rocks. It appears that insufficient fluid pressure was reached to cause the degree of brecciation and vein formation within the fault that occurred at the No.3 Zone at Stop 25.

Outcrop description

The main lithologies at Stop 24 are coherent rhyolite and felsic volcaniclastic rocks of unit 6 and pyroxene-crystal rich volcaniclastic rocks of unit 7. The Boundary zone map shown in **Figure 36** is based on 2011 and 2012 mapping and is an updated interpretation from that of Fieldhouse (1999) and Beaumont-Smith and Lavigne (2008). A detailed sketch (**Figure 37**), demostrates the relationship between bedding and the main S_1 flattening foliation of the clasts, which are rotated in an anticlockwise sense into the shear zone, together with the mafic dikes, all of which imply sinistral shear (Figure 37). However the shear zone is not well developed and the fabric is not prominent in proximity to the shear zone. The clasts show a strong refraction, as they are rotated into the shear zone. The felsic

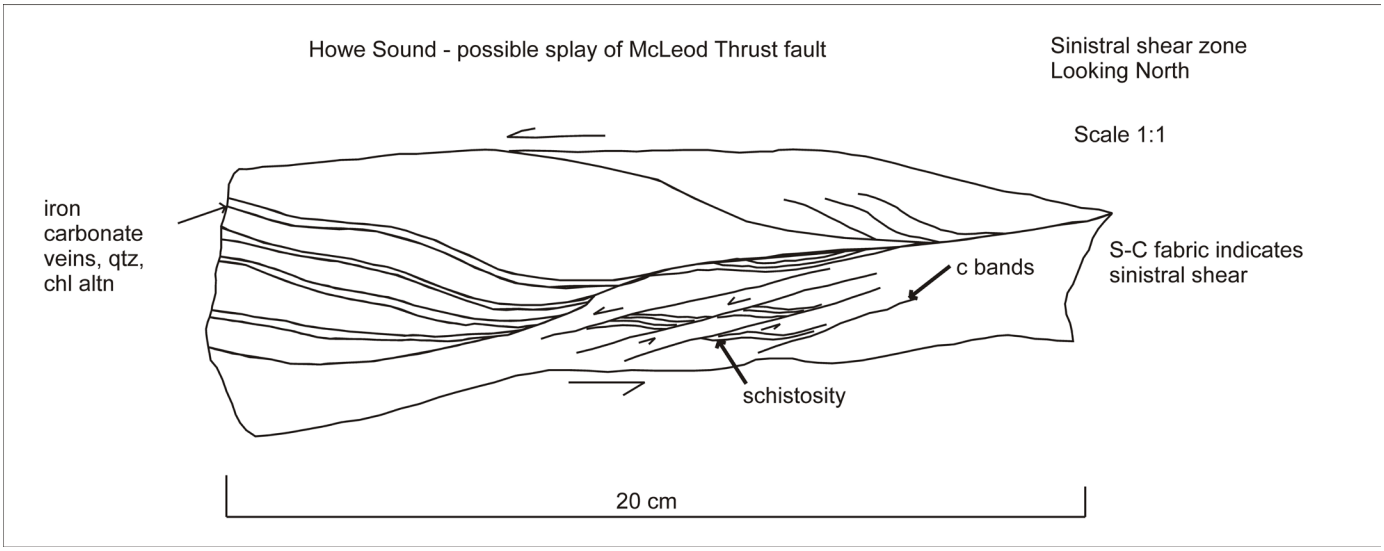

Figure 35: *Sketch to show the S-C fabric which represents a potential splay of the MRT (identified on Figure 33).*

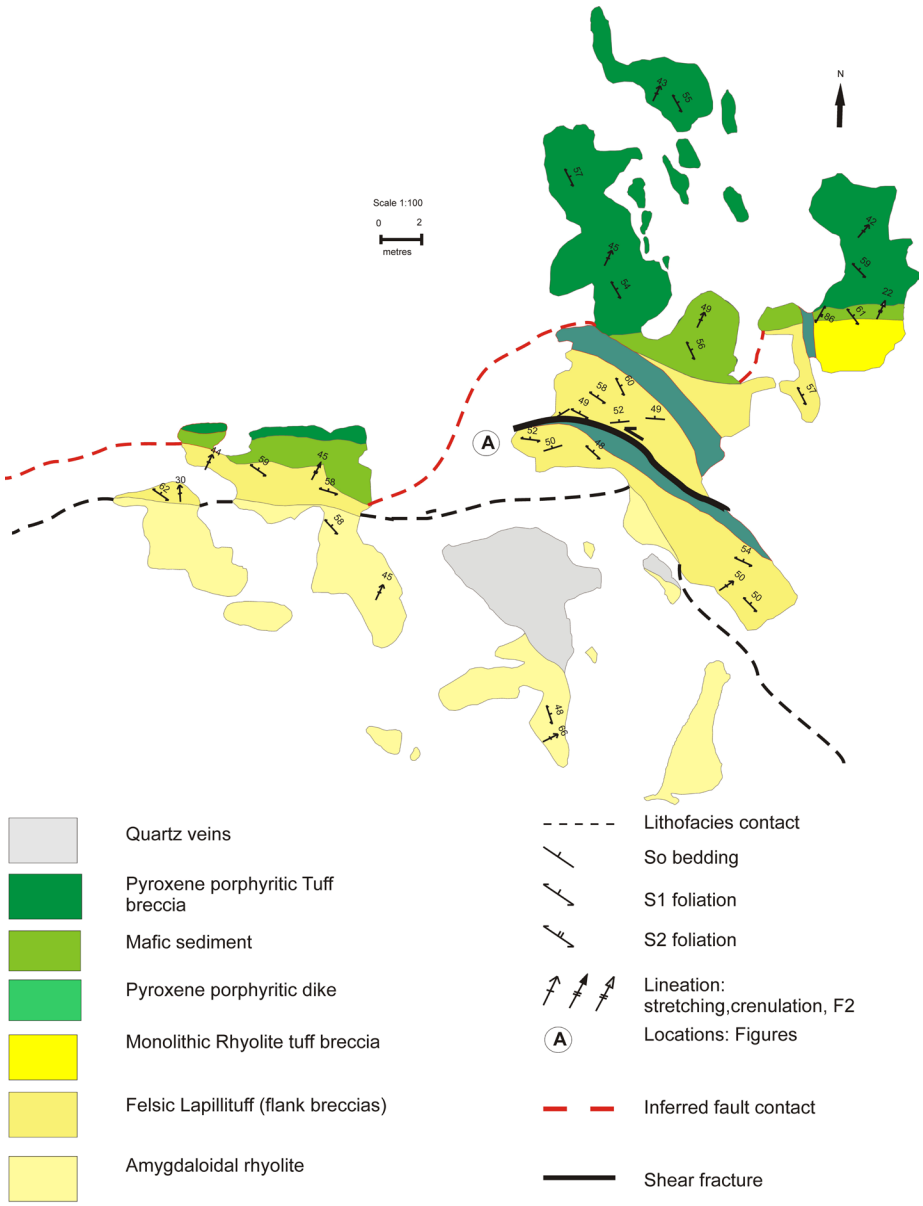

Figure 36: *Outcrop map of the Boundary zone showing at Stop 24.*

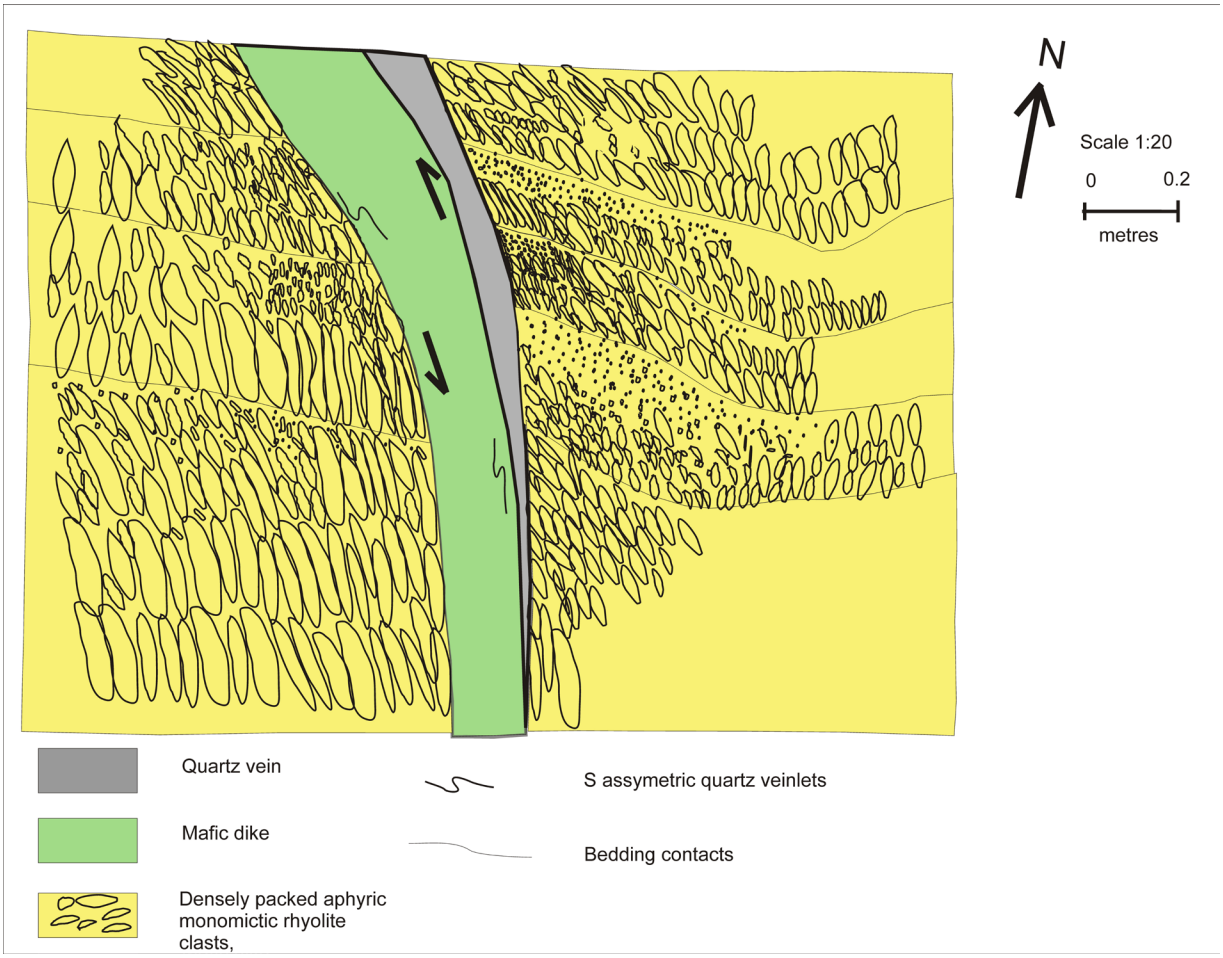

Figure 37: *Sketch to show the sinistral shear fracture at the Boundary Zone at location A (identified on* ***Figure 36****).*

rocks comprise a massive aphyric rhyolite flow with quartz filled amygdules located at the top of the flow, which is in contact with the flank breccias stratigraphically above. These rhyolite breccias are monolithic and well-bedded (**Figure 37**). At this outcrop bedding strikes east-northeast and dips steeply. The clasts display a strong flattening foliation, consistent with S_1 which is here a north-northwest orientation and a strong lineation, which dips moderate to shallow to the northeast.

The rhyolite and felsic breccias are interpreted to face (top) to north based on the south to north progression from a massive aphyric coherent rhyolite flow, to *in situ* breccias and flank breccias, all of which are monolithic and derived from autobrecciation and mass wasting of the coherent rhyolite dome. This succession confirms that younging is towards the north. Previous work by Beaumont-Smith and Lavigne (2008) had indicated that this portion of the stratigraphy was overturned, but based on our facing directions at this outcrop this in no longer a tenable interpretation. The north facing at this outcrop is compatible with the consistent north facing of almost all the rocks in the thrust panel.

To reach Stop 25, return to vehicles. Drive another 650 m (westward becoming northward) on the gravel road. You will reach a junction with a small gravel road on the left and see a large clearing. Turn left at this junction and immediately park vehicles along the road. You will see a small pond on the northeast side of the road. The No. 3 zone exposure is located right by the pond.

STOP 25 (UTM: 6084071N; 433238E): The No. 3 zone

Introduction

The second main deposit on the QMX mine property is the No.3 zone. This zone is a fault-hosted vein occurrence, consisting of a main shear vein and numerous extensional ladder veins. The No. 3 zone has two surface exposures which show the changing orientation of the main shear structure: at the main quartz-vein showing (Location A) and in the portal area (Location B). The main quartz-vein area shows the shear vein striking due west however the portal area displays a main west-northwest- to northwest-trending shear, which has rotated northwards to merge with the MRT.

Gold mineralization is located within a 50 m wide fault zone at the folded contact between the coarse pyroxene mafic volcaniclastic rocks (unit 7, as defined by Rubingh et al., 2012a), and the plagioclase-phyric pillowed flows of the Birch Lake basalt. Mineralization is hosted within quartz-albite-iron carbonate veins as coarse visible gold and it is associated with acicular arsenopyrite within the wallrocks and wallrock fragments (Galley et al., 1991).

Location A

At this stop, located at the main showing of the No. 3 zone, we can observe two thick white quartz veins and a series of narrow extensional veins at an angle to the main veins. The trace of the main foliation is rotated into the zone in an anticlockwise sense and there are thick laminated quartz veins and brecciated wall rock fragments. All these textures indicate sinistral shear and they are consistent with a shear vein – extensional vein system as discussed by Galley et al. (1991). At the No. 3 zone, mineralization was emplaced during sinistral shear overprinting the Nor Acme anticline; however the MRT also overprints the Nor Acme anticline. The No. 3 zone emplacement could be associated with thrusting on the MRT, or alternatively it could have formed during sinistral shear and overprinting of the MRT. This stop exhibits several generations of veins and, on an outcrop scale, the S_1 and S_2 fabrics are both rotated into parallelism with the main shear fracture, indicating D_2 timing for mineralization.

Location B

At this stop (The No. 3 zone portal), we can examine a recently enlarged outcrop from 2012 mapping. The sinistral shear fracture at this outcrop is interpreted to show the continuation of the structure previously observed at the vein showing of the No. 3 zone. This stop highlights the crosscutting relationships of different structures and fabric elements which are illustrated in **Figure 38**.

Bedding at this stop is defined by the normal grading of clasts of the coarse pyroxene mafic volcaniclastic rocks (unit 7, as defined by Rubingh et al., 2012a). The beds are 1–2 m thick and the clasts which are 3–80 cm in size are all similar in composition and texture. They are characterized by 15% pyroxene (3–25 mm) and 5–7% plagioclase (2–4 mm) phenocrysts in a light-coloured ground mass. The main observation here is that the main west-northwest- to northwest-trending shear fracture of unknown displacement cuts the beds; anticlockwise rotation of the clasts into the shear indicates sinistral movement.

Facing directions are weakly defined to the north, based on weak normal grading and the beds are folded with an S_1 axial-planar fabric, defined by flattened clasts, but there is no associated penetrative foliation. We can observe here the S_1 fabric axial planar to S_0 which is the same generation as the macroscopic F_1 folds such as the Nor Acme fold (**Figure 39**a). The S_1 fabric is also axial planar to folded, gold-bearing, quartz–albite–iron carbonate veins, and these veins display an S_2 cleavage which overprints the vein (Figure 39b). The overprinting relationship between S_2 and the rotation of S_1 into the main shear fracture constrains the timing of the shear fracture to either late D_1 or early D_2.

The S_3 fabric is a steep north-northeast-trending fracture cleavage, which is observed to cut the shear zone and overprint all fabric elements. There are north-trending shears associated with the S_3 fabric, east-trending tension gashes, and small-amplitude folds which fold the S_2 fabric (some of which display Z-asymmetry) and display an S_3 axial planar cleavage (**Figure 39**a), similar to the relationships observed at stop 24. These D_3 fabric elements may therefore reorient structures associated with mineralization; however these interpretations are preliminary and could change with further structural analysis.

To reach Stop 26, return to vehicles to continue travelling 1.8 km along the gravel road. During dry weather conditions the first 900 m is 4x4 accessible. The last 900 m are an ATV trail that requires walking. Stop 26 is located on the right (north) side of the trail along a power line.

STOP 26 (UTM: 6084810N; 432097E): McLeod Road Thrust

Introduction

This stop is important as we can examine the S_2 regional fabric in the Burntwood Group and observe how it changes in orientation towards the MRT, which lies exposed at the base of the hill. At Stop 22 we observed the same overprinting relationship of the S_2 fabric and the MRT. Regional mapping during 2012 has identified S_2 as a moderately defined, northwest- to north-northeast-trending, moderately northeast- to east-dipping, penetrative spaced cleavage, defined by the alignment of hornblende in mafic rocks and biotite in felsic rocks. The S_2 fabric of the MB panel displays a clockwise relationship to S_1; it overprints the Howe Sound Fault, the MRT and the Nor-Acme anticline. The mineral lineation (L_2) is rarely observed and trends north-northeast to east, which is similar to the orientation of the stretching lineation (L_1) defined by the clasts (Rubingh et al., 2012a).

At this stop, at the MRT contact, the relationship of the regional S_2 fabric in the Burntwood Group can be compared with the volcanics. What were previously identified as sinistral transcurrent shear-sense indicators are alternatively related to thrust imbrication of the panel during D_2.

Outcrop description

The S_2 fabric in the Burntwood Group rotates in an anticlockwise sense as it approaches the MRT; however, it is observed to transect the MRT at an angle of >30° and is therefore not related to initial thrust imbrication of the panel. This S_2 cleavage is axial planar to S-asymmetric F_2 folds which are folding the S_1 shear foliation and this axial planar S_2 cleavage is parallel to the regional S_2 fabric in the Burntwood Group, which cuts across the MRT. Therefore, the S_2 fabric as observed here may be related to sinistral reactivation of the MRT (Rubingh et al., 2012a; **Figure 40**).

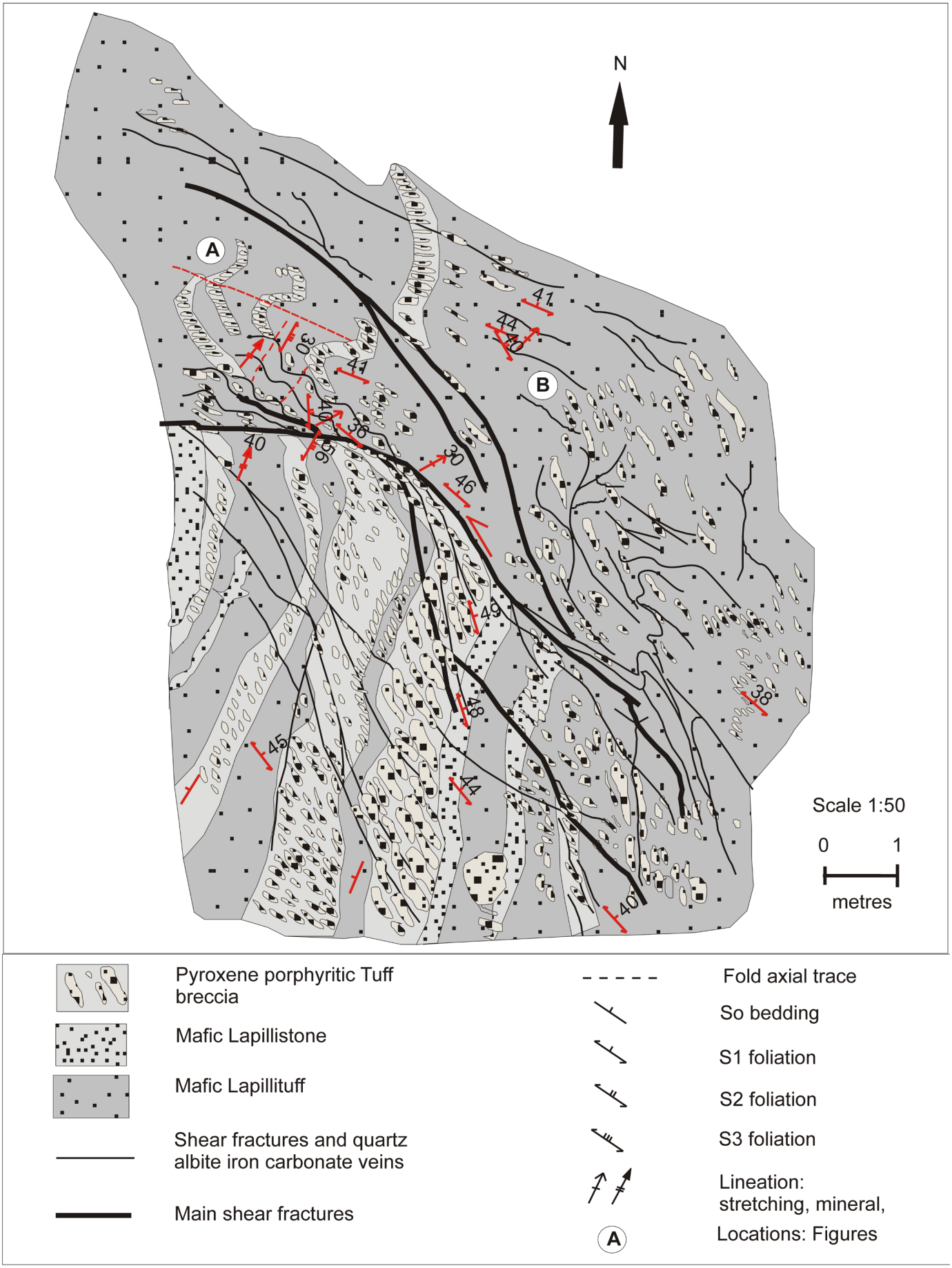

Figure 38: *Sketch to show the fabric relationships at the No.3 Zone portal (Rubingh et al., 2012a).*

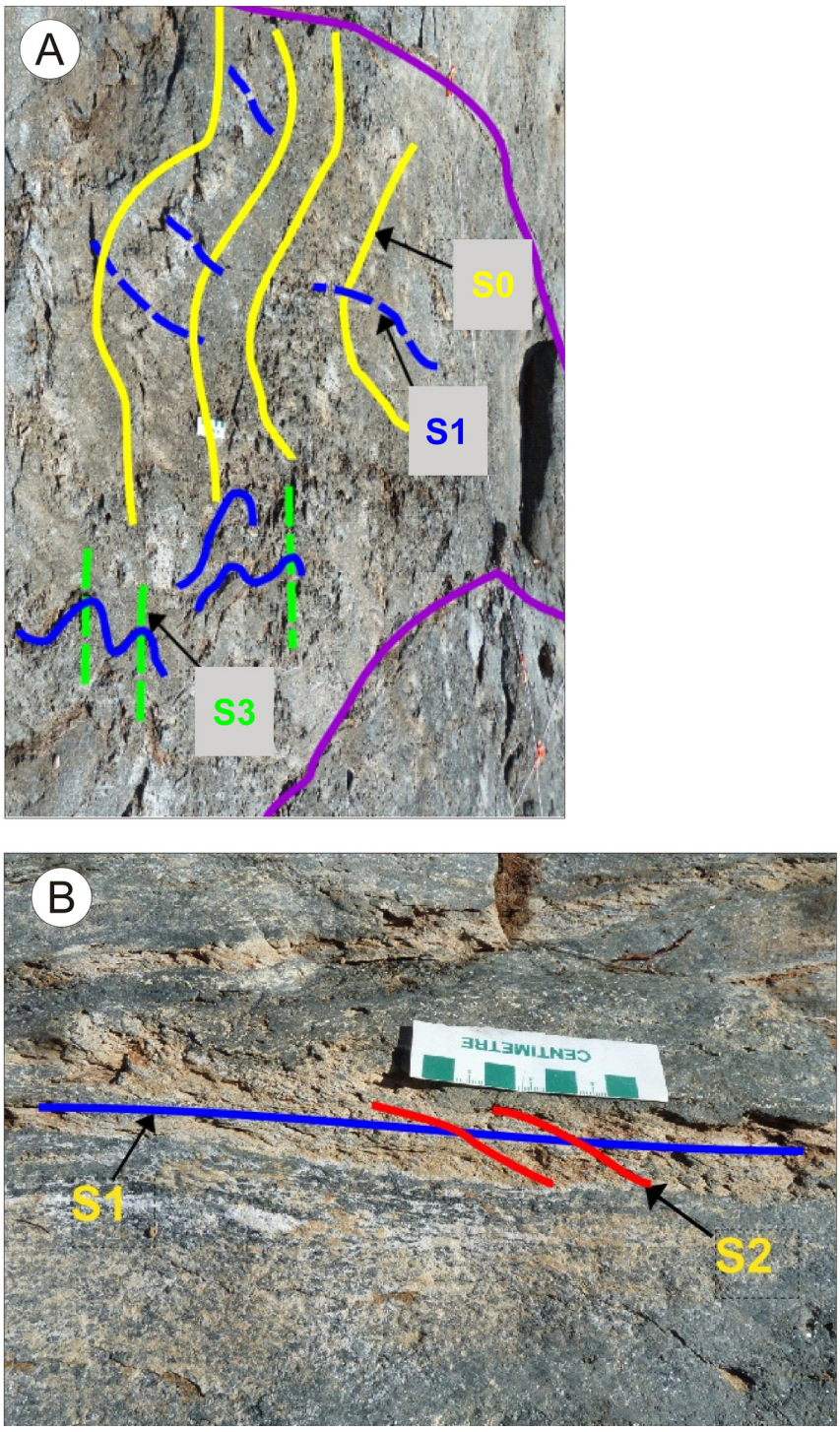

Figure 39: *a) F_1 folds with an axial planar fabric and S_3 axial planar cleavage to small tight folds, b) S_2 cleavage overprints iron carbonate vein.*

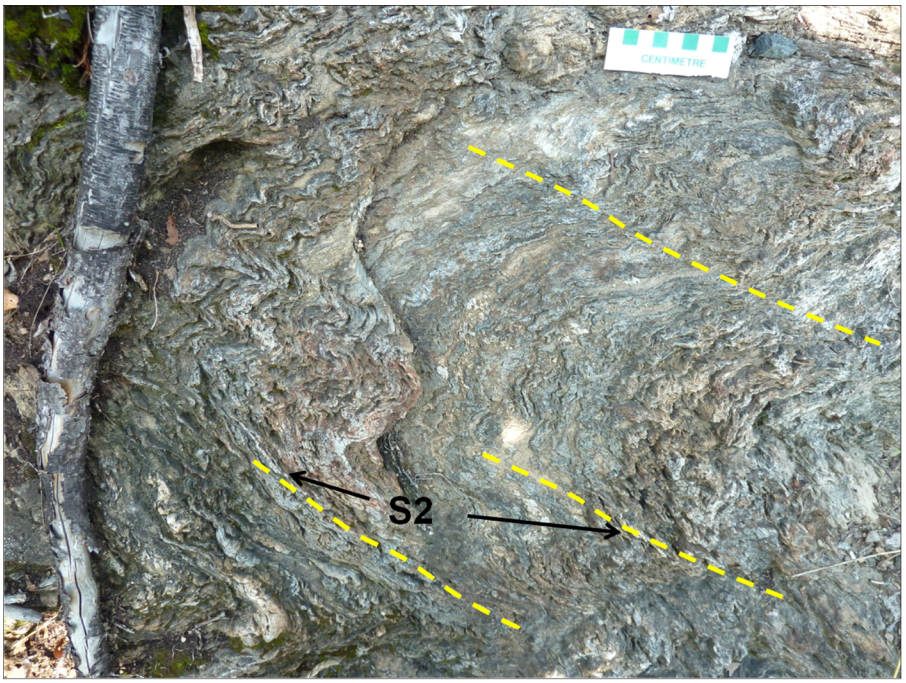

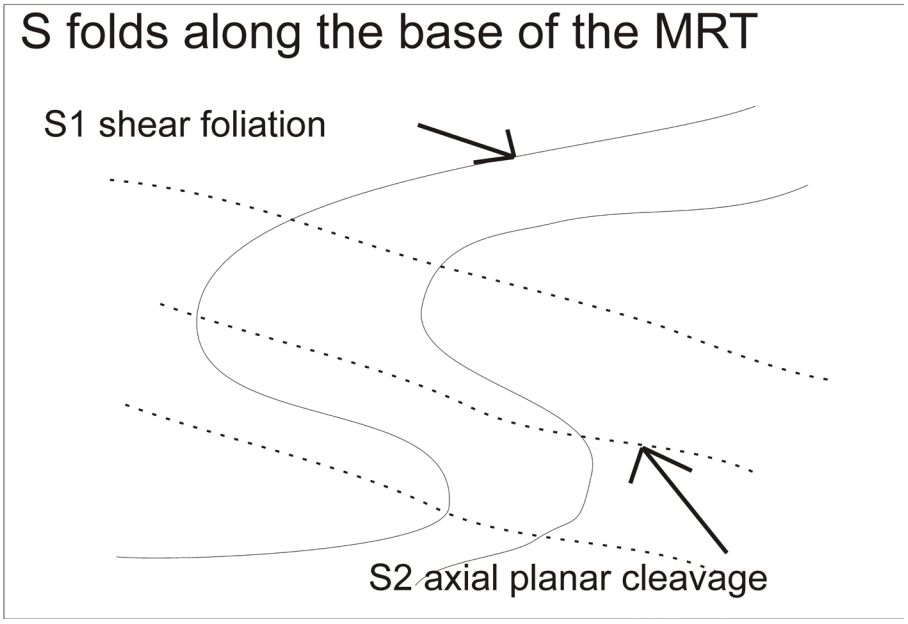

Figure 40: *Sketch of features on outcrop at Stop 26, Location C. The southerly unit comprises silicified/feldspathized Welch pillowed basalt of the Anderson sequence and the northerly unit consists of lobe facies rhyolite. The contact between the two units is likely a* D_{1-2} *thrust fault.*

Part 3: Geological Setting of the Au-rich Lalor Lake Zn-Cu VMS mine (by Alan Bailes, Craig Taylor, Sarah Bernauer and Darren Simms)

Introduction

A half day underground tour of the Lalor Lake deposit rounds out the field trip to Snow Lake area. The mine, which began underground production in August, 2012, is being rapidly developed. Consequently, exact locations and descriptions of tour stops are not available at the time of writing this guidebook.

Part 3 provides a brief history of the Lalor Lake VMS deposit and its geological setting. The objective is to provide field trip participants with a broad understanding of the deposit and a context for understanding features that they will be shown during the underground mine tour by Lalor Lake mine staff. Much of the material in this section is from information provided by HudBay staff geologists as well from reports written for HudBay Minerals Inc. by various consultants.

Deposit history

The Chisel Lake area has been explored for VMS deposits by HudBay Minerals Inc. since 1955 with many small to mid-level tonnage deposits discovered (**Table 1**). The deposits have been rich in base metals, with good precious metal content. They have also been easy to mill due to coarse grain size resulting from metamorphic recrystallization.

Although the Chisel Lake area has extensive domains of altered rocks, which encouraged continued exploration for a large deposit, the Lalor Lake deposit was difficult to find until a deep-penetrating EM survey was conducted over the Chisel Lake–Photo Lake–Lalor Lake area in 2003. This survey identified several large deep targets (**Figure 41**), with the one associated with the Lalor Lake deposit drilled in March 2007. The discovery drill hole, DUB168, intersected 16.45 m of 17.26% zinc, including a 7.99 m section of 31.93% zinc. In August 2010 HudBay Minerals Inc. published the 43-101 compliant reserves given in Table 1, which included poorly constrained gold and copper-gold mineralization that will be drilled off from an underground exploration drift to be started in 2014 (**Figure 42**).

An extensive exploration drill program on the Lalor Lake property was undertaken between 2007 and 2012 with the property then taken over by the mine department for underground development. The exploration drilling indicated that strata traced down to the mineralization dipped steeply to the north and topped to the southwest (Bailes 2009 and 2011) whereas the host strata for the mineralization dipped shallowly to the northeast. One interpretation of this feature is that it results from a shallow north dipping thrust fault (**Figure 22** and **Figure 43**). Rocks below the hypothetical thrust fault are characterized by strong alteration, sulphide mineralization and La/Yb ratios typically >15 (Bailes 2009). Rocks above the interpreted fault have negligible alteration and sulphide mineralization, and typically have La/Yb<5.

Development drilling at Lalor Lake mine (**Figure 43, Figure 44**) provides a much more accurate delineation of units and shows that the rocks hosting the mineralization are probably isoclinally and recumbently folded (Bailes, 2012). Sulphide mineralization at the Lalor Lake mine consists of two main types. The first is typical Zn-Cu massive sulphide mineralization, largely occurring in the main #10 sulphide lens (**Figure 42** and **Figure 43**). The second (sometimes collectively referred to as footwall lenses) contains massive to disseminated, commonly carbonate-bearing sulphides occurring in the #20, #31, #30 and #40 lenses (**Figure 43** and **Figure 44**).

The #10 sulphide lens is hosted in mafic heterolithic tuff breccias with La/Yb>15. These mafic breccias have been subdivided into a Lower and Upper unit with the #10 lens marking the contact between them. The Lower mafic tuff breccia is typically strongly altered and characterized by metamorphic mineral assemblages that range form biotite-chlorite bearing mesocratic types to sericite-biotite-quartz rich leucocratic end members. The level of alteration typically increases in intensity with proximity to the base of the #10 massive sulphide lense. Close to the base of the #10 lens the sulphide content increases in conjunction with increases in chlorite and biotite. Pervasive chlorite ± biotite commonly occurs as vein-halos, typically accompanied by elevated sulphides (pyrite, pyrrhotite and chalcopyrite) and porphyroblasts of gahnite, cordierite and anthophyllite. The chlorite-rich vein-halo domains are interpreted to be primary hydrothermal fluid channel-ways. This unit is locally characterized by large pophyroblasts of metamorphic minerals such as kyanite, staurolite and garnet, and in vein haloes cordierite and anthopyllite. This zone of alteration, which involves considerable addition of Mg(Fe) and K as chlorite and sericite, corresponds with rocks displaying elevated Hashimoto (Ishakawa) Alteration Index (**Figure 43**). This type of alteration, although also associated with other sulphide lenses, is clearly most closely spatially (and genetically?) related to the massive Zn-Cu sulphide mineralization as represented by the #10 lens.

The "FW" sulphide lenses (e.g., #20, #31, #30 and #40 lenses) occur in a unit of highly altered dacite and rhyodacite, with some of the larger sulphide lenses along its contact with an underlying aphyric basalt unit (**Figure 43** and **Figure 44**). The altered dacite and rhyodacite, which is characterized by addition of Ca, contains a wide assortment of minerals and displays a wide variety of textures. The most prominent minerals in these rocks are calcite/dolomite, talc/chlorite and tremolite, with lesser epidote group minerals, diopside, amphibole,orthoamphibole and grossular garnet. They are also characterized by trace to 20% disseminated sulphide minerals (typically pyrite and/or pyrrhotite, but often including noteworthy sphalerite, chalcopyrite and galena). The elevated sulphide and base metal content of the Ca-rich alteration zone results in diffuse and difficult to define ore lenses, some of which have elevated gold content. The Ca-rich rocks display an elevated Chlorite-Carbonate-Pyrite Index (CCPI; Ishikawa et al., 1976). Rocks containing elevated CCPI preferentially occur within the dacite-rhyodacite sequence and, to a lesser extent, the stratigraphically underlying aphyric basalt. Rocks with a high CCPI are rare in rocks stratigraphically overlying the dacite-rhyodacite,

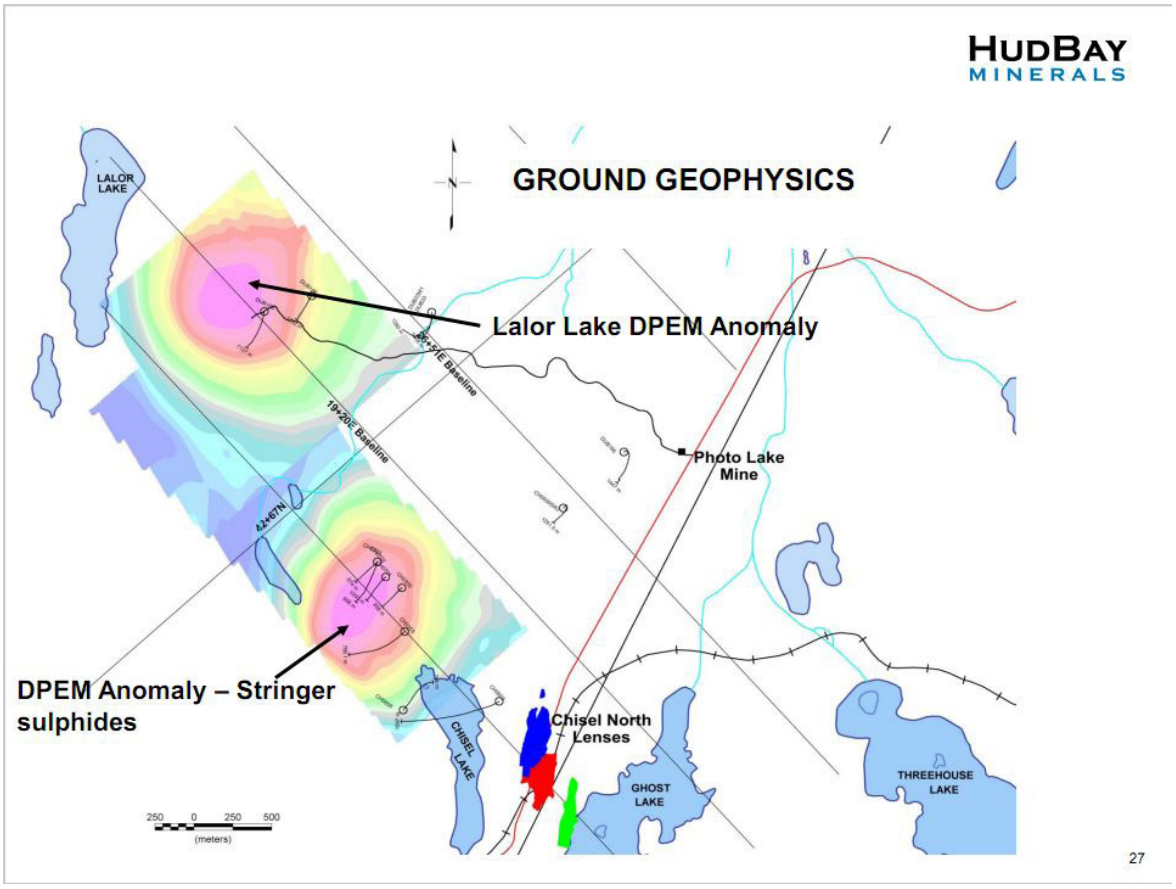

Figure 41: *Deep EM anomalies from gound geophysics over the Chisel Lake-Photo Lake-Lalor Lake property. Note the drill holes on the Chisel North anomaly that encountered stringer sulphides and the DUB168 discovery drill hole on the Lalor Lake anomaly.*

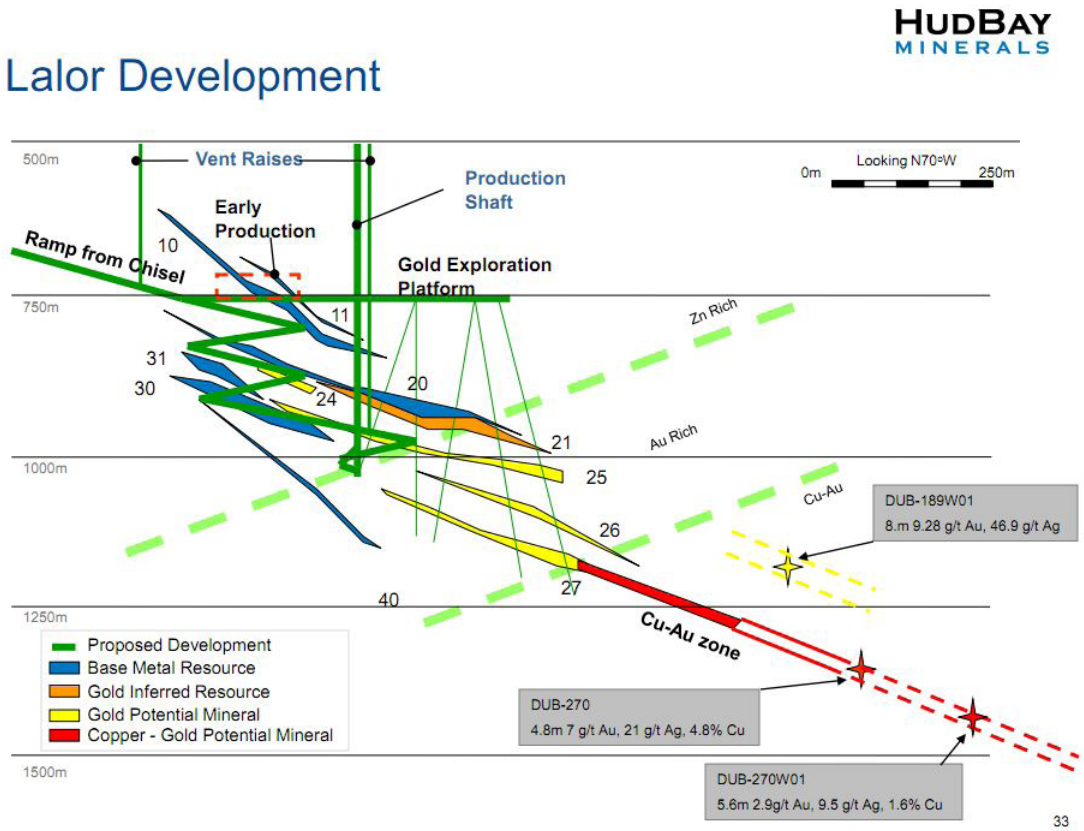

Figure 42: *Proposed Lalor Mine development plan (December 2010) in cross section.*

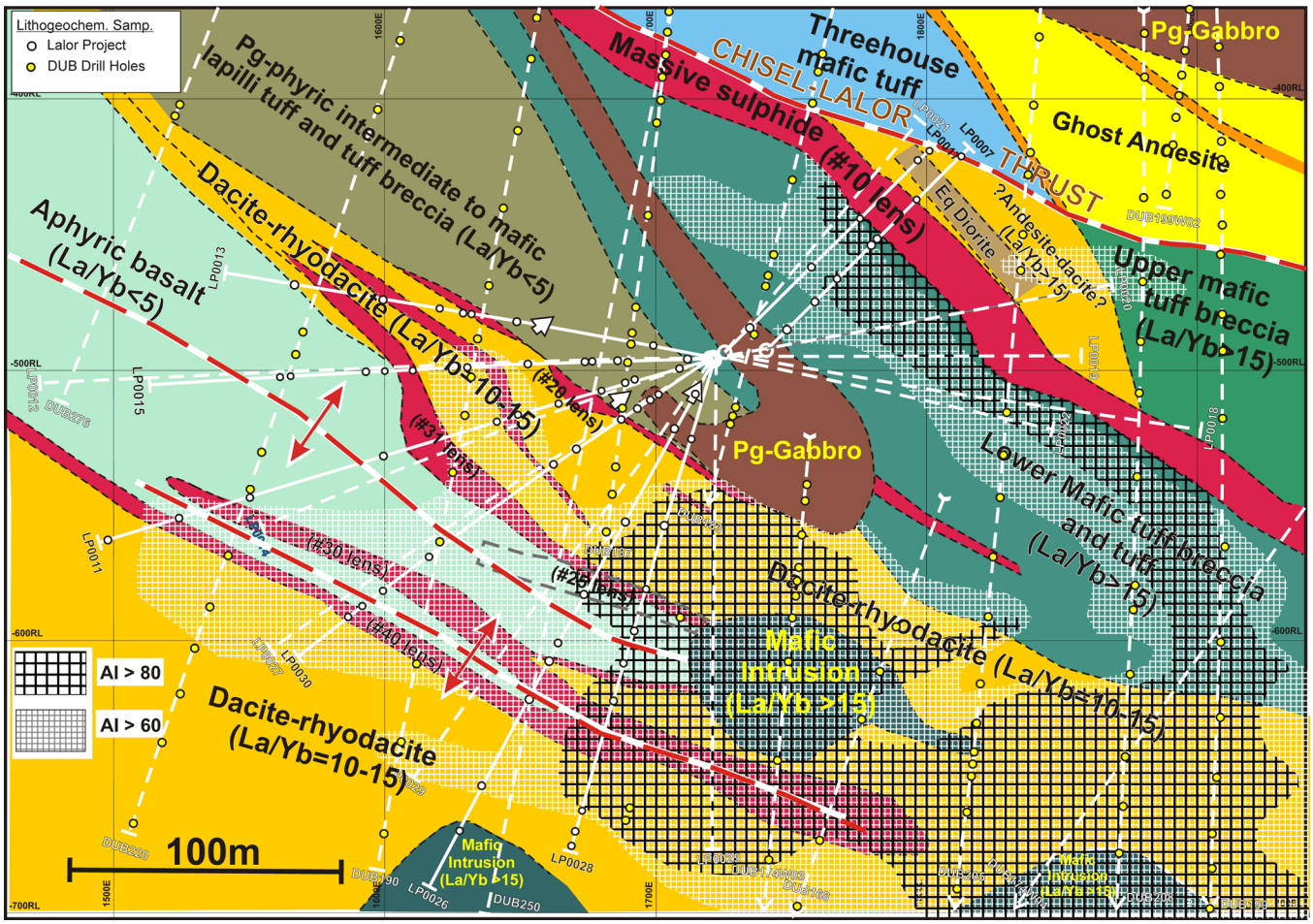

Figure 43: *Major geological units encountered in drill core projected onto S5200N (Bailes, 2012) at the Lalor Lake mine. Drill holes re-logged are shown by solid white lines. Other drill holes (including those from the DUB exploration drilling) are shown as dashed white lines. This figure is a composite with information from off section in adjacent drill holes projected to provide more control on unit distribution. The Chisel-Lalor thrust fault, which is a hypothetical structure needed to explain the distribution of units in the Lalor Lake deposit area (Bailes, 2008, 2009, 2011), is shown on this cross section although not identified in the Lalor Project (LP) drill holes. A reclined fold structure, which is depicted in this figure, is hypothesized to explain the termination of the aphyric basalt unit and the repetition of the dacite-rhyodacite both above and below the aphyric basalt. Normally size graded beds in the plagioclase-phyric intermediate to mafic tuff indicate this unit tops upwards. Hydrothermally altered rocks below the #10 massive sulphide lens are consistent with the host mafic breccias facing upwards . The distribution of rocks with Alteration Indices > 80 plotted on S5200N overlap with portion of the rocks define a zone of alteration that extends from the dacite-rhyodacite unit and traverses through the Lower mafic tuff breccia to the base of the #10 lens.*

suggesting that this style of alteration predated the overlying mafic tuff breccia and development of the #10 sulphide lens. The common association of gold with carbonate-rich rock in VMS systems suggests that this style of alteration and its subsequent metamorphism may play a role in controlling and defining the distribution Au in the Lalor Lake mine (D. Tinkham, pers. comm., 2012).

References

Alt, J.C. 1995: Subseafloor processes in mid-ocean ridge hydrothermal systems, Seafloor Hydrothermal Systems: Physical, Chemical, Biological, and Geological Interactions, AGU Geophysical Monograph 91, p. 85-114.

Ansdell, K.M. 1993: U-Pb zircon constraints on the timing and provenance of fluvial sedimentary rocks in the Flin Flon and Athapapuskow basins, Flin Flon Domain, Trans- Hudson Orogen, Manitoba and Saskatchewan*; in* Radiogenic Age and Isotopic Studies: Report 7, Geological Survey of Canada, Paper 93-2, p. 49-57.

Ansdell, K.M., Kyser, T.K., Stauffer, M. and Edwards, G. 1992: Age and source of detrital zircons from the Missi Group: a Proterozoic molasse deposit, Trans-Hudson Orogen, Canada; Canadian Journal of Earth Sciences, v. 29, p. 2583-2594.

Ansdell, K.M., Lucas, S.B., Connors, K. and Stern, R.A. 1995: Kisseynew metasedimentary gneiss belt, Trans-Hudson Orogen (Canada): Back-arc origin and collisional inversion; Geology, v. 23, p. 1039-1043.

Ansdell, K.M., Connors, K., Stern, R.A. and Lucas, S.B. 1999: Coeval sedimentation, magmatism, and fold-thrust belt development in the Trans-Hudson Orogen: geochronological evidence from the Wekusko Lake area, Manitoba, Canada; *in* NATMAP Shield Margin Project, Volume 1; Canadian Journal of Earth Sciences, v. 36, no. 2, p. 293-312.

Ashton, K.E., Lewry, J.F., Heaman, L.M., Hartlaub, R.P., Stauffer, M.R. and Tran, H.T. 2005: The Pelican Thrust Zone: basal detachment between the Archaean Sask Craton and Palaeoproterozoic Flin Flon–Glennie Complex, western Trans-Hudson Orogen. Canadian Journal of Earth Sciences, v. 42, p. 685–706.

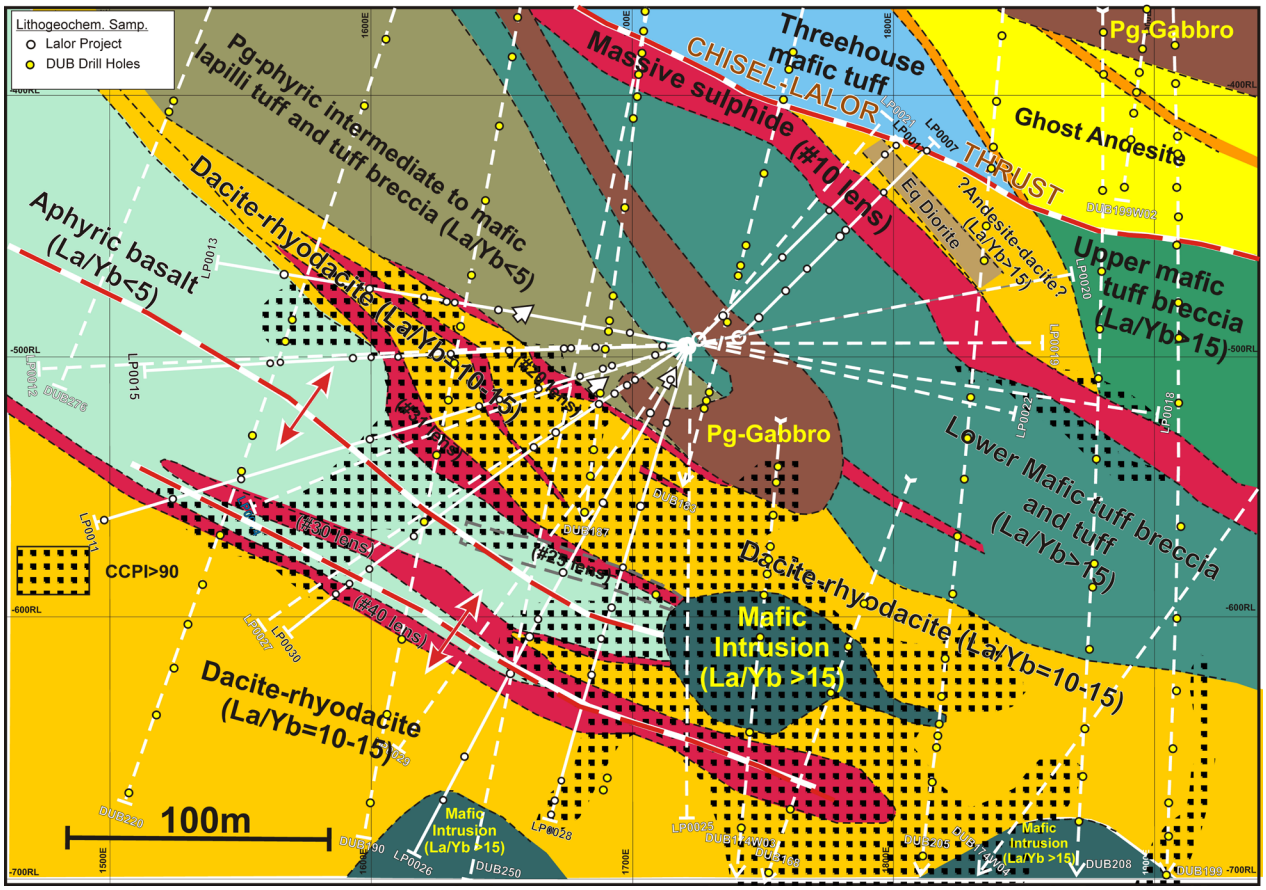

Figure 44: *The distribution of rocks with a chlorite-carbonate-pyrite index (CCPI) >90 at the Lalor Lake mine are shown on S5200N by the overlaid dot pattern (Bailes, 2012). Rocks with a CCPI>90 correlate with domains where carbonate-rich and calc-silicate rocks were logged. Rocks within the domain displaying CCPI>90 also have elevated chlorite and sulphides, with many containing sphalerite and galena.*

Bailes, A.H. 1971: Preliminary compilation of the geology of the Snow Lake-Flin Flon-Sherridon area, Manitoba Mines and Natural Resources, Mines Branch, Geological Paper 71-1, 27 p.

Bailes, A.H. 1980: Origin of early Proterozoic volcaniclastic turbidites, south margin of the Kisseynew sedimentary gneiss belt, File Lake, Manitoba; *in* Early Precambrian Volcanology and Sedimentology in the Light of the Recent, Precambrian Research, v. 12, no. 1-4, p. 197-225.

Bailes, A. H. 1986: Chisel-Morgan lakes project; *in* Report of Field Activities 1986, Manitoba Energy and Mines, Minerals Division, p. 71-76.

Bailes, A.H. 2008: Geological Setting of the Lalor and Photo Lake VMS Deposit; Consulting Report for HBED, September 2008, 46 p. (with accompanying CD-ROM).

Bailes, A.H. 2009: Geological and Geochemical Investigation of Altered Rocks Hosting the Lalor VMS Deposit; Consulting Report for HBED, December 2009, 96 p. (with accompanying CD-ROM).

Bailes, A.H. 2011: A Review of Structural Features Associated with VMS Deposits in the Chisel-Lalor-Photo lakes area; Consulting Report for HBED, February 2011, 31 p.

Bailes, A.H. 2012: Preliminary Report on the Stratigraphic and Structural Controls on the Mineralization at the Lalor Lake mine; Consulting Report for HudBay Minerals Inc, November, 2012, 63 p. (with accompanying CD-ROM).

Bailes, A.H. 2012b: Stratigraphic and Structural Controls on VMS Mineralization in the Chisel-Ghost Lakes Area: Consulting Report for HudBay Minerals Inc., November, 2012, 62 p. (with accompanying CD-ROM).

Bailes, A.H. and McRitchie, W.D. 1978: The transition from low to high grade metamorphism in the Kisseynew sedimentary gneiss belt, Manitoba; *in* Metamorphism in the Canadian Shield, J. A. Fraser and W. W. Heywood (eds.), Geological Survey of Canada, Paper 78-10, p. 155-178.

Bailes, A.H. and Galley, A.G. 1993: Geology of the Anderson-Stall volcanic-hosted massive sulphide area, Snow Lake, Manitoba; Geological Survey of Canada, Open File 2776, 1 map. scale 1:10_000.

Bailes. A.H. and Simms, D. 1994: Implications of an unconformity at the base of the Threehouse formation, Snow Lake (NTS 63K/16); in Manitoba Energy and Mines, Minerals Division, Report of Activities, 1994, 85-88.

Bailes, A.H., Simms, D., Galley, A.G. and Young, J. 1997: Geological setting of the Photo Lake volcanic-hosted massive sulphide deposit, Snow Lake, Manitoba, NTS 63K/16SE (part); Manitoba Energy and Mines, Open File Report 97-5, 1 colour map scale 1:5000.

Bailes, A.H. and Galley, A.G. 1996: Setting of Paleoproterozoic volcanic-hosted massive sulphide deposits, Snow Lake; *in* EXTECH I, A multidisciplinary approach to massive sulphide research: Rusty Lake-Snow Lake greenstone belt, Manitoba, (ed.) G.F. Bonham-Carter, A.G. Galley and G.E.M. Hall,: Geological Survey of Canada Bulletin, v. 426, p. 105-138.

Bailes, A.H. and Galley, A.G. 1999: Evolution of the Paleoproterozoic Snow Lake arc assemblage and geodynamic setting for associated volcanic-hosted massive sulphide 88 deposits, Flin Flon Belt, Manitoba, Canada: Canadian Journal of Earth Science, v. 36, p. 1789-1805.

Bailes, A.H. and Galley, A.G. 2007: Geology of the Chisel–Anderson lakes area, Snow Lake, Manitoba (NTS areas 63K16SW and west half of 63J13SE); Manitoba Science, Technology, Energy and Mines, Manitoba Geological Survey, MAP Geoscientific map 2007-1, 1 colour map with accompanying notes. scale 1:20 000.

Bailes, A.H., Galley, A.G., Paradis, S., and Taylor, B.E. in press: Large Synvolcanic Alteration Zones associated with Snow Lake VMS Deposits, Flin Flon Belt, Manitoba, Canada; *in* Paleoproterozoic Tectonics and Ore Deposits of the Western Trans-Hudson Orogen, Special Issue of Economic Geology.

Bailes, A.H. and Schledewitz, D.C.P. 1998: Geology and geochemistry of Paleoproterozoic volcanic rocks between the Mcleod Road and Birch Lake faults, Snow Lake area, Flin Flon Belt (parts of NTS 63K/16 and 63J/13); *in* Report of Activities 1998, Manitoba Energy and Mines, Geological Services, p. 4-13.

Bailes, A.H., Hunt, P.A. and Gordon, T.M. 1991: U-Pb zircon dating of possible synvolcanic plutons in the Flin Flon belt at Snow Lake, Manitoba; Radiogenic Age and Isotopic Studies: Report 4, Geological Survey of Canada, Paper 91-2, p. 35-43

Bailes, A.H. Galley, A.G. Skirrow, R.G. and Young, J. 1996: Geology of the Chisel volcanic-hosted massive sulphide area, Snow Lake, Manitoba; Geological Survey of Canada; Manitoba Department of Energy and Mines, Mineral Resources Division, Open File, Open File Report 3262 95-4, scale 1:5000.

Bailes, A.H., Gordon, T.M. and Hunt, P.A. 1988: U-Pb geochronology of the Richard Lake tonalite, a possible synvolcanic pluton in the Snow Lake area, Manitoba Energy and Mines, Minerals Division, 1998 Report of Field Activities, p. 63-65.

Bailes, A., Gilmore, K., Levers, J. and Janser, B. 2009: The Lalor Deposit – Surprise at Depth [abstract]; Manitoba Mining and Minerals Convention 2009, Winnipeg, Manitoba, November 19-21, 2009, Program, p. 57-58.

Beccaluva, L. and Serri, G. 1988: Boninitic and low-Ti subduction-related lavas from intraoceanic arc-back arc systems and low-Ti ophiolites: a reappraisal of their petrogenesis and original tectonic setting; Tectonophysics, v. 146, p. 291-315.

Beaumont-Smith, C.J. and Lavigne, J. 2008: Structural geology and gold metallogenesis of the New Britannia mine area, Snow Lake, Manitoba (NTS 63K16); in Report of Activities 2008, Manitoba Science, Technology, Energy and Mines, Manitoba Geological Survey, p. 7–17

Bickford, M.E., Collerson, K.D., Lewry, J.F., Van Schmus, W.R. and Chiarenzelli, J.R. 1990: Proterozoic collisional tectonism in the Trans-Hudson orogen, Saskatchewan, Geology, v. 18, p. 14-18.

Connors, K.A. 1996: Unraveling the boundary between turbidites of the Kisseynew Domain and volcano-plutonic rocks of the Flin Flon domain in the eastern Trans-Hudson Orogen, Canada; Canadian Journal of Earth Sciences, v. 33, p. 811-829.

Connors, K.A. and Ansdell, K.M. 1994: Revision of stratigraphy and structural history in the Wekusko Lake area, eastern Trans-Hudson Orogen; *in* Report of Activities 1994, Manitoba Energy and Mines, Geological Services, p. 104-107.

Connors, K., Ansdell, K.M. and Lucas, S.B. 1999: Coeval sedimentation, magmatism, and fold-thrust development in The Trans-Hudson Orogen; propagation of deformation into an active continental arc setting, Wekusko Lake area, Manitoba; *in* NATMAP Shield Margin Project, Volume 1; Canadian Journal of Earth Sciences, v. 36, no. 2, p. 275-291.

Corrigan, D., Galley, A.G. and Pehrsson, S. 2007: Tectonic evolution and metallogeny of the southwestern Trans-Hudson Orogen; *in* Mineral deposits of Canada: a synthesis of major deposit-types, district metallogeny, the evolution of geological provinces, and exploration methods; Special Publication no. 5, p. 881-902.

Couture, J.-F. 1986: Géologie de la Formation de Gilman dans la partie centrale du Canton de Roy, Chibougamau, Québec: M.Sc. thesis, Université du Québec à Chicoutimi, Québec, 138 p.

Crawford, A., Falloon, T.J. and Green, D.H. 1989: Classification, petrogenesis and tectonic setting of boninites*; in* Boninites, A.J. Crawford (ed.), Unwin Hyman, p. 1-49.

David, J., Bailes, A.H. and Machado, N. 1996: Evolution of the Snow Lake portion of the Paleoproterozoic Flin Flon and Kisseynew belts, Trans-Hudson Orogen, Manitoba, Canada; Precambrian Research, v. 80, p. 107-124.

Duncan, R.A. and Green, D.H. 1987: The genesis of refractory melts in the formation of oceanic crust; Contributions to Mineralogy and Petrology, v. 96, p. 326-342.

Falloon, T.J., Malahoff, A., Zonenshain, L.P. and Bogdanov, Y. 1992: Petrology and geochemistry of back-arc basin basalts from Lau Basin spreading ridges at 15°, 18°, and 19°; Contributions to Mineralogy and Petrology, v. 47, p. 1-35.

Fieldhouse, I. 1999: Geological setting of gold mineralization in the vicinity of the New Britannia Mine, Snow Lake, Manitoba; M.Sc. thesis, University of Manitoba, 135 p. scale 1:2400 240.

Franklin, J.M, Gibson, H.L., Jonasson, I.R. and Galley, A.G. 2005: Volcanogenic Massive Sulphide Deposits: in Hedenquist, J.W., Thompson, J.F.H., Goldfarb, R.J., and Richards, J.P., eds., Economic Geology, 100th Anniversary Volume, The Economic Geology Publishing Company, p. 523-560.

Froese, E. and Moore, J.M. 1980: Metamorphism in the Snow Lake area, Manitoba, Geological Survey of Canada, Paper 78-27, 16 p., + 1 map at 1:50_000.

Fulton, P.J. 1999: Distribution of gold mineralization at the New Britannia Mine in Snow Lake, Manitoba: implications for exploration and processing; M.Sc. thesis, University of Manitoba, 207 p.

Gale, G.H. 2002: Geology of the New Britannia Mine, Snow Lake (NTS 63K16), Manitoba; in Report of Activities 2002, Manitoba Industry, Trade and Mines, Manitoba Geological Survey, p. 83-86.

Galley, A.G. 1993: Semi-conformable alteration zones in volcanogenic massive sulphide districts: Journal of Geochemical Exploration, v. 48, p. 175-200.

Galley, A.G. 1996: Paleoproterozoic volcanic-related massive sulphide deposits: Tectonic and depositional environments, The Gangue, v. 54, p. 10-13.Galley, A.G. and Ames, D.E. 1998: Skarns associated with Precambrian VMS deposits: Geological Associaiton of Canada, A-61.

Galley, A.G., 2003, Composite synvolcanic intrusions associated with Precambrian VMS- related hydrothermal systems, Mineralium Deposita, v. 38, p. 443-473.

Galley, A.G., Bailes, A.H., Syme, E.C., Bleeker, W., Macek, J.J. and Gordon, T.M. 1991: Geology and mineral deposits of the Flin Flon and Thompson Belts, Manitoba (field trip 10); International Association on the Genesis of Ore Deposits, Symposium [1991]; Geological Survey of Canada, Open File 2165, 136 p.

Galley, A.G., Bailes, A.H. and Kitzler, G. 1993: Geological setting and hydrothermal evolution of the Chisel Lake and North Chisel Zn-Pb-Ag-Au massive sulphide deposit, Snow Lake, Manitoba: Exploration and Mining Geology, vol. 2, p. 271-295.

Galley, A.G. and Bailes, A.H. 2002: Volcanogenic massive sulphide-related hydrothermal alteration events within the Paleoproterozoic Snow Lake Arc Assemblage, Geological Association of Canada-Mineralogical Association of Canada Joint Annual Meeting 2002, Saskatoon, Saskatchewan, Canada, Field Trip A2 Guidebook, 94 p.

Galley, A.G., Franklin, J.M. and Ames, D.E. 1988: Geological setting of gold mineralization, Snow Lake, Manitoba; Geological Survey of Canada, Open File 1700, scale 1:5000.

Galley, A.G. and Scoates, J.S. 1990: The relationship of dikes to hydrothermal alteration in the Edwards Lake formation, Snow Lake, Manitoba (NTS 63K/16); *in* Manitoba Energy and Mines, Minerals Division, Report of Activities 1990, p. 162-169.

Ghent, E.D. and Stout, M.Z. 1981: Geobarometry and geothermometry of plagioclase-biotite-garnet-muscovite assemblages, Contributions to Mineralogy and Petrology, v. 76, p. 92-97.

Gibson, H.L., Watkinson, D.H. and Comba, C.D.A. 1983: Silicification: Hydrothermal alteration in an Archean geothermal system within the Amulet Rhyolite formation, Noranda, Quebec: Economic Geology, v. 78, p. 954-971.

Hannington, M.D., Poulsen, K.H. and Thompson, J.F.H. 1999: Volcanogenic gold in the massive sulphide environment, *in* C. T. Barrie, and Hannington, M.D., ed., Volcanic-Associated Massive Sulfide Deposits: Processes and Examples in Modern and Ancient Settings, Reviews in Economic Geology, v. 8, p. 325-356.

Hannington, M.D., Kjarsgaard, I.M., Galley, A.G. and Taylor, B. 2003: Mineral-chemical studies of metamorphosed hydrothermal alteration in the Kristineberg volcanogenic massive sulfide district, Sweden; Mineralium Deposita, v. 38, p. 423-442.

Harrison, J.M. 1949: Geology and mineral deposits of the File-Tramping Lakes area, Manitoba; Geological Survey of Canada, Memoir 250, 92 p.

Harrison, J.M. 1951: Precambrian correlation and nomenclature, and problems of the Kisseynew gneisses in Manitoba; Geological Survey of Canada, Bulletin 20, 53 p.

Hodges, D.J. and Manojvic, P.M. 1993: Application of lithogeochemistry to exploration for deep VMS deposits in high grade metamorphic rocks, Snow Lake, Manitoba; Journal of Geochemical Exploration, vol. 48, p. 201-224.

Hoffman, P.F. 1988: United Plates of America, the birth of a craton - Early proterozoic assembly and growth of Laurentia; *in* Annual review of earth and planetary sciences; vol. 16, p. 543-603.

Hogg, N. 1957: The Nor-Acme Mine; in Structural geology of Canadian ore deposits: congress volume : a symposium, Canadian Institute of Mining and Metallurgy, 6th Commonwealth Mining and Metallurgical Congress, p. 262.

Holk, G.J. 1998: Stable isotope studies of silicfication at Snow Lake, The Use of Regional-Scale Alteration Zones and Subvolcanic Intrusions in the Exploraiton for Volcanic-Associated Massive Sulfide Deposits, p. 393-400.

Ishikawa, Y, Sawaguchi, T., Iwaya, S. and Horiuchi, M. 1976: Delineation of prospecting targets for Kuroko deposits based on modes of volcanism of underlying dacite and alteration halos: Mining Geology, v. 26, p. 105–117 (in Japanese with English abs.).

Kalogeropoulos, S.I. and Scott, S.D. 1989: Mineralogy and geochemistry of an Archean tuffaceous exhalite: the Main Contact Tuff, Millenbach mine area, Noranda, Quebec: Canadian Journal of Earth Sciences, v. 26, p. 88-105.

Kennedy, G.C. 1950: A portion of the system silica-water; Economic Geology, 45, 629-653.

Kleeman, U. and Reinhardt, J. 1994: Garnet-biotite thermometry revisited: The effect of Al^{VI} and Ti in biotite, European Journal of Mineralogy, v. 6, p. 925-941.

Kraus, J. 1998: Structural and metamorphic studies in the Snow Lake area, Trans-Hudson Orogen, Manitoba, central Canada; University of New Brunswick, Fredericton, New Brunswick, 229 p.

Kraus, J. and Menard, T. 1995: Metamorphism of the File Lake formation, Snow Lake : preliminary results; *in* Report of Activities 1995, Manitoba Energy and Mines, Geological Services, p. 160-163.

Kraus, J. and Menard, T. 1997: A thermal gradient at constant pressure; implications for low- to medium-pressure metamorphism in a compressional tectonic setting, Flin Flon and Kisseynew domains, Trans-Hudson Orogen, central Canada, The Canadian Mineralogist, v. 35, no. 5, p. 1117-1136.

Kraus, J. and Williams, P.F. 1994a: Clevage development and timing of metamorphism in the File Lake Formation across the Threehouse Synform, Snow Lake, Manitoba: a new paradigm; *in* Lithoprobe: Trans-Hudson Orogen Transect: report of fourth transect meeting, Z. Hajnal and J. F. Lewry (eds.), University of Saskatchewan, Lithoprobe Report 38, p. 230-237.

Kraus, J. and Williams, P.F. 1994b: Structure of the Squall Lake area, Snow Lake (NTS 63K/16); *in* Report of Activities 1994, Manitoba Energy and Mines, Geological Services, p. 189-193.

Kraus, J. and Williams, P.F. 1999: Structural development of the Snow Lake allochthon and its role in the evolution of the southeastern Trans-Hudson Orogen in Manitoba, central Canada; Canadian Journal of Earth Sciences, v. 36. no. 11, p. 1881–1899.

Lafrance, B., Gibson, H.L., Pehrsson, S., Schetselaar, E., DeWolfe, Y.M. and Lewis, D. *in press*: Structural reconstruction of the Flin Flon volcanogenic massive sulfide mining district, Saskatchewan and Manitoba, Canada; *in* Paleoproterozoic Tectonics and Ore Deposits of the Western Trans-Hudson Orogen, Special Issue of Economic Geology.

Lewry, J.F. and Collerson, K.D. 1990: The Trans-Hudson Orogen: Extent, Subdivision and Problems; *in* The Early Proterozoic Trans-Hudson Orogen of North America, J. F. Lewry and M. R. Stauffer (eds.), Geological Association of Canada,Special Paper 37, p. 1-14.

Liaghat, S. and MacLean, W.H. 1992: The Key Tuffite, Matagami mining district: Origin of the tuff components and mass changes: Exploration and Mining Geology, vol. 1, p. 197-207.

Lucas, S.B., Stern, R.A. and Syme, E.C. 1996: Flin Flon greenstone belt: intraoceanic tectonics and the development of continental crust (1.92-1.84 Ga); Geological Society of America Bulletin, vol. 108, p. 602-629.

Machado, N. and Zwanzig, H. 1995: U-Pb geochronology of the Kisseynew Domain in Manitoba: Provenance ages for the metasediments and timing of magmatism, *in* Z. Hajnal and J. Lewry (eds.), Report of 1994 THOT Transect Meeting. LITHOPROBE Report 38, p. 133-142.

Machado, N., Zwanzig, H.V. and Parent, M. 1999: U-Pb ages of plutonism, sedimentation, and metamorphism of the Paleoproterozoic Kisseynew metasedimentary belt, Trans-Hudson Orogen (Manitoba, Canada); Canadian journal of earth sciences, v. 36, no. 11, p. 1829-1842.

Menard, T. and Gordon, T. M. 1995: Syntectonic alteration of VMS deposits, Snow Lake, Manitoba; *in* Report of Activities 1995, Manitoba Energy and Mines, Geological Services, p. 164-167.

Mercier-Langevin, P., Hannington, M.D., Dubé, B. and Bécu, V. 2011: The gold content of volcanogenic massive sulfide deposits; Mineralium Deposita, v. 46, p. 509-539.

Percival, J.A., Zwanzig, H.V. and Rayner, N. 2006: New tectonostratigraphic framework for the northeastern Kisseynew Domain, Manitoba (parts of NTS 63O); *in* Report of Activities 2006, Manitoba Science, Technology, Energy and Mines, Manitoba Geological Survey, p. 74-84.

Piché, M., Guha, J., Daigneault, R.D., Sullivan, J.R. and Bouchard, G. 1990: Les gisements volcanogène du camp minier de Matagami: Structure, stratigrphie et implications métallogéniques, *in* P.V.M. Rive, Y. Gagnon, J.M. Lulin, G. Riverin and A. Simard, ed., The Northwestern Quebec Polymetallic Belt, Can. Inst. Min. Metall., Special vol. 21, p. 327-336.

Rosenbauer, J.R. and Bischoff, J.L. 1983: Uptake and transport of heavy metals by heated seawater: A summary of the experimental results, *in* P. A. Rona, Bostrom, K., Laubier, L., and Smith, K.L., ed., Hydrothermal Processes at Seafloor Spreading Centres, New York, Plenum, p. 177-198.

Rubingh, K.E. 2011: Stratigraphy of the McLeod Road–Birch Lake thrust panel, Snow Lake, west-central Manitoba (parts of NTS 63K16 and 63J13); in Report of Activities 2011, Manitoba Innovation, Energy and Mines, Manitoba Geological Survey, p. 68–78.

Rubingh, K.E., Lafrance, B. and Gibson, H.L. 2012a: Lithostratigraphy and structural geology of the McLeod Road–Birch Lake thrust panel, Snow Lake, west-central Manitoba (parts of NTS 63K16, 63J13); in Report of Activities 2012, Manitoba Innovation, Energy and Mines, Manitoba Geological Survey, p. 104–114.

Rubingh, K.E., Lafrance, B., Gibson, H.L. and Gagné, S. 2012b: Preliminary lithostratigraphic map of the McLeod Road-Birch Lake thrust panel, Snow Lake, west-central Manitoba (parts of NTS 63K16, 63J13); Manitoba Innovation, Energy and Mines, Manitoba Geological Survey, Preliminary Map PMAP2012-07, scale 1:5000.

Russell, G.A. 1957: Structural studies of the Snow Lake-Herb Lake area; Manitoba Mines and Natural Resources; Mines Branch, Publication 55-3, 33 p. + 1 map at 1:31_680

Seyfried, W.E. and Bischoff, J.L. 1977: Hydrothermal transport of heavy metals by seawater: the role of seawater/basalt ratio; Earth and Planetary Science Letters, vol. 34, p. 71-77.

Seyfried, W. E., Jr., Berndt, M.E. and Seewald, J.S. 1988: Hydrothermal alteration processes at mid-ocean ridges: Constraints from diabase alteration experiments, hot spring fluids and composition of the oceanic crust: Canadian Mineralogist, vol. 26, p. 787-804.

Skirrow, R.G. 1987: Silicification in a lower semiconformable alteration zone near the Chisel Lake Zn-Cu massive sulphide deposit, Manitoba; M.Sc. thesis, Carleton University, Ottawa, Ontario, 171 p.

Skirrow, R.G. and Franklin, J.M. 1994: Silicification and metal leaching in subconcordant alteration zones beneath the Chisel Lake massive sulphide deposit, Snow Lake, Manitoba; Economic Geology, vol. 89, p. 31-50.

Stern, R.A., Syme, E.C. and Lucas, S.B. 1995a: Geochemistry of 1.9 Ga MORB- and OIB-like basalts from the Amisk collage, Flin Flon belt, Canada: Evidence for an intra-oceanic origin; Geochimica et Cosmochimica Acta, vol. 59, p. 3131-3154.

Stern, R.A., Syme, E.C., Bailes, A.H. and Lucas, S.B. 1995b: Paleoproterozoic (1.86-1.90 Ga) arc volcanism in the Flin Flon belt, Trans-Hudson Orogen, Canada; Contributions to Mineralogy and Petrology, vol. 119, p. 117-141.

Stern, R.A., Syme, E.C., Bailes, A.H., Galley, A.G., Thomas, D.J. and Lucas, S.B. 1992: Nd isotopic stratigraphy of Early Proterozoic Amisk Group metavolcanic rocks from the Flin Flon belt*; in* Radiogenic Age and Isotopic Studies, Report 6, Geological Survey of Canada, Paper 92-2, p. 73-84.

Studer, R.D. 1982: Geology of the Stall Lake copper deposit, Snow Lake, Manitoba: Canadian Institute of Mining and Metallurgy Bulletin, vol. 75, p. 66-72.

Surka, M.M. 2001: Metal mobility during silicification of the 1.89 Ga Welch Lake primitive arc basalts, Snow Lake arc assemblages, Snow Lake, Manitoba , B.Sc. Honour`s thesis, University of Manitoba, 102 p.

Swinden, H.S. 1996: The application of volcanic geochemistry to the metallogeny of volcanic-hosted sulphide deposits in central Newfoundland, *in* D. A. Wyman, ed., Trace Element Geochemistry of Volcanic Rocks: Applications for Massive Sulphide Exploration, Short Course Notes, Geological Association of Canada, p. 239-279.

Syme, E.C., Bailes, A.H. and Lucas, S.B. 1995: Geology of the Reed Lake area (parts of NTS 3K/9 and 10); in Report of Activities 1995, Manitoba Energy and Mines, Geological Services, p. 42–60.

Syme, E.C., Lucas, S.B., Bailes, A.H. and Stern, R.A. 1999: Contrasting arc and MORB-like assemblages in the Paleoproterozoic Flin Flon Belt, Manitoba, and the role of intra-arc extension in localizing volcanic-hosted massive sulphide deposits; National Research Council of Canada, Canadian journal of earth sciences, v. 36, no. 11, p. 1767-1788.

Taylor, B.E. and Timbal, A. 1998: Regional stable isotope studies in the Snow Lake area; CAMIRO Project 94E07 Annual Report, p. 271-280.

Trembath, G.D. 1986: The compostional variation of staurolite in the area of Anderson Lake Mine, Snow Lake, Manitoba, Canada: MSc thesis, University of Manitoba, Winnipeg, 187 p.

Walford, P.C. and Franklin, J.M. 1982: The Anderson Lake Mine, Snow Lake, Manitoba; *in* R.W. Hutchinson, C.D. Spence and J.M. Franklin (eds.), Precambrian Sulfide Deposits, Geological Association of Canada, Special Paper 25, p. 481-523.

Zaleski, E. Froese, E. and Gordon, T.M. 1991: Metamorphic petrology of Fe-Zn-Mg-Al alteration zones at the Linda volcanogenic massive sulphide deposit, Snow Lake, Manitoba; Canadian Mineralogist, v. 29, p. 995-1017.